



AFRL-RX-WP-TP-2009-4086

**AN ASSESSMENT OF BINARY METALLIC GLASSES:
CORRELATIONS BETWEEN STRUCTURE, GLASS
FORMING ABILITY AND STABILITY (PREPRINT)**

Daniel B. Miracle, Dmitri Louzguine-Luzgin, Larissa Louzguina-Luzgina, and Akihisa Inoue
Metals Branch
Metals, Ceramics and NDE Division

APRIL 2009

Approved for public release; distribution unlimited.

See additional restrictions described on inside pages

STINFO COPY

**AIR FORCE RESEARCH LABORATORY
MATERIALS AND MANUFACTURING DIRECTORATE
WRIGHT-PATTERSON AIR FORCE BASE, OH 45433-7750
AIR FORCE MATERIEL COMMAND
UNITED STATES AIR FORCE**

REPORT DOCUMENTATION PAGE				Form Approved OMB No. 0704-0188	
<p>The public reporting burden for this collection of information is estimated to average 1 hour per response, including the time for reviewing instructions, searching existing data sources, gathering and maintaining the data needed, and completing and reviewing the collection of information. Send comments regarding this burden estimate or any other aspect of this collection of information, including suggestions for reducing this burden, to Department of Defense, Washington Headquarters Services, Directorate for Information Operations and Reports (0704-0188), 1215 Jefferson Davis Highway, Suite 1204, Arlington, VA 22202-4302. Respondents should be aware that notwithstanding any other provision of law, no person shall be subject to any penalty for failing to comply with a collection of information if it does not display a currently valid OMB control number. PLEASE DO NOT RETURN YOUR FORM TO THE ABOVE ADDRESS.</p>					
1. REPORT DATE (DD-MM-YY) April 2009		2. REPORT TYPE Journal Article Preprint		3. DATES COVERED (From - To) 01 April 2009- 01 April 2009	
4. TITLE AND SUBTITLE AN ASSESSMENT OF BINARY METALLIC GLASSES: CORRELATIONS BETWEEN STRUCTURE, GLASS FORMING ABILITY AND STABILITY (PREPRINT)				5a. CONTRACT NUMBER In-house	
				5b. GRANT NUMBER	
				5c. PROGRAM ELEMENT NUMBER 62102F	
6. AUTHOR(S) Daniel B. Miracle (AFRL/RXLMD) Dmitri Louzguine-Luzgin, Larissa Louzguina-Luzgina and Akihisa Inoue (Tohoku University of Japan)				5d. PROJECT NUMBER 4347	
				5e. TASK NUMBER RG	
				5f. WORK UNIT NUMBER M02R4000	
7. PERFORMING ORGANIZATION NAME(S) AND ADDRESS(ES) Metals Branch (RXLMD) Metals, Ceramics and NDE Division Materials and Manufacturing Directorate Wright-Patterson Air Force Base, OH 45433-7750 Air Force Materiel Command, United States Air Force				8. PERFORMING ORGANIZATION REPORT NUMBER AFRL-RX-WP-TR-2009-4086	
9. SPONSORING/MONITORING AGENCY NAME(S) AND ADDRESS(ES) Air Force Research Laboratory Materials and Manufacturing Directorate Wright-Patterson Air Force Base, OH 45433-7750 Air Force Materiel Command United States Air Force				10. SPONSORING/MONITORING AGENCY ACRONYM(S) AFRL/RXLMD	
				11. SPONSORING/MONITORING AGENCY REPORT NUMBER(S) AFRL-RX-WP-TP-2009-4086	
12. DISTRIBUTION/AVAILABILITY STATEMENT Approved for public release; distribution unlimited.					
13. SUPPLEMENTARY NOTES To be submitted to International Materials Review PAO Case Number and clearance date: 88ABW-2009-1039, 17 March 2009. The U.S. Government is joint author on this work and has the right to use, modify, reproduce, release, perform, display, or disclose the work.					
14. ABSTRACT The objective of this work is to explore the influence of the atomic structure of binary metallic glasses on glass-forming ability and thermal stability. A broad assessment of binary metallic glasses is given, with information on 619 distinct binary alloys from 162 binary glass systems. For each of these glasses, the structure is quantified with the efficient cluster-packing (ECP) model, using reported glass constitutions as input. The glass transition temperatures T_g , crystallization temperatures T_x , and liquidus temperatures T_l are taken from the literature to compute the thermal stability parameters $Trg = T_g / T_l$, Tx / T_l , $gxxTTT$ and $= Tx / (T_g + T_l)$. Comparison of the atomic structures with reported amorphous thickness and thermal stability parameters gives the following major results. Binary glasses show a strong preference for solute-to-solvent atomic radius ratios, R , that produce efficient local atomic packing, consistent with earlier results.					
15. SUBJECT TERMS metallic glass, atomic structure, topology, stability					
16. SECURITY CLASSIFICATION OF:			17. LIMITATION OF ABSTRACT: SAR	18. NUMBER OF PAGES 86	19a. NAME OF RESPONSIBLE PERSON (Monitor) Jonathan Spowart 19b. TELEPHONE NUMBER (Include Area Code) N/A
a. REPORT Unclassified	b. ABSTRACT Unclassified	c. THIS PAGE Unclassified			

An assessment of binary metallic glasses: Correlations between structure, glass forming ability and stability

Daniel B. Miracle^{a*}, Dmitri Louzguine-Luzgin^{b,c}, Larissa Louzguina-Luzgina^{b,c**} and Akihisa Inoue^{b,c}

a. Air Force Research Laboratory, Materials and Manufacturing Directorate, Dayton, OH USA

b. WPI Advanced Institute of Materials Research, Tohoku University, Sendai, JAPAN

c. Institute of Materials Research, Tohoku University, Sendai, JAPAN

Abstract

The objective of this work is to explore the influence of the atomic structure of binary metallic glasses on glass-forming ability and thermal stability. A broad assessment of binary metallic glasses is given, with information on 619 distinct binary alloys from 162 binary glass systems. For each of these glasses, the structure is quantified with the efficient cluster-packing (ECP) model, using reported glass constitutions as input. The glass transition temperatures T_g , crystallization temperatures T_x , and liquidus temperatures T_l are taken from the literature to compute the thermal stability parameters $T_{rg} = T_g/T_l$, T_x/T_l , $\Delta T_x = T_x - T_g$ and $\gamma = T_x/(T_g + T_l)$. Comparison of the atomic structures with reported amorphous thickness and thermal stability parameters gives the following major results. Binary glasses show a strong preference for solute-to-solvent atomic radius ratios, R , that produce efficient local atomic packing, consistent with earlier results. Of the thirteen R values that provide efficient local atomic packing in metallic glasses, only five are commonly reported. Minimum and maximum solute atom fractions, F_α , are predicted as a function of R from structural considerations, including the minimum needed to fill cluster-forming α solute sites and the maximum based on an iso-structural condition. With only one exception, all of the binary glass alloys fall within these bounds, which cover a broad range of compositions and relative atom sizes. A more limited range of structural topologies is displayed by the most stable binary metallic glasses. These include glasses with $\Delta T_x > 20$ K and

* Corresponding author, daniel.miracle@wpafb.af.mil

** part-time employee at WPI AIMR

Corresponding Author:

Dr. Daniel B. Miracle
Air Force Research Laboratory, 2230 Tenth Street
Wright-Patterson AFB, OH 45433-7817 USA
Email: Daniel.miracle@wpafb.af.mil

the binary bulk metallic glasses (BMGs), with unusual glass-forming ability and a reported thickness of at least 1 mm, found in the Ca-Al, Cu-Hf, Cu-Zr, Hf-Cu, Ni-Nb and Zr-Cu systems. These glasses have R values near 0.710, 0.799, 1.116 or 1.248 that produce structure-forming solute-centered clusters with $\langle 9 \rangle$, $\langle 10 \rangle$, $\langle 15 \rangle$ and $\langle 17 \rangle$ solvent atom sites as nearest neighbors, respectively. The most stable binary glasses are also always solute-rich, representing solute atom fractions that depend on R and range from $0.33 \leq F_\alpha \leq 0.64$ for $R = 0.617$ to $0.17 \leq F_\alpha \leq 0.39$ for $R = 1.433$. This provides enough solute atoms, α , to fill all of the α , β and γ solute sites and roughly 1/3 of the Ω (solvent) sites in the ECP structural model. This suggests that α_Ω anti-site defects, where α solutes occupy Ω sites, are important in the glass-forming ability of the most stable glasses. This stabilizing effect results from an increase in the number of more stable α - Ω bonds, and by producing topologies that enable efficient global atomic packing. A major conclusion of this study is that the best metallic glasses satisfy both the R and solute-rich criteria simultaneously, providing a useful predictive tool for the exploration and discovery of new binary BMGs. The most stable metallic glasses also have absolute differences in solvent and solute bulk moduli $|B_\Omega - B_\alpha|$ less than 60 GPa, and have absolute differences in solvent and solute Pauling electronegativities $|\chi_\Omega - \chi_\alpha|$ equal to ~ 0.3 or ~ 0.6 . The structural parameters studied here show no systematic influence on the thermal stability parameters T_{rg} , T_x/T_l , ΔT_x or γ .

Keywords: metallic glass, atomic structure, topology, stability

1. Introduction

It has long been suggested that metallic glass stability and glass-forming ability (GFA) are influenced by atomic structure, but it has been difficult to systematically explore this idea until recently. The efficient cluster packing (ECP) model gives a simple approach to specify and characterize metallic glass structures [1, 2]. From this model, metallic glass structures can be constructed from topology alone (the relative sizes and numbers of constituent atoms). The ECP model shows that metallic glass structures are comprised of a solvent atom and one to three solute species of different sizes which are taken from 11 available atomic sizes that give efficient local atomic packing. Considering the distinct number of ways that the different structural sites can be filled by the available atom sizes, and from the type of defect states that can exist, 276 topologically unique atomic structures have been outlined for metallic glasses [2]. Aside from the expectation that structures with higher global packing efficiency may give more stable glasses, there is no fundamental basis for predicting stability from topology alone. It is thus not known if some of these 276 structures are intrinsically more stable than others, or if all provide a roughly equal topological contribution to metallic glass stability.

Using an ECP analysis, the structural topology can be obtained from the alloy specification, which gives the constituent atom species (and hence atomic sizes) and their concentrations. As the alloy specification is given for essentially every glass reported in the literature, and since many thousands of distinct metallic glasses have been produced and reported in the past 48 years, an enormous amount of information is available from which structural topology can be assessed. The critical cooling rate needed to produce a fully amorphous product is a principal metric of GFA, but it is difficult to measure and is rarely reported. A more practical measure of GFA is the maximum amorphous thickness that can be produced, and this information can be taken from the literature to establish correlations between structural topology and GFA. Thermal stability can be represented by primary parameters such as glass transition temperature (T_g) and crystallization temperature (T_x), and by derived quantities such as reduced glass transition temperature ($T_{rg} =$

T_g/T_l , where T_l is the liquidus temperature), T_x/T_l , the temperature interval $\Delta T_x = T_x - T_g$, and $\gamma = T_x/(T_g + T_l)$ [3].

The goal of this assessment is to explore the influence of metallic glass structure and topology on GFA and thermal stability. To bound the problem to a workable subset and to simplify structural determination, the present work considers only binary metallic glasses. The data needed to explore correlations between atomic structure, GFA and metallic glass stability are collected from the literature. The ECP model is used to define the structural topology and defect state for each metallic glass in this assessment. Analysis of the topological characteristics and glass stability are conducted to identify relationships between these quantities. These relationships are used to develop more quantitative insights into the role of structure on the GFA and stability of metallic glasses.

2. Approach

2.1 Data collection

An extensive review of the literature was conducted to collect the data needed for binary metallic glasses. Only metallic glasses produced by quenching from the liquid are considered. Amorphous solids produced by techniques such as mechanical alloying, electro-deposition and vapor deposition are not included. Data retrieved from the literature include alloy specification, amorphous thickness and representative temperatures T_g , T_x , T_l . The compositions used in the present review are usually nominal compositions given by the pre-melting weight of the elements— measured compositions are rarely reported. Measured weight loss is sometimes given, and this data supports reporting compositions to 2 or 3 significant digits. Minority species picked up during processing may be present and may influence results, but such information is rarely available. Liquidus temperatures were taken from binary phase diagrams [4] where this value was not provided in the cited papers. Common thermal stability parameters derived from T_g , T_x and T_l were calculated, including T_{rg} , T_x/T_l , ΔT_x and γ . Atomic radii used here are based on a recent assessment [2], on published values [5-8] and on measured interatomic separations in

metallic glasses, and are given in [Table 1](#). The radii of several elements have been modified slightly from earlier assessments (see Section 4.8). The assessed precision is ± 6 pm. The elastic properties of the constituent elements are taken from [8] to explore the suggestion that this property may influence GFA [9], and Pauling electronegativities are taken from [8] to explore a possible correlation with GFA. Where available, additional structure-specific data such as density and partial coordination numbers are also tabulated from the cited literature. The collected data and the citations are compiled in [Table A1](#) of the Appendix.

2.2 Structural assessment

The solvent (Ω) and solute (α) species produce structure-forming clusters that consist of a central α site surrounded by Ω sites. These clusters are centered at positions in space that approximate to a cubic close-packed (ccp) lattice. Additional solute sites are formed in the structure, including β sites that are surrounded by an octahedron of these clusters and γ sites surrounded by a tetrahedron of clusters. In binary glasses, there are thus two species i (solvent atoms Ω and solute atoms α) and four sites j (Ω , α , β and γ). The number of structural sites can be counted in the ECP model, where \hat{S}_j is the total number of j sites per α site [1, 2]. By definition, $\hat{S}_\alpha = 1$. From ccp symmetry, there is 1 β site and 2 γ sites for every α site, so that $\hat{S}_\beta = 1$ and $\hat{S}_\gamma = 2$. Each α site in the structure creates \hat{S}_Ω Ω sites. The value of \hat{S}_Ω is given by the geometry of efficient local atomic packing around α sites, and depends only on the ratio $R = r_\alpha / r_\Omega$ between the solute radius, r_α , and solvent radius, r_Ω , as shown by equation 5 in [10]. The total number of structural sites is $\sum_j S = \sum_j \hat{S}_j = \hat{S}_\Omega + 4$ [2]. These relationships are illustrated in [Table 2](#).

Metallic glass structures are specified by the way in which the sites are occupied. For binary alloys, eight structural site occupancies, $S(i_j)$, give the number of j sites that are occupied by i species, normalized by the number of α sites in the structure ([Table 2](#)). Quantitative comparisons with structure-specific measurements [2] give no support for a structurally significant presence of solvent anti-site defects on solute sites, so that $S(\Omega_\alpha) = S(\Omega_\beta) = S(\Omega_\gamma) = 0$. The total number of Ω

atoms per α site in the structure, \bar{S}_Ω , is thus given by $S(\Omega_\Omega)$ (see [Table 2](#)). The $S(\alpha_j)$ values can be obtained from the metallic glass constitution by determining the total number of α atoms in the structure normalized by the number of α sites, \bar{S}_α . The atom fractions are given by

$$F_\alpha = \bar{S}_\alpha / (\bar{S}_\alpha + \bar{S}_\Omega) \quad 1a$$

$$F_\Omega = \bar{S}_\Omega / (\bar{S}_\alpha + \bar{S}_\Omega) \quad 1b$$

so that

$$F_\alpha / F_\Omega = \bar{S}_\alpha / \bar{S}_\Omega \quad 2$$

where F_i is the atom fraction of species i and \bar{S}_i is the total number of i atoms in the structure normalized by the number of α sites. As a basic identity from the discussion above, and assuming that all Ω sites are occupied

$$\hat{S}_\Omega = S(\Omega_\Omega) + S(\alpha_\Omega) \quad 3$$

Substituting $\bar{S}_\Omega = S(\Omega_\Omega)$ from above gives

$$\hat{S}_\Omega = \bar{S}_\Omega + S(\alpha_\Omega) \quad 4$$

Rearranging terms and combining with [Equation 2](#) gives the general result

$$\bar{S}_\alpha = (F_\alpha / F_\Omega) (\hat{S}_\Omega - S(\alpha_\Omega)) \quad 5$$

that depends only on metallic glass constitution (through the terms F_α and F_Ω), on geometry (through the term \hat{S}_Ω) and on the number of α atoms that occupy Ω sites. Specific solutions are developed below for [Equation 5](#) in solute-lean and solute-rich glasses.

In solute-lean glasses, the number of solute atoms is less than or equal to the number of solute sites, so that $\bar{S}_\alpha \leq 4$. Since α atoms fill solute sites before Ω sites [2], there are no solute anti-site defects on Ω sites in solute-lean glasses, and $S(\alpha_\Omega) = 0$. Inserting this in [Equation 5](#) gives the final result for solute-lean glasses

$$\bar{S}_\alpha = (F_\alpha / F_\Omega) \hat{S}_\Omega \quad 6$$

An important number of solute sites will be vacant when $\bar{S}_\alpha < 4$, so that $S(\alpha_\alpha)$, $S(\alpha_\beta)$ and $S(\alpha_\gamma)$ may be less than the maximum values. Solute-rich glasses have all solute sites occupied by α and enough extra to occupy some Ω sites, forming α_Ω anti-site defects. Since there are four solute sites per α site

$$\bar{S}_\alpha = S(\alpha_\Omega) + 4 \quad 7$$

Rearranging terms and substituting in Equation 5 gives

$$\bar{S}_\alpha = F_\alpha / F_\Omega (\bar{S}_\Omega - \bar{S}_\alpha + 4) \quad 8$$

Collecting \bar{S}_α terms and simplifying gives the final result for solute-rich glasses

$$\bar{S}_\alpha = F_\alpha (\bar{S}_\Omega + 4) \quad 9$$

\bar{S}_α is thus given by Equation 6 if $F_\alpha / F_\Omega (\bar{S}_\Omega + 4) \leq 4$, otherwise it is given by Equation 9. $S(\alpha_j)$ values are determined from \bar{S}_α by filling α solute sites first (to the maximum value of $S(\alpha_\alpha) = 1$), then β sites (to the maximum value of $S(\alpha_\beta) = 1$) then γ (to the maximum value of $S(\alpha_\gamma) = 2$) and finally Ω sites, until $S(\alpha_\alpha) + S(\alpha_\beta) + S(\alpha_\gamma) + S(\alpha_\Omega) = \bar{S}_\alpha$ and the solutes are all accounted for. $S(\Omega_\Omega)$ is determined from Equation 3 once $S(\alpha_\Omega)$ is known.

Normally, solute and solvent elements are taken to be the minority and majority species, respectively. However, this definition becomes ambiguous near the equiatomic composition, especially when the solute and solvent species are different sizes. For example, when $R = 0.80$, each α site is at the center of an efficiently-packed cluster with 10 Ω atoms in the first coordination shell, so that each α site in the structure produces 10 Ω sites. When all of the α sites are filled by α , $F_\alpha = 1/11 = 0.091$; when all of the α and β sites are filled by α the solute atom fraction is $F_\alpha = 2/12 = 0.167$; and when all of the α , β and γ sites are filled by α the solute atom fraction is $F_\alpha = 4/14 = 0.286$. This structure represents many transition metal-metalloid binary glasses such as Co-P and Pd-Si, and also metal-metal glasses such as Zr-Cu and Zr-Ni. Now consider a glass where α is larger than Ω . For example, $R = 1.25$ in Al-Y and Cu-Zr glasses, where each α site now produces 17 Ω sites. In this glass, all of the α sites are occupied when $F_\alpha = 1/18 = 0.056$; all of the α and β sites are occupied when $F_\alpha = 2/19 = 0.105$; and all of the α , β and γ sites are occupied when $F_\alpha = 4/21 = 0.190$. From a structural perspective, larger solutes are thus more potent, since they produce more Ω sites than do smaller solutes.

If we continue to add Cu solutes to the Zr-Cu glasses described above, and we continue to add Zr solutes to the Cu-Zr glasses, we can imagine that an iso-structural condition will eventually be produced. We define the iso-structural condition as the singular structure where the

same structural description is obtained regardless of which atom is used as the solute and which is the solvent. This will occur at the equi-atomic composition when the two atoms are the same size, but it will occur at a different composition in structures with non-equal spheres, since different sized atoms have different structural potency.

The concept of inverse structures is introduced here to give a rigorous, structure-specific definition for solvent and solute species in binary structures with different atom sizes. Consider a glass with solute and solvent radii r_α and r_Ω . \hat{S}_Ω and other structural parameters are defined using $R = r_\alpha/r_\Omega$ and atom fractions F_α and F_Ω as described earlier. An inverse structure can also be described for the same glass, using $R^I = r_\Omega/r_\alpha$, $F_\alpha^I = F_\Omega$ and $F_\Omega^I = F_\alpha$. In this way, the solute of a normal structure is the solvent in the inverse structure. The iso-structural condition is defined when the total number of solute atoms per solute site in the normal structure equals the total number of solute atoms per solute site in the inverse structure, $\bar{S}_\alpha = \bar{S}_\alpha^I$. This always occurs for solute-rich glasses, so using Equation 9 and the relation $F_\alpha^I = F_\Omega = 1 - F_\alpha$ gives

$$F_\alpha \left(\hat{S}_\Omega + 4 \right) = (1 - F_\alpha) \left(\hat{S}_\Omega^I + 4 \right) \quad 10$$

Rearranging terms gives the α atom fraction at which the iso-structural condition is met

$$F_\alpha^{iso} = \frac{\hat{S}_\Omega^I + 4}{\hat{S}_\Omega + \hat{S}_\Omega^I + 8} \quad 11$$

From Equation 11, $F_\alpha^{iso} = 0.5$ only when $\hat{S}_\Omega = \hat{S}_\Omega^I$, and this occurs only when $R = R^I = 1$. When $R < 1$, $\hat{S}_\Omega < \hat{S}_\Omega^I$ and $F_\alpha^{iso} > 0.5$, and when $R > 1$, then $\hat{S}_\Omega > \hat{S}_\Omega^I$ and $F_\alpha^{iso} < 0.5$. In the present analysis, structural parameters are determined for both cases: when the α constituent is taken as the smaller atomic species ($R < 1$) and when the α constituent is taken as the larger atomic species ($R > 1$). The solute is defined as the species that gives the smaller value of \bar{S}_α . Throughout this work, the terms α and Ω are used to represent the solute and solvent species, respectively, as established by this criterion.

An adjustment is made in \hat{S}_Ω to account for a change in the number of structural sites that accompanies a significant number of α_Ω defects in solute-rich glasses. An effective solvent radius is given as

$$\tilde{r}_\Omega = r_\Omega \left[(\Omega_\Omega) / \hat{S}_\Omega \right] + r_\alpha \left[(\alpha_\Omega) / \hat{S}_\Omega \right] \quad 12$$

where r_i is the atom radius. Since \hat{S}_Ω depends on the effective solvent size, Equation 12 is solved iteratively. This correction applies only to solute-rich glasses, or about 40% of the alloys in this study. The average adjustment to \hat{S}_Ω is less than 5%, and is never more than 15%. Throughout this work, the term \hat{S}_Ω is understood to incorporate this correction.

This structural analysis has been applied to all of the binary metallic glass alloys in this assessment. The glass constitutions are given as solute and solvent species and solute atom fractions, F_α . The structural parameters include the nominal radius ratio R , the effective radius ratio $\tilde{R} = r_\alpha / \tilde{r}_\Omega$, \hat{S}_Ω , \bar{S}_α , \bar{S}_Ω and $S(i_j)$ values. These data are included in Table A1 of the Appendix.

3. Results

The elements found in binary metallic glasses are presented in Section 3.1, followed by the phenomenological correlations between the measured amorphous thickness and the resulting thermal stability parameters (Section 3.2). The remainder of the results is devoted to establishing the influence of atomic structure (Sections 3.3 through 3.5) and physical properties of the constituent elements (Sections 3.6 and 3.7) on the thermal stability and thickness of binary metallic glasses.

3.1 Elements found in binary metallic glasses

A total of 619 distinct metallic glass alloy compositions are identified from 162 different binary systems (Table A1). An A-B glass system is counted separately from the B-A glass system in the present study, since they are topologically distinct and are separated by the iso-structural condition defined by the composition in Equation 11. Forty-one elements are solvents and 49 elements are solutes, representing a total of 56 different elements (Figure 1). Solute or solvents are taken from alkaline earth metals, early and late transition metals, lanthanides and actinide elements. Other metal elements include Al, Ga, Sn and Pb. Nearly all of the metalloids, including B, Si, Ge, As, Sb and Te, and nearly half of the non-metals, including C, N and P, are

constituents of binary metallic glasses. Binary metallic glasses containing alkali metals, inert gas and halogen elements were not found in this assessment. Most metallic elements have been used to produce binary metallic glasses, and the number of binary glass systems contained in this assessment represents over 5% of the binary systems possible from the 56 elements represented. While metallic glasses are unusual, it is no longer true that they are rare.

Figure 1 near here.

3.2 Influence of thermal parameters on GFA

While binary glasses generally have poor GFA, sixteen binary bulk metallic glass (BMG) alloys, defined as glasses that can be produced by melt quenching to thicknesses ≥ 1 mm, are reported in six binary systems (Table A2). With the exception of the Ca-Al BMG, the binary BMGs are pairs of early and late transition metals. These include the inverse glass-forming pairs of Cu-Hf and Hf-Cu, and of Cu-Zr and Zr-Cu. Only single compositions are reported for Ca-Al and Hf-Cu BMGs, but the remaining four BMG systems cover F_α ranges of 0.02 to 0.05. These BMGs allow analysis of relationships between the maximum reported amorphous thickness and thermal stability parameters such as T_{rg} , ΔT_x , T_x/T_l and γ . Correlations between thickness and these thermal stability parameters are shown in Figure 2. Binary BMGs require minimum values of approximately 0.55 for T_{rg} ; 0.59 for T_x/T_l ; 0.38 for γ ; or 10 K for ΔT_x . Once these minimum values are achieved, there seems to be no systematic increase in amorphous thickness with increasing thermal stability.

Figure 2 near here.

In addition to relationships between thickness and derived thermal stability parameters, correlations may also exist between thickness and the basic thermal quantities T_l , T_x and T_g . Figure 3 shows the GFA, represented by the reported amorphous thickness, and derived thermal stability parameters plotted against these three basic thermal parameters. A wide range in

temperatures is reported for binary metallic glasses. The most stable glasses tend toward the lower half of the temperature range found for T_l (Figure 3a) and the upper half of the temperature range for T_g (Figure 3c). Once again, the small number of relatively stable binary metallic glasses makes an unambiguous determination of these trends difficult.

Figure 3 near here.

3.3 Solute atom fraction and solute-to-solvent radius ratio in binary metallic glasses

The two principal topological parameters in binary metallic glass structures are the relative size and relative number of Ω and α atoms. These parameters are plotted in Figure 4, where the relative number of atoms is given by the solute atom fraction, F_α . The vertical bars indicate a range in reported compositions for a given binary glass system. Radius ratios range from 0.609 to 1.456 (the value $R = 0.443$ for Gd-C is a singular exception that significantly extends the range of R values), and F_α ranges from 0.06 to 0.625. There are essentially no metallic glasses with $R \sim 1$ (Mg-Zr is the sole exception), in agreement with the long-held empirical observation that a radius ratio difference greater than 12% is needed for good GFA [11-15]. The dashed line in Figure 4 indicates the boundary between solute-lean and solute-rich glasses. Binary BMGs are indicated separately by filled symbols, and it is found that all binary BMGs are solute-rich. Structurally, these BMGs have no vacant solute sites and have significant numbers of solute anti-site defects. The solid line indicates the iso-structural composition as a function of R , and is the upper limit on F_α . With the exception of Ca-Al, binary BMGs tend toward the iso-structural composition. The dotted line represents the values of F_α needed to satisfy the condition $\bar{S}_\alpha = 1$, proposed here as the minimum solute atom fraction needed to form a metallic glass by liquid quenching (see Section 3.5)

Figure 4 near here.

A histogram of the relative atomic sizes of Ω and α in binary metallic glass systems is shown in Figure 5. The nominal radius ratio, $R = r_\alpha / r_\Omega$, from each of the 162 binary glass systems is placed in a bin with an interval between R and $R+0.02$. The vertical bars in this figure give the total number of systems where R falls within the indicated interval. The values from all of the vertical bars in Figure 5 sum to 179, as the Gd-C system occurs at a value of R much lower than the range included in this figure. A clear preference for specific radius ratios is shown, consistent with earlier work [10]. The specific radius ratios, R^* , needed to give efficient local atomic packing of Z solvent atoms around a central α solute (Table 3) are indicated by the vertical lines in Figure 5. Metallic glasses most commonly have a radius ratio near $R^*=0.799$, indicating a structure that is comprised of solute-centered atomic clusters with $Z=10$ and designated as a $\langle 10 \rangle$ glass [1]. Additional significant peaks are shown at $R^*=0.710$, $R^*=0.902$, $R^*=1.116$ and $R^*=1.248$ representing $\langle 9 \rangle$, $\langle 12 \rangle$, $\langle 15 \rangle$ and $\langle 17 \rangle$ structures, respectively. Far fewer glasses have radius ratios near $R^*=0.617$, $R^*=1.311$ and $R^*=1.433$. An insignificant number of $\langle 6 \rangle$, $\langle 7 \rangle$, $\langle 13 \rangle$, $\langle 14 \rangle$, $\langle 16 \rangle$ and $\langle 19 \rangle$ binary metallic glasses have been reported. Four of the 6 binary BMG systems have R near $R^*=0.799$ or $R^*=1.248$, and the remaining 2 have R near 0.710 and 1.116. This dataset suggests that GFA is best for $\langle 9 \rangle$, $\langle 10 \rangle$, $\langle 12 \rangle$, $\langle 15 \rangle$ and $\langle 17 \rangle$ glasses.

Figure 5 near here.

Additional trends are highlighted by replotting the data of Figure 5 to count the number of glasses within an increment $R+\Delta R$ and an increment $F_\alpha+\Delta F_\alpha$. The Kriging gridding method [16], commonly used to convert irregularly-spaced data into contour and surface plots, was applied using an interval of 0.05 for both ΔR and ΔF_α with an overlap of 0.025. The integrated number of alloys per specified interval in R and F_α is shown in Figure 6. Glasses with $R \cong 0.799$ that span a composition interval from about $0.16 \leq F_\alpha \leq 0.24$ are most commonly reported. Glasses with $R \cong 1.25$ are the next most common within the composition range $0.09 \leq F_\alpha \leq 0.13$. Lesser peaks occur near $R = 0.67$ and $F_\alpha = 0.19$; $R = 0.73$ and $F_\alpha = 0.33$; $R = 0.79$ and $F_\alpha = 0.39$; $R = 0.81$ and $F_\alpha = 0.30$; and $R = 1.25$ and $F_\alpha = 0.37$.

Figure 6 near here.

3.4 Influence of solute-to-solvent radius ratio on GFA and stability

In the following series of plots, the GFA (represented throughout this work by the maximum reported fully amorphous thickness) and the glass stability (represented by the thermal parameters T_{rg} , T_x/T_l , ΔT_x and γ) are compared with metallic glass characteristics, emphasizing glass topology but also including physical characteristics. Figure 7 plots these parameters against R . Binary BMGs, where the thickness is ≥ 1 mm, occur near R^* values that suggest structure-forming clusters with Z of $\langle 9 \rangle$, $\langle 10 \rangle$, $\langle 15 \rangle$ and $\langle 17 \rangle$. A strong correlation is also seen for ΔT_x , where the highest reported values occur near $R^* = 0.799$ and $R^* = 1.248$, reinforcing the dominance of $\langle 10 \rangle$ and $\langle 17 \rangle$ structures. The values of T_{rg} span a range from 0.346 to 0.638, but show neither a strong correlation with specific values of R nor a systematic variation with R . The same is true for T_x/T_l , which ranges from 0.222 to 0.680, and for γ , which varies from 0.263 to 0.417. Linear regressions for these three parameters all have shallow slopes and correlation coefficients below 0.6. Similar trends are shown for other structural parameters that are explicit functions of R , such as the number of structural sites around each α site, \hat{S}_Ω , and the coordination number, Z , given by the closest integer to \hat{S}_Ω .

Figure 7 near here.

3.5 Influence of solute atom fraction on GFA and stability

There is only a weak dependence of T_{rg} , T_x/T_l and γ on F_α (Figure 8). While the slopes obtained by linear regression are slightly larger than for the comparison with R in Figure 7, they are still rather small and the correlation coefficient remains low, so that the natural scatter in the experimental data is likely to overcome the slight systematic variation in these terms with F_α . However, there is a strong influence of F_α on the maximum reported thickness and ΔT_x . All binary BMGs are solute-rich, so that the highest values of thickness and ΔT_x occur for glasses

where F_α is greater than 0.33 (Figures 4, 8). The boundary between solute-rich and solute-lean structures varies significantly with R (Figure 4), and so it is difficult to show the effect of this structural transition in Figure 8.

To illustrate the influence of the solute-lean to solute-rich structural transition, the stability parameters are shown against the number of α atoms per α site in the structure, \bar{S}_α in Figure 9. With Fe_{91}B_9 as the only exception, all of the glasses have $\bar{S}_\alpha \geq 1$. Since α atoms fill α sites first, this shows that the α sites are typically fully occupied by α atoms in binary metallic glasses. This validates a major earlier assumption of the ECP model, and underscores the dominant role of α -centered clusters in forming the structural scaffold for metallic glasses. Since there is 1 β site and 2 γ sites for each α site, the α , β and γ solute sites are all filled when $\bar{S}_\alpha = 4$, which defines the boundary between solute-lean structures with solute vacancies and solute-rich glasses with α_Ω solute anti-site defects. All binary BMGs have $\bar{S}_\alpha > 4$. The number of α_Ω defects produced when α atoms occupy Ω sites can be obtained by subtracting 4 from \bar{S}_α in Figure 9. Thus, the best binary glasses usually have from 2 to 4 α_Ω defects per α site. The GFA and stability parameters are plotted against the fraction of Ω sites occupied by α in Figure 10. Solute-lean glasses have a value of $S(\alpha_\Omega)/\hat{S}_\Omega = 0$ in this plot, and the best glasses have roughly between 20-40% of the Ω sites filled by α .

Figures 8-10 near here.

3.6 Influence of r_Ω , T_i , and constituent element elastic properties on GFA and stability

Topological and thermodynamic modeling of metallic glasses has predicted an increase in T_{rg} with increasing solvent atom radius, r_Ω , and/or solvent shear modulus, G_Ω ; with decreasing liquidus temperature, T_l ; with decreasing solute bulk modulus, B_α ; and with decreasing difference between Ω and α bulk moduli, $|B_\Omega - B_\alpha|$ [9]. In nominal agreement with these predictions, T_{rg} is seen to increase slightly with decreasing T_l (Figure 3a), with decreasing B_α (Figure 11) and with decreasing $|B_\Omega - B_\alpha|$ (Figure 12). The magnitude of the change in T_{rg} with

the indicated parameters is small, and linear regression gives a rather small fitting coefficient, from 0.28 to 0.47. Further consideration (Section 4.6) suggests that there is no significant effect of these parameters on T_{rg} . There is no apparent influence of r_{Ω} (Figure 13) or G_{Ω} (Figure 14) on T_{rg} . With the exception of T_l , these parameters show no significant effect on T_x/T_l and γ (Figures 11-14). Since these two parameters are inversely proportional to T_l , decreasing T_l leads to a slight increase in T_x/T_l and γ , as expected (Figure 3a).

These same physical characteristics exert a range of distinct influences on ΔT_x and GFA. As in the comparisons of Section 3.4 and Section 3.5, ΔT_x and GFA both follow the same trends. A clear threshold dependence is shown in Figure 12, where all of the most stable glasses have $|B_{\Omega} - B_{\alpha}|$ values less than 60 GPa. Although less clear, a similar trend is suggested for T_l (Figure 3a) and B_{α} (Figure 11), where the most stable binary glasses are found only for the lower half of the ranges in T_l and B_{α} values shown. There seems to be no influence of r_{Ω} (Figure 13) and G_{Ω} (Figure 14) on ΔT_x and GFA.

Figures 11-14 near here.

3.7 Influence of electronegativity on GFA and stability

A comparison is made between electronegativity, χ , of the constituent elements and the GFA and stability. The absolute value of the difference in Pauling electronegativity of the solvent and solute constituents is used here, $|\chi_{\Omega} - \chi_{\alpha}|$. Binary glasses with the best GFA have discrete electronegativity differences of either ~ 0.3 or ~ 0.6 (Figure 15). These small differences in electronegativity suggest a component of covalent bonding with a slightly polar nature between Ω and α , similar to the bonding in intermetallic systems such as Ni-Al, Co-Al, Mo-Si and Fe-C. The preference shown here for specific differences in electronegativities may be an artifact of the small number of binary BMG systems- only 4 distinct pairs of atom species are found in this assessment. More complicated electronegativity functions were also considered here, including

an averaged electronegativity weighted by the constituent atom fractions [17]. No correlations were found with these other electronegativity functions.

Figure 15 near here.

4. Discussion

4.1 Binary metallic glasses are simple proxies for the more expansive family of metallic glasses

Binary metallic glasses represent a broad and diverse category of relatively simple metallic glasses. They cover a wide range of elements that include most of the element types in the periodic table. A small number of relatively stable glasses is also found, whether measured by an amorphous thickness of more than 1 mm or by thermal stability parameters. These characteristics qualify binary metallic glasses as a simple proxy for the more expansive field of metallic glasses. As structural complexity is a hallmark of disordered solids, the relative simplicity of binary metallic glass structures and the relative ease of measuring structure-specific properties such as partial pair distribution functions recommend binary metallic glasses for more extensive characterization. There are surprisingly few studies that measure the influence of glass composition on structure-specific properties. The influence of systematic changes in binary composition on density, partial coordination numbers and free volume (via indentation, relaxation or positron annihilation) are expected to significantly clarify structural descriptions. Further insights may be available by coupling new experimental data with the structural analysis techniques developed here. Additional structural studies in binary glasses using techniques such as scanning tunneling microscopy and 3D atom probe are suggested for future work.

4.2 Thermal stability parameters give post-mortem correlations with GFA

The data here support the common view that GFA, as measured by the maximum amorphous thickness, depends upon thermal stability. However, once threshold values are achieved for the thermal stability parameters T_{rg} , T_x/T_l , ΔT_x and γ , the data show no further correlation ([Figure 2](#)

and Table A2). For example, a binary BMG is produced with a thickness of 2 mm when $T_{rg} = 0.556$, but increasing T_{rg} to 0.638 does not increase the maximum thickness produced. Further, thicknesses less than 2 mm and as low as $<100 \mu\text{m}$ are also produced over roughly the same range in T_{rg} . Reported thicknesses are typically not the maximum thickness possible for values less than about $100 \mu\text{m}$ in the binary glasses assessed here, and this may contribute to this poor correlation. The majority of literature data come from studies to discover new glass-forming compositions or to measure some property of the metallic glass. Processing techniques such as melt spinning and suction casting are often used, since they enable rapid production and require only a small amount of material. Thermal stability can be evaluated in glasses found in these studies, but significant extra material and effort is needed to define the maximum fully amorphous thickness possible. This extra work involves the systematic variation of process variables such as wheel speed in melt-spinning or mold size in casting. Such efforts are rarely reported for binary glasses. Given the possibility that glasses with a large ΔT_x may also be binary BMGs, casting studies to establish the maximum fully amorphous thickness of the glasses with large ΔT_x but small currently reported thicknesses are suggested. Also contributing to the lack of a systematic variation in GFA with thermal stability parameters may be the limited number of relatively stable binary BMGs. A critical evaluation similar to the analysis provided here of more complex metallic glasses, where BMGs are more common, may give additional insight and is suggested for future work.

The data in Figure 3 support the suggestion that the amorphous thickness in binary metallic glasses is maximized when threshold values of T_l and T_g are achieved. The temperatures proposed from these figures ($T_l < 1500 \text{ K}$ and $T_g > 600 \text{ K}$) are broadly consistent with the expectation that T_{rg} is maximized for BMGs.

4.3 Atomic structure gives predictive correlation with GFA: Radius ratios

Relationships between thermal stability parameters and GFA are satisfying from a scientific standpoint, as they validate insights into the physics underlying glass formation. However, they

lack practical appeal since they do not provide a predictive capability, as the glass must first be produced to generate the thermal stability parameters. However, the results here show clear correlations between GFA and structural parameters. These correlations give an important predictive capability, since the structure can be described from only atom sizes (which are readily available) and concentrations (which can be independently specified). The solute-to-solvent radius ratio, R , is one of single best structural parameters to predict the occurrence, GFA and thermal stability of binary metallic glasses. Of the 15 specific radius ratios necessary for efficient local atomic packing, only 5 are commonly observed in metallic glasses, and only 4 produce the most stable glasses. Metallic glasses with R required for <9>, <10>, <12>, <15> and <17> structures are commonly reported; <8>, <18> and <20> structures are uncommon; and <6>, <7>, <13>, <14>, <16> and <19> structures are rare or not reported (Table 3). The best GFA is achieved for <9> structures with $R \sim 0.710$, for <10> structures with $R \sim 0.799$, for <15> structures with $R \sim 1.116$ and for <17> structures with $R \sim 1.248$. Essentially no <13> or <14> glasses were found in this assessment, confirming the empirical rule that a significant size difference is needed between solute and solvent species to form metallic glasses. A more mechanistic understanding is given by the elastic strain [12] or strain energy [18] needed to destabilize competing crystalline structures. The rarity of <6>, <7>, <16> and <19> glasses is surprising, and there is no explanation at present for this observation.

4.4 Atomic structure gives predictive correlation with GFA: Atom fraction

The structural perspective developed here gives minimum and maximum values of F_α required for metallic glasses (Figure 4). With only one exception, all of the 619 binary metallic glasses fall within these bounds. While the bounds on F_α substantiate this structural perspective, it does not provide a compelling aid in the exploration and development of metallic glasses, as a wide range of compositions are included. However, the observation that all of the most stable binary metallic glasses are solute-rich and generally approach the iso-structural condition is a major insight that gives a useful predictive tool for the development of BMGs. This finding has

direct structural implications that include the suggestion that metallic glass stability is diminished by solvent anti-site defects on solute sites, Ω_{solute} , and by solute vacancies, V_{solute} . Ω_{solute} defects are expected to dominate in solvent-rich glasses, where there are insufficient solute atoms to fill solute sites. The data in [Figures 4 and 9](#) show that metallic glasses are formed only when F_{α} is sufficient to fill at least all the α sites. While it is possible that these same compositions could be produced by structures where solute sites are filled both by α and by Ω , thus producing Ω_{solute} defects, there is no data supporting the presence of Ω_{solute} defects. Further, these defects would produce inefficient local atomic packing that is inconsistent with the basic principle of the efficient filling of space that dominates the occurrence of metallic glasses. While Ω_{solute} defects are not expected to be structurally significant for the reasons discussed here, they may nevertheless occur as thermally-induced defects in small concentrations.

Although metallic glasses are often produced with V_{solute} defects, they do not exist in any binary BMG or in glasses with ΔT_x larger than 20 K ([Figure 9](#)). Qualitatively, the reason that the most stable glasses do not have V_{solute} defects can be understood from the energy penalty (the PdV term of Gibbs free energy, where P is pressure and V is volume) paid by a condensed solid for free volume— ‘free’ volume isn’t free. Even though vacancy defects in metallic glasses consist of many unoccupied spaces that are small fractions of an atomic volume which are locally distributed about a vacancy site [2], the energy penalty is nevertheless expected to be significant. The free volume provided by vacancies also increases atom mobility, which further degrades the stability of metallic glasses.

In addition to the destabilizing effect of Ω_{solute} and V_{solute} defects, the preference for solute-rich glasses suggests a stabilizing influence of solutes on β , γ and Ω sites may also exist. β and γ sites are surrounded by Ω atoms from the 1st shells of the bounding α clusters, so that roughly \hat{S}_{Ω} new Ω – α bonds are formed for every α atom that occupies a β or γ site (β_{α} and γ_{α} defects). Although the actual magnitudes of atomic bond energies are not known in condensed solids, application of the regular solution model [19] suggests that α – Ω bonds are more stable than the weighted average of α – α and Ω – Ω bonds in metallic glasses, so that solute occupancy of β and γ

sites increases metallic glass stability. A qualitative thermodynamic argument gives a simple basis for the observation shown here that the most stable glasses have roughly between 20-40% of the Ω sites filled by α . Each α_Ω defect replaces an Ω atom in the 1st shell of an α -centered cluster with an α atom. Considering only bonds within this cluster, removing the Ω atom breaks one α - Ω bond with the central solute atom and 4 or 5 Ω - Ω bonds within the first coordination shell, and placing an α atom on this site forms one α - α bond and 4 or 5 α - Ω bonds. It is quite likely that α_Ω defects thus give an enthalpic bond energy term that helps stabilize metallic glasses. Considering efficiently-packed clusters with coordination numbers $8 \leq Z \leq 20$ [20], it can be shown empirically that no more than about 1/3 of the Ω sites in the 1st coordination shell can be replaced by α before α - α contacts are introduced in the 1st shell. Beyond this fraction, the number of new α - α contacts increases rapidly and the number of new α - Ω bonds decreases. The finding in this assessment that no more than about 1/3 of the Ω sites are occupied by α (Figure 10) is in broad agreement with this qualitative enthalpic argument. Of course, α_Ω defects are also likely to give an entropic term that stabilizes solute-rich glasses.

4.5 Influence of atomic structure on thermal stability

The linear regression for T_{rg} in Figures 7-9 suggests a weak structural dependence, but this approach gives equal weight to each datapoint regardless of GFA. T_{rg} is clearly seen to be independent of R when only T_{rg} values from binary BMGs are considered, as shown by the regression line in Figure 7. T_{rg} values below this upper bound represent alloys with poorer GFA. The present work shows that all binary BMG structures simultaneously have both a discrete value of R that enables efficient local atomic packing, and a solute-rich composition that fills α , β , and γ sites and roughly 1/3 of the Ω sites. For a glass structure that satisfies the R criterion, poorer GFA and lower T_{rg} values can result when F_α is insufficient for BMG formation. This can be illustrated by data from Zr-Cu glasses (Table A1). Zr-Cu BMGs have F_{Cu} values that range from 0.45 to 0.50 and T_{rg} values that range from 0.552 to 0.585, while Zr-Cu glasses with lower F_{Cu} , but the same value of R , do not form BMGs and have T_{rg} values that range from 0.496 to

0.542. Chemical considerations may also contribute to poorer GFA and lower T_{rg} , as similar R values can be obtained for chemically distinct alloys. The same results extend to the influence of R on T_x/T_l and γ (Figure 7), and to the impact of solute atom fraction on T_{rg} , T_x/T_l and γ (Figures 8-10). Careful consideration of the data in Figures 7-10 thus shows no influence of structure on T_{rg} , T_x/T_l , or γ .

Values of ΔT_x appear to correlate strongly with structure, and seem to follow the same trends as GFA (Figure 3a and Figures 7-15). This apparent difference results from the expanded numerical scale and from the greater degree of variability in ΔT_x relative to the other stability parameters. Compressing ΔT_x data to the same vertical scale as for T_{rg} , T_x/T_l and γ shows that the same structural independence is observed for ΔT_x . As mentioned in Section 3.2, the limited ΔT_x dataset is also an important factor contributing to the lack of a compelling correlation. Critical analysis of the structural influence in more complex glasses is suggested, where many more BMGs exist.

4.6 Other predictive correlations and interrelationships between GFA and thermal stability

A weak systematic influence of B_α and $|B_\Omega - B_\alpha|$ on T_{rg} is suggested by Figures 11 and 12. However, applying the approach described in the previous section of considering only T_{rg} values from binary BMGs shows that there is no significant influence. This same data shows a clear partitioning of the most stable glasses— BMGs and glasses with large values of ΔT_x — to the lowest values of $|B_\Omega - B_\alpha|$. The effect of $|B_\Omega - B_\alpha|$ on GFA and on ΔT_x (Figure 12) is a new result that validates a prediction from earlier thermodynamic modeling [9]. There is presently no physical basis for explaining the apparent preferred discrete values of $|\chi_\Omega - \chi_\alpha|$ in the most stable binary glasses, and this observation may result from the rather small number of relatively stable binary alloy systems.

The maximum global atomic packing fraction is expected to be a key topological parameter in the stability of metallic glass structures, but there are very few approaches for predicting the packing fraction in binary systems of spheres. Developed for the packing of ceramic particles,

and based on the filling of interstices between larger particles by much smaller particles, the Furnas model [21-23] has been extended empirically to the packing of binary systems of spheres with R ranging from 0.1 to 0.5 [24]. A shallow maximum in the packing fraction is observed in these systems at a volume fraction of smaller particles, X_f , of 0.37 ± 0.10 . Although the applicability of the concept of smaller spheres filling the interstices of larger spheres diminishes with decreasing difference in size, the efficient packing of larger spheres around a smaller sphere, directed by volume minimization and by chemical interactions, suggests that this approach may give useful insights into atomic packing in metallic glasses. Converting X_f to F_α for glasses with $0.6 \leq R \leq 0.9$, and truncating F_α at the iso-structure composition, F_α^{iso} , the F_α range over which maximal global packing is expected is shown as a function of R by the cross-hatched regions in [Figure 4](#). The predicted solute atom fractions are all solute rich and reach the iso-structural composition. Maximal global packing efficiency can be obtained for glasses with $0.6 \leq R \leq 0.9$, and the compositions predicted for $R \cong 0.8$ match surprisingly well the actual compositions for binary BMGs with <10> structures. Maximal packing efficiency is also predicted for $0.6 \leq R \leq 0.9$ when $F_\alpha > F_\alpha^{iso}$, where the inverse structure is the appropriate description of the glass structure. Applying the appropriate conversion for R and F_α (see Section 2.2), the current prediction shows that maximal global packing efficiency can also be achieved for $1.11 \leq R \leq 1.46$. Reasonable agreement is shown between the predicted and observed values of R and F_α for the binary BMGs with $R > 1$. The trend of achieving maximal global packing efficiency with solute-rich compositions, and the general agreement with selected BMG compositions is encouraging, but additional work is needed to develop more accurate models for predicting global packing efficiency in systems of binary spheres.

The ECP model provides an alternate approach for calculating packing fraction, but density estimates from the ECP model currently have errors as large as 40% [2]. This is insufficient for consideration as a topological criterion. Local topology as given by nearest-neighbor atomic coordination may also provide insights to stability. However, the equations for partial coordination numbers from the ECP model are valid over a restricted composition range that

currently doesn't include solute-rich glasses. Density and partial coordination numbers have direct structural implications, and refinements to the methods by they are calculated within the ECP model are needed to explore these parameters. Measurements of these properties are available in the literature, and have been included in [Table A1](#) for completeness.

The most compelling predictive correlations in this work are shown for the structural parameters R and \bar{S}_α (and the related terms F_α and $S(\alpha_\Omega)/\hat{S}_\Omega$), and for the physical parameters $|B_\Omega - B_\alpha|$ and $|\chi_\Omega - \chi_\alpha|$. It was suggested in Section 4.5 that it may be necessary for both R and \bar{S}_α to be satisfied simultaneously in the most stable binary glasses. Once the R criterion is met, the role of \bar{S}_α can be evaluated, since F_α can be changed while holding R constant, and without changing the chemical bonding between constituent elements. This analysis shows that \bar{S}_α is essential, since the excellent GFA of a binary BMG that satisfies the R criterion becomes dramatically degraded when F_α is reduced below a critical value. It is difficult to determine if R plays the same critical role, since it is not possible to fix F_α and vary R without also changing the constituent elements in the structure, and hence also changing the underlying chemical bonding between elements. However, since global packing efficiency cannot be accomplished without efficient local atomic packing, and since the R criterion provides efficient local atomic packing, then it is concluded that both R and F_α criteria must be met simultaneously to form the most stable metallic glasses. Since all of the most stable glasses in this assessment satisfy all four of the criteria above simultaneously, it is worth considering if all are necessary to form a BMG. It may be that only a subset of these four criteria is sufficient for BMG formation. It is also possible that there are other criteria which cannot yet be established with the data available. The limited number of binary BMGs makes a critical assessment of this issue difficult at present.

4.7 Inverse glass systems

Inverse glass systems are companion structures where the solute-to-solvent radius ratio, R , and the solvent-to-solute radius ratio, $1/R$, both match values required for efficient local atomic packing. The <10> and <17> structures are inverse systems, since <10> glasses have

$R_{10}^* = 0.799$ and $1/R_{10}^* = 1.252$, which almost exactly match the values $1/R_{17}^* = 0.801$ and $R_{17}^* = 1.248$ for <17> glasses. Only one other pair of structures, <12> glasses with $R_{12}^* = 0.902$ and $1/R_{12}^* = 1.109$ and <15> glasses with $R_{15}^* = 1.116$ and $1/R_{15}^* = 0.896$, match nearly as closely. None of the other structures have a topologically matched inverse system. Thus, the inverse of a <16> glass would have $1/R_{16}^* = 0.845$, which matches neither $R_{10}^* = 0.799$ nor $R_{12}^* = 0.902$ (R_{11}^* glasses are topologically unstable [1, 2]). Satisfying the R criterion enables efficient local atomic packing around solute atoms. As F_α increases beyond the iso-structural composition, then the solute species becomes the solvent and vice versa. Since BMGs tend toward the iso-structure composition, and since BMGs are likely to be distinguished as structures with maximal global packing efficiency (Section 4.6), then inverse structures may play an important consideration in BMG stability.

BMGs are obtained for both of the inverse glass systems Zr-Cu and Cu-Zr, as well as for Hf-Cu and Cu-Hf inverse systems. Not only do these represent the companion system pair with the best fit (<10> and <17>), but the actual radius ratios also most closely match the ideal radius ratios needed for efficient local atomic packing. Specifically, the actual R values for these four systems (Table A1) vary by less than 0.5% from the ideal R^* values for <10> and <17> structures. Ni-Nb binary BMGs could conceivably have a companion Nb-Ni inverse structure, since $1/R_{15}^* = 0.896$, which is very close to $R_{12}^* = 0.902$. The actual R values for these companion glasses (Table A1) deviate from the ideal values $R_{15}^* = 1.116$ and $R_{12}^* = 0.902$ by about 2%, and this may be a factor in the lack of a Nb-Ni binary BMG. Ca-Al glasses are not expected to have a companion inverse glass system, since $1/R_9^* = 1.408$, which is midway between the R needed for <19> and <20> glasses. However, the actual R for Ca-Al is 0.723, so that R for Al-Ca is 1.383 (Table A1). These are within about 1.2% of the ideal R values for <9> and <19> glasses. Although Al-Ca glasses exist, they are not reported to be BMGs (Table A1).

Using the binary Zr-Cu alloy system as an example, the relationships between inverse glasses are illustrated in Figure 16. The binary system is divided unambiguously by the iso-structure composition into Zr-Cu glasses and Cu-Zr glasses. The iso-structure composition is bounded by

solute-rich glasses on each side. Cu-rich Zr-Cu BMGs approach the iso-structure composition on one side, while Zr-rich Cu-Zr BMGs approach the iso-structure composition from the other. These two inverse glass systems are structurally distinct— one is a Zr-based glass with a <10> structure, and the other a Cu-based glass with a <17> structure. Only at the iso-structure composition can the glass be described equally well as a Cu-based or a Zr-based glass. The radius ratio criterion is satisfied for these inverse glasses across the full range of F_α . Both enthalpic (Section 4.4) and packing fraction (Section 4.6) contributions stabilize solute-rich glasses near the iso-structural composition. The composition of the boundary between solute-lean and solute rich glasses depends on R , and varies from $0.25 \leq F_\alpha \leq 0.33$ for $0.902 \leq R \leq 0.617$, and from $0.79 \leq F_\alpha \leq 0.83$ for $1.116 \leq R \leq 1.433$. As shown in Figure 4, the iso-structure composition varies from 0.53 for $R = 0.902$ to 0.63 for $R = 0.617$. The compositions shown in Figure 16 for the iso-structural composition and for the boundaries between solute-lean and solute-rich glasses are for glasses in the Zr-Cu binary system.

4.8 Reassessment of atomic radii

The good alignment of the present radius ratios with R^* values required for efficient local atomic packing improves on earlier results from a more limited dataset [10]. Only binary systems are counted here, rather than distinct alloy compositions, to avoid any bias introduced by more extensive characterization of some systems resulting from practical considerations such as the extent of the glass-forming region, the ease of GFA and the availability of constituent elements. The improved agreement here is achieved in part by a more detailed assessment of atomic radii. The values used here represent a small increase in the radius of B, r_B , (from 85 pm to 88 pm) and a decrease in r_{Ni} (from 128 pm to 126 pm) relative to earlier assessments. Previous r_{Ni} values were obtained from pure elements, and r_B was derived by difference from the measured Ni–B separation in $Ni_{81}B_{19}$ [[25]]. These earlier values gave $R = 0.664$, which was too small to give good agreement with the measured coordination number of Ni around B of 9.3. The approach used here acknowledges that atomic radii are slightly smaller for unlike atomic bonding. Thus, a

slightly smaller value of r_{Ni} is used, which gives a slightly larger value of r_B when determined by difference from the same Ni–B separation in $Ni_{81}B_{19}$. The new values used here give $R = 0.698$, in better agreement with the value of 0.710 required for an efficiently packed B-centered cluster with 9 Ni atoms in the first coordination shell. Radii used here for Fe, Rh, Ti, Nb, Au and Hf are reduced by 2 pm each, and r_{Ta} is reduced by 3 pm relative to earlier assessed values. Adjustments were also made to radii for Ba, Ca, Gd, Pt, Nd and Th. All of the modifications in this present assessment are within the stated precision of ± 6 pm.

5. Summary

Binary glasses are a large and diverse subset of metallic glasses, representing 56 different elements and most element types in the periodic table. Six hundred and thirty seven binary alloys are identified from 162 different binary systems. These 162 binary systems represent over 5% of the possible binary systems that can be produced from the 56 constituent elements, so that binary metallic glasses, although still uncommon, are not rare. Sixteen binary bulk metallic glass (BMG) alloys, being produced in the fully amorphous condition at thicknesses ≥ 1 mm, are found from 6 systems in this assessment: Ca-Al, Cu-Hf, Cu-Zr, Hf-Cu, Ni-Nb and Zr-Cu. The constitutional breadth, relative structural simplicity and availability of relatively stable alloys recommend binary glasses as convenient proxies for the broader family of more complex metallic glasses.

Metallic glasses are analyzed using the efficient cluster packing (ECP) model, which shows that binary structures consist of 2 species (solvent Ω and solute α) and 4 sites (Ω , α , and additional solute sites β and γ). An approach is developed for evaluating the 8 resulting site occupancy values that define the structural topology, using as input only the relative atomic sizes and atom fractions of the glasses. Other extensions of the ECP model developed here include definition of solute-lean glasses as structures with insufficient α atoms to fill all solute sites, and definition of solute-rich glasses as structures with enough α to fill all available solute sites and to form α_Ω anti-site defects comprised of solute atoms on Ω sites. A description of inverse

structures is developed, where the solute and solvent species of a normal structure are interchanged. This is used to define the iso-structure condition, which gives an unambiguous structure-based definition of solute and solvent species that is important for solute-rich glasses near the equiatomic composition.

Binary metallic glasses include solute-to-solvent radius ratios from $0.602 \leq R \leq 1.456$, (the single exception is Gd-C with $R = 0.443$) producing structure-forming, solute-centered clusters with coordination numbers from $7 \leq Z \leq 20$. Consistent with earlier work, a strong preference is shown for special radius ratios, R^* , that give efficient local atomic packing in the 1st coordination shell. This work shows that not all R^* values are equally effective in producing metallic glasses. Binary glasses are most commonly produced with radius ratios near $R^* \cong 0.799$ that give <10> structures, where efficiently packed clusters consisting of a central solute atom surrounded by ~10 solvent atoms form the structural scaffold. Other commonly observed structures include <9>, <12>, <15> and <17> glasses with radius ratios near 0.710, 0.902, 1.116 and 1.248, respectively. Binary glasses are formed less frequently with <8>, <18> and <20> structures, while glasses with R that give <7>, <13>, <14>, <16> and <19> structures are rare or not reported. Thus, only 5 of the 13 radius ratios for metallic glasses are common.

Solute atom fractions in binary metallic glasses range from $0.06 \leq F_\alpha \leq 0.625$. Rather than using a simple definition of solute species based on atom fraction alone, a structural definition is developed as an explicit function of R . Maximum values of F_α increase above 0.5 with decreasing R for $R < 1$ due to decreased structural potency of smaller solute atoms, and maximum values decrease from 0.5 with increasing R for $R > 1$. The minimum F_α values occur when α sites are fully occupied by α solutes, and an explicit structural dependence shows that the minimum F_α values decrease with increasing R . With only one exception, all of the 619 binary alloys cited here fall within the compositional bounds derived from these structural considerations. α sites are always occupied in binary glasses, but only by α atoms (the single exception is Fe₉₁B₉). Ω sites are always filled, either by Ω atoms or by α atoms, forming α_Ω anti-site defects. β and γ sites may be vacant or can be filled by α , but not by Ω . A significant number

of solute-lean glasses (with vacant β and/or γ sites) and a significant number of solute-rich glasses (with α_Ω anti-site defects) are shown in this analysis.

The criteria outlined above for R and F_α define the broad topological requirements for glass formation by liquid metal quenching. However, the most stable glasses have outstanding GFA and thermal stability, and satisfy a more restrictive set of conditions. These most stable glasses represent only 4 values of R^* , including 0.710 for <9> structures; 0.799 for <10> structures; 1.116 for <15> structures and 1.248 for <17> structures. Further, the most stable glasses are limited to solute-rich compositions that depend on R and range from $F_\alpha > 0.17$ for $R = 1.433$ to $F_\alpha > 0.33$ for $R = 0.617$. From a structural perspective, these glasses all have $\bar{S}_\alpha > 4$ and do not have vacancy defects on either Ω or α sites. Solute sites are all occupied by α , and a significant number of α_Ω defects occur. The stabilizing influence of α_Ω defects is suggested to result from a bond enthalpy term, whereby the number of more stable Ω – α bonds in the structure is increased relative to the number of less stable α – α and Ω – Ω bonds. Observed compositions are consistent with a structural argument that predicts that the maximum fraction of Ω sites that can be occupied by α is about 1/3 in the most stable metallic glasses. The R criterion enables efficient *local* atomic packing, while models for maximal *global* packing efficiency suggest that the R and F_α must be met simultaneously. In agreement with this, all of the most stable glasses in this assessment do satisfy both the R and F_α topological constraints simultaneously, representing a significant structural influence on GFA and stability. This finding gives a practically important predictive capability, as the most stable binary metallic glasses are restricted to a relatively narrow range of structural topologies.

In addition to the influence of R and the inter-related quantities F_α and \bar{S}_α , the present work also shows an influence of physical characteristics on GFA and thermal stability. The most stable glasses all have an absolute difference in constituent element bulk moduli of $|B_\Omega - B_\alpha| < 60$ GPa. The absolute difference in Pauling electronegativity of Ω and α atoms, $|\chi_\Omega - \chi_\alpha|$, also shows a good correlation with reported amorphous thickness and the thermal stability parameter, ΔT_x . All of the most stable glasses have $|\chi_\Omega - \chi_\alpha|$ equal to either ~ 0.3 or ~ 0.6 . The thermal stability

parameters T_{rg} , T_x/T_t , ΔT_x and γ do not show any systematic trends with the topological parameters studied here. Like structure, these relationships provide a predictive capability, as these features can be established before a glass is produced.

Additional work is suggested to solidify and extend the structural insights developed here. Very few studies of binary metallic glasses measure critical thickness, and this information is expected to improve the statistical validity of the correlations explored here. The measurement of structure-specific properties such as density and partial coordination numbers would also enhance structural understanding, especially if carried out in glasses where the constitution and structure are varied systematically. From the structural and analytical foundation provided here, a similar critical assessment of more complex glasses is recommended, where the number of relatively stable BMGs is significantly higher than for binary systems.

Acknowledgements

DBM thanks the Air Force Office of Scientific Research for funding during a sabbatical to the Institute of Materials Research, Tohoku University, Sendai, Japan. DL and LL acknowledge the Air Force Office of Scientific (Tokyo Office, Dr. J.P. Singh, Program Manager) for funding this effort. This work was also supported by the Research and Development Project on Advanced Metallic Glasses, Inorganic Materials and Joining Technology from MEXT, Japan.

References

- [1] D. B. Miracle, "A structural model for metallic glasses," *Nature Materials*, vol. 3, pp. 697-702, 2004.
- [2] D. B. Miracle, "The efficient cluster packing model- an atomic structural model for metallic glasses," *Acta Mater.*, vol. 54, pp. 4317-4336, 2006.
- [3] Z. P. Lu and C. T. Liu, "A new glass-forming ability criterion for bulk metallic glasses," *Acta Mater.*, vol. 50, pp. 3501-3512, 2002.
- [4] H. Okamoto, P. R. Subramanian, and L. Kacprzak, "Binary Alloy Phase Diagrams," T. B. Massalski, Ed., 2nd ed. Materials Park, OH USA: ASM, International, 1990.
- [5] E. Teatum, J. K. Gschneidner, and J. Waber, "Compilation of calculated data useful in predicting metallurgical behavior of the elements in binary alloy systems," Los Alamos National Laboratory, University of California, Los Alamos, New Mexico LA-2345, 1960.
- [6] J. C. Slater, "Atomic radii in crystals," *J. Chem. Phys.*, vol. 41, pp. 3199-3204, 1964.
- [7] C. H. MacGillavry and G. Reick, "Interatomic Distances in Metallic Crystals," in *International Tables for X-Ray Crystallography*, V. III Physical and Chemical Tables, K. Lonsdale, Ed., 2nd ed. Dordrecht, Holland: Kluwer Academic Publishers, 1985, pp. 277-285.
- [8] M. Winter, "WebElements: the periodic table on the WWW," vol. 2007: The University of Sheffield and WebElements Ltd, UK, 2008.
- [9] O. N. Senkov, D. B. Miracle, and H. M. Mullens, "Topological criteria for amorphization based on a thermodynamic approach," *J. Appl. Phys.*, vol. 97, pp. 103502, 2005.
- [10] D. B. Miracle, W. S. Sanders, and O. N. Senkov, "The influence of efficient atomic packing on the constitution of metallic glasses," *Phil. Mag. A*, vol. 83, pp. 2409-2428, 2003.
- [11] D. E. Polk and B. C. Giesen, "Metallic Glasses," 1978.
- [12] T. Egami and Y. Waseda, "Atomic size effect on the formability of metallic glasses," *J. Non-Cryst. Sol.*, vol. 64, pp. 113-134, 1984.
- [13] L. Battezzati and M. Baricco, "An analysis of volume effects in metallic glass formation," *J. Less Common Metals*, vol. 145, pp. 31-38, 1988.
- [14] R. W. Cahn, "Metallic Glasses," in *Materials Science and Technology*, vol. Vol. 9 Glasses and Amorphous Materials, J. Zarzycki, Ed. Cambridge, UK: VCH, 1991, pp. 493-548.
- [15] A. Inoue, "Bulk amorphous alloys with soft and hard magnetic properties," *Mat. Sci. Eng.*, vol. A226-228, pp. 357-363, 1997.
- [16] G. Matheron, "Principles of geostatistics," *Economic Geology*, vol. 58, pp. 1246-1266, 1963.
- [17] Z. P. Lu, C. T. Liu, and Y. D. Dong, "Effects of atomic bonding nature and size mismatch on thermal stability and glass-forming ability of bulk metallic glasses," *J. Non-Cryst. Sol.*, vol. 341, pp. 93-100, 2004.
- [18] D. B. Miracle and O. N. Senkov, "Topological criterion for metallic glass formation," *Mat. Sci. Eng.*, vol. A347, pp. 50-58, 2003.

- [19] D. R. Gaskell, *Introduction to the Thermodynamics of Materials*, 3rd ed. Washington, DC USA: Taylor & Francis, 1995.
- [20] D. B. Miracle, E. A. Lord, and S. Ranganathan, "Candidate atomic cluster configurations in metallic glass structures," *Trans. JIM*, vol. 47, pp. 1737-1742, 2006.
- [21] C. C. Furnas, "The relations between specific volume voids, and size composition in systems of broken solids of mixed size," *Report of Investigations*, vol. No. 2894, 1928.
- [22] C. C. Furnas, "Grading Aggregates, I- mathematical relations for beds of broken solids of maximum density," *Industrial and Engr. Chem.*, vol. 23, pp. 1052-1058, 1931.
- [23] F. O. Anderegg, "Grading Aggregates II- The application of mathematical formulas to mortars," *Industrial and Engr. Chem.*, vol. 23, pp. 1058-1064, 1931.
- [24] J. Zheng, W. B. Carlson, and J. S. Reed, "The Packing Density of Binary Powder Mixtures," *J. European Cer. Soc.*, vol. 15, pp. 479-483, 1995.
- [25] P. Lamparter, W. Sperl, S. Steeb, and J. Bletry, "Atomic structure of amorphous metallic $\text{Ni}_{81}\text{B}_{19}$," *Z. Naturforsch.*, vol. 37a, pp. 1223-1234, 1982.
- [26] A. Inoue, N. Nishiyama, K. Hatakeyama, and T. Masumoto, "New amorphous alloys in Al-Ca and Al-Ca-M (M=Mg or Zn) systems," *Mater. Trans. JIM*, vol. 35, pp. 282-285, 1994.
- [27] A. Inoue, K. Ohtera, A. P. Tsai, H. Kimura, and T. Masumoto, "Glass transition behavior of Al-Y-Ni and Al-Ce-Ni amorphous alloys," *Japanese Journal of Applied Physics*, vol. 27, pp. L1579-L1582, 1988.
- [28] H. A. Davies and J. B. Hull, "Some aspects of splat-quenching in an inert atmosphere and of the formation of non-crystalline phases in Al-17.3 at. % Cu, germanium and tellurium," *J. Mat. Sci.*, vol. 9, pp. 707-717, 1974.
- [29] A. Inoue, T. Zhang, K. Kita, and T. Masumoto, "Mechanical strengths, thermal stability and electrical resistivity of aluminum-rare earth metal binary amorphous alloys," *Mat. Trans. JIM*, vol. 30, pp. 870-877, 1989.
- [30] A. Inoue and T. Masumoto, "New amorphous alloys with significant supercooled liquid region and large reduced glass transition temperature," *Mat. Sci. Eng.*, vol. A134, pp. 1125-1128, 1991.
- [31] A. Inoue, H. Yamaguchi, T. Zhang, and T. Masumoto, "Al-La-Cu amorphous alloys with a wide supercooled liquid region," *Mat. Trans. JIM*, vol. 31, pp. 104-109, 1990.
- [32] A. Inoue, T. Ochiai, Y. Horio, and T. Masumoto, "Formation and mechanical properties of amorphous Al-Ni-Nd alloys," *Mat. Sci. Eng.*, vol. A179/A 180, pp. 649-653, 1994.
- [33] J. H. Perepezko, R. J. Hebert, and G. Wilde, "Synthesis of nanostructures from amorphous and crystalline phases," *Mat. Sci. Eng.*, vol. A 375-377, pp. 171-177, 2004.
- [34] E. Matsubara, Y. Waseda, A. Inoue, H. Ohtera, and T. Masumoto, "Anomalous X-ray Scattering on Amorphous $\text{Al}_{87}\text{Y}_8\text{Ni}_5$ and $\text{Al}_{90}\text{Y}_{10}$ Alloys," *Z. Naturforsch.*, vol. 44a, pp. 814-820, 1989.
- [35] P. Predecki, B. C. Giessen, and N. J. Grant, "New metastable alloy phases of gold, silver, and aluminium," *Trans. Metall. Soc. AIME*, vol. 233, pp. 1438-1439, 1965.
- [36] H. S. Chen and K. A. Jackson, "The Influence of Alloy Composition on Glass Formation and Properties," presented at Metallic Glasses, Metals Park, OH USA, 1978.

- [37] W. Klement, R. H. Willens, and P. Duwez, "Non-crystalline structure in solidified gold-silicon alloys," *Nature*, vol. 187, pp. 869,870, 1960.
- [38] M. Maret, A. Soper, G. Etherington, and C. N. J. Wagner, "Structure of $\text{Be}_{43}\text{Hf}_x\text{Zr}_{57-x}$ metallic glasses," *J. Non-Cryst. Sol.*, vol. 61-62, pp. 313-318, 1984.
- [39] F. Sommer, G. Duddek, and B. Predel, "New glassy alloys," *Z. Metallkde.*, vol. 69, pp. 587-590, 1978.
- [40] R. St.Amand and B. C. Geissen, "Easy glass formation in simple metal alloys: amorphous metals containing calcium and strontium," presented at Scripta Metall., 1978.
- [41] B. C. Giessen, J. Hong, L. Kabecoff, D. E. Polk, and R. Raman, "Compositional dependence of the thermal stability and related properties of metallic glasses I: T(g) for $\text{Ca}_{0.65}\text{M}_{0.35}$ and $\text{Zr}_{0.475}\text{Cu}_{0.475}\text{M}_{0.05}$ glasses," *FIX*.
- [42] F. Q. Guo, S. J. Poon, and G. J. Shiflet, "CaAl-based bulk metallic glasses with high thermal stability," *Appl. Phys. Lett.*, vol. 84, pp. 37-39, 2004.
- [43] Z. Diao, Y. Yamada, T. Fukunaga, T. Matsuda, and U. Mizutani, "Electronic structure and electron transport properties of amorphous Ca-Al-Ga and Ca-Mg-Ga alloys," *Mat. Sci. Eng.*, vol. A181/A182, pp. 1047-1050, 1994.
- [44] U. Mizutani, M. Sasaura, V. L. Moruzzi, and T. Matsuda, "Electronic structure and electron transport in Ca-Mg-Cu metallic glasses," *Mat. Sci. Eng.*, vol. 99, pp. 295-299, 1988.
- [45] A. Berrada, J. Durand, N. Hassanain, and B. Loegel, "Anisotropy versus exchange in amorphous heavy-rare-earth based RE_4Au alloys," *J. Appl. Phys.*, vol. 50, pp. 7621-7623, 1979.
- [46] Y. Obi, H. Morita, and H. Fujimori, "Magnetic properties of amorphous Co-Mn-B alloys," *IEEE Trans Magnetics*, vol. 16, pp. 1132-1134, 1980.
- [47] K. Shirikawa, Y. Waseda, and T. Masumoto, "Densities of metal-metalloid amorphous alloys," *Sci. Rep. Res. Inst. Tohoku University (Sendai)*, vol. 29A, pp. 229-239, 1981.
- [48] Y. Waseda and H. S. Chen, "A structural study of metallic glasses containing boron (FeB, CoB, and NiB)," *phys. stat. sol. (a)*, vol. 49, pp. 387 - 392, 1978.
- [49] A. Inoue, T. Masumoto, M. Kikuchi, and T. Minemura, "Effect of compositions on the crystallization of (Fe, Ni, Co)-Si-B amorphous alloys," *Sci. Rep. Res. Inst. Tohoku University (Sendai)*, vol. 27A, pp. 127-146, 1979.
- [50] A. Inoue, A. Kitamura, and T. Masumoto, "The effect of aluminium on mechanical properties and thermal stability of (Fe,Co,Ni)-Al-B ternary amorphous alloys," *J. Mat. Sci.*, vol. 16, pp. 1895-1908, 1981.
- [51] F.-X. Li, F. Li, G.-H. Tu, and W.-R. Chen, "The behavior of electrical resistivity in amorphous $\text{Co}_{100-x}\text{B}_x$ alloys," *Mat. Sci. Eng.*, vol. 99, pp. 227-229, 1988.
- [52] G. Steinbrink, B. Punge-Witteler, and U. Koester, "Influence of an oxygen atmosphere and surface treatments on surface crystallization of (Co, Ni)-B glasses," *Mat. Sci. Eng.*, vol. 133, pp. 624-629, 1991.
- [53] A. Inoue, A. Kitamura, and T. Masumoto, "Ni-B and Co-B amorphous alloys with high boron concentration," *Mat. Trans. JIM*, vol. 47, pp. 404-407, 1979.
- [54] R. Ray, R. Hasegawa, C.-P. Chou, and L. A. Davis, "Iron-boron glasses: density, mechanical and thermal behavior," *Scripta Metall.*, vol. 11, pp. 973-978, 1977.

- [55] F. Spaepen, "Structure and flow of amorphous alloys," presented at Proc. 3rd International Conference on Rapidly Quenched Metals, 1979.
- [56] P. Lamparter and S. Steeb, "Structure of amorphous and molten alloys," in *Structure of Solids*, vol. Volume 1, *Materials Science and Technology, A Comprehensive Treatment*, V. Gerold, Ed. Weinheim, Germany: VCH, 1993, pp. 217-288.
- [57] A. Inoue, K. Kobayashi, C. Suryanarayana, and T. Masumoto, "An amorphous phase in Co-rich Co-Ti alloys," *Scripta Metall.*, vol. 14, pp. 119-123, 1980.
- [58] M. Nose and T. Masumoto, "Characteristics of (Fe, Co and/or Ni)-Zr amorphous alloys," *Sci. Rep. Res. Inst. Tohoku University (Sendai)*, vol. 28A, pp. 222-236, 1980.
- [59] K. H. J. Buschow and N. M. Beekmans, "Thermal stability and electronic properties of amorphous Zr-Co and Zr-Ni alloys," *Phys. Rev. B*, vol. 19, pp. 3843- 3846, 1979.
- [60] K. Shirakawa, K. Fukamichi, J. Kanehira, and T. Masumoto, "Spontaneous hall effect and magnetostriction of Co-Cr-Zr amorphous alloys," presented at Proc. 4th International Conference on Rapidly Quenched Metals, Sendai, Japan, 1981.
- [61] J.-C. Chen, Z.-X. Wang, W.-S. Zhan, J.-G. Zhao, B.-G. Shen, X. N. Zheng, and Q.-H. Chen, "The scattering mechanism of resistivity in amorphous Fe_{90-x}Co_xZr₁₀ alloys," *Mat. Sci. Eng.*, vol. 99, pp. 215-217, 1988.
- [62] K. Osamura, R. Suzuki, and Y. Murakami, "SAXS study on the structure of amorphous metallic alloys," presented at Proc. 4th International Conference on Rapidly Quenched Metals, Sendai, Japan, 1981.
- [63] L. Tanner and R. Ray, "Metallic glass formation and properties in Zr and Ti alloyed with Be-I the binary Zr-Be and Ti-Be systems," *Acta metall.*, vol. 27, pp. 1727-1747, 1979.
- [64] T. Zhang, A. Inoue, and T. Masumoto, "Amorphous (Ti,Zr,Hf)-Ni-Cu ternary alloys with a wide supercooled liquid region," *Mat. Sci. Eng.*, vol. A181/A182, pp. 1423-1426, 1994.
- [65] L. Xia, D. Ding, S. T. Shan, and Y. D. Dong, "The glass forming ability of Cu-rich Cu-Hf binary alloys," *J. Phys.: Condens. Matter*, vol. 18, pp. 3543-3548, 2006.
- [66] A. Inoue, W. Zhang, and J. Saida, "Synthesis and fundamental properties of Cu-based bulk glassy alloys in binary and multi-component systems," *Materials Transactions*, vol. 45, pp. 1153-1162, 2004.
- [67] A. J. Brunner, P. Oelhafen, and H.-J. Guntherodt, "X-ray photoelectron spectroscopy on amorphous Cu_xTe_{100-x} and Ni_xTe_{100-x}," *Mat. Sci. Eng.*, vol. 99, pp. 277-280, 1988.
- [68] K. Aoki and T. Masumoto, "Formation and Crystallization of Rapidly Quenched Ti-Al-Cu and Ti-Ni-Cu Amorphous Alloys," *Advanced Materials*, vol. 3, pp. 393-398, 1989.
- [69] S. Whang and B. C. Giessen, "Wear properties of some Ti alloy glasses," presented at Proc. 4th International Conference on Rapidly Quenched Metals, Sendai, Japan, 1981.
- [70] R. Ray, B. C. Giessen, and N. Grant, "New non-crystalline phases in splat cooled transition metal alloys," *Scripta Metall.*, vol. 2, pp. 357-359, 1968.
- [71] M. Sakata, N. Cowlan, and H. A. Davies, "Relations between chemical short range order and stability in CuTi glasses," presented at Proc. 4th International Conference on Rapidly Quenched Metals, Sendai, Japan, 1981.
- [72] L. A. Davis, C.-P. Chou, L. E. Tanner, and R. Ray, "Strengths and stiffnesses of metallic glasses," *Scripta Metall.*, vol. 10, pp. 937-940, 1976.

- [73] A. Inoue, C. Suryanarayana, and T. Masumoto, "Microstructure and superconductivity in annealed Cu-Nb-(Zr, Ti, Hf) ternary amorphous alloys obtained by liquid metal quenching," *J. Mat. Sci.*, vol. 16, pp. 1391-1401, 1981.
- [74] K. Suzuki, H. Fujimori, and K. Hashimoto, "Amorphous Metals," T. Masumoto, Ed. Tokyo, Japan: Ohmsha, Ltd., 1982, pp. 291 (in Japanese).
- [75] K. H. J. Buschow, "Thermal stability of amorphous Zr-Cu alloys," *J. Appl. Phys.*, vol. 52, pp. 3319-3323, 1981.
- [76] R. C. Budhani, T. C. Goel, and K. L. Chopra, "Formation and stability of Cu-Zr glasses prepared by melt-spinning and gun-quenching," presented at Proc. 4th International Conference on Rapidly Quenched Metals, Sendai, Japan, 1981.
- [77] F. Spaepen and D. Turnbull, "Formation of Metallic Glasses," presented at Rapidly Quenched Metals Second International Conference, Cambridge, MA, 1976.
- [78] D. Xu, B. Lohwongwatana, G. Duan, W. L. Johnson, and C. Garland, "Bulk metallic glass formation in binary Cu-rich alloy series - Cu_{100-x}Zr_x (x = 34, 36, 38.2, 40 at.%) and mechanical properties of bulk Cu₆₄Zr₃₆ glass," *Acta Mater.*, vol. 52, pp. 2621-2624, 2004.
- [79] N. AUTHORS, "NEED TITLE."
- [80] D. Wang, Y. Lia, B. B. Sun, M. L. Sui, K. Lu, and E. Ma, "Bulk metallic glass formation in the binary Cu-Zr system," *Appl. Phys. Lett.*, vol. 84, pp. 4029-4031, 2004.
- [81] A. S. Argon and H. Y. Kuo, "Free energy spectra for inelastic deformation of five metallic glass alloys," *J. Non-Cryst. Sol.*, vol. 37, pp. 241-266, 1980.
- [82] K. Fukamichi, S. Suzuki, and K. Sato, "Refrigerant characteristics of R-Al and R-Si amorphous alloys," *Sci. Rep. Res. Inst. Tohoku University (Sendai)*, vol. 36A, pp. 48-58, 1991.
- [83] K. Fukamichi, M. Kikuchi, S. Arakawa, and T. Masumoto, "Invar-Type new ferromagnetic amorphous Fe-B alloys," *Solid State Comm.*, vol. 23, pp. 955-958, 1977.
- [84] R. Hasegawa and R. Ray, "Iron-boron metallic glasses," *J. Appl. Phys.*, vol. 49, pp. 4174-4178, 1978.
- [85] M. Kijek, B. Cantor, and R. W. Cahn, "Diffusion in amorphous alloys," *Scripta Metall.*, vol. 14, pp. 1337-1340, 1980.
- [86] H. S. Chen, "Thermal and mechanical stability of metallic glass ferromagnets," *Scripta Metall.*, vol. 11, pp. 367-369, 1977.
- [87] U. Gonser, M. Ghafari, M. Ackermann, H. P. Klein, J. Bauer, and H. G. Wagner, "Crystallization of Fe(B,Si) amorphous alloys observed by Mossbauer spectroscopy and calorimetry," presented at Proc. 4th International Conference on Rapidly Quenched Metals, Sendai, Japan, 1981.
- [88] Y. Waseda and H. S. Chen, "On the structure of metallic glasses of transition metal-metalloid systems," *Sci. Rep. Res. Inst. Tohoku University (Sendai)*, vol. 28A, pp. 143-155, 1980.
- [89] T. Zingg, T. Richmond, G. Leemann, H. Jenny, H. Bretscher, and H.-J. Guntherodt, "Electronic transport properties of glassy Fe-Sc alloys," *Mat. Sci. Eng.*, vol. 99, pp. 179-182, 1988.

- [90] K. H. J. Buschow and A. M. v. d. Kraan, "Magnetic properties of amorphous $\text{Th}_{1-x}\text{Fe}_x$ alloys," *phys. stat. sol. (a)*, vol. 53, pp. 665-669, 1979.
- [91] K. Buschow and N. Beekmans, "On the thermal stability and the electrical resistivity of amorphous Th-Fe alloys," *phys. stat. sol. (a)*, vol. 56, pp. 505-511, 1979.
- [92] H. Kobayashi, H. Onodera, and H. Yamamoto, "Mössbauer Studies of Magnetic Inhomogeneity in Amorphous Fe-Zr-B Alloys," *J. Phys. Soc. Japan*, vol. 55, pp. 331-340, 1986.
- [93] A. Inoue, A. Kitamura, and T. Masumoto, *J. Mat. Sci.*, vol. 16, pp. 1895-1908, 1981.
- [94] J. Horvath, J. Ott, K. Pfahler, and W. Ulfert, "Tracer diffusion in amorphous alloys," *Mat. Sci. Eng.*, vol. 97, pp. 409-413, 1988.
- [95] H. U. Krebs, W. Biegel, A. Bienenstock, D. J. Webb, and T. H. Geballe, "Phase separation in amorphous Zr-Fe alloys determined by anomalous X-ray scattering and magnetization measurements," *Mat. Sci. Eng.*, vol. 97, pp. 163-167, 1988.
- [96] K. Buschow, "Magnetic coupling of rare earth moments in amorphous alloys," *Solid State Comm.*, vol. 27, pp. 275-278, 1978.
- [97] K. H. J. Buschow and N. M. Beekmans, "Magnetic and electrical properties of amorphous alloys of Gd and C, Al, Ga, Ni, Cu, Rh or Pd," presented at Proc. 4th International Conference on Rapidly Quenched Metals, Sendai, Japan, 1981.
- [98] K. H. J. Buschow, H. A. Algra, and R. A. Henskens, "Magnetic properties and ferromagnetic resonance in amorphous Gd alloys," *J. Appl. Phys.*, vol. 51, pp. 561-566, 1980.
- [99] D. Sellmyer, G. Hadjipanayis, and S. G. Cornelison, "Electrical and magnetic properties of rare-earth-gold glasses," *J. Non-Cryst. Sol.*, vol. 40, pp. 437-445, 1980.
- [100] K. Fukamichi, M. Kikuchi, T. Masumoto, and M. Matsuura, "Magnetic properties and invar effects of amorphous Gd-Co ribbons," *Phys. Lett.*, vol. 73A, pp. 436-438, 1979.
- [101] D. Louzguine and A. Inoue, "Influence of a supercooled liquid on devitrification of Cu-, Hf- and Ni- based metallic glasses," *Mat. Sci. Eng.*, vol. A357-377, pp. 346-350, 2004.
- [102] K. H. J. Buschow and N. M. Beekmans, "Formation, decomposition and electrical transport properties of amorphous Hf-Ni and Hf-Co alloys," *J. Appl. Phys.*, vol. 50, pp. 6348-6352, 1979.
- [103] K. Jansson and M. Nygren, "Investigation of the thermal stability and crystallization process of amorphous $\text{Hf}_{0.67}\text{T}_{0.33-x}\text{M}_x$ alloys, with T = Co or Ni, M = P or Si, by DSC, DTA and X-ray diffraction techniques," *Mat. Sci. Eng.*, vol. A133, pp. 462-467, 1991.
- [104] A. Inoue, Y. Takahashi, C. Suryanarayana, and T. Masumoto, "Superconducting properties and microstructure of crystallized Hf-Nb-Si and Hf-V-Si amorphous alloys," *J. Mat. Sci.*, vol. 17, pp. 1753-1764, 1982.
- [105] A. Inoue, H. S. Chen, J. T. Krause, and T. Masumoto, "Young's modulus sound velocity and Young's modulus of Ti-, Zr- and Hf-based amorphous alloys," *J. Non-Cryst. Sol.*, vol. 68, pp. 63-73, 1984.
- [106] N. I. Varich, A. A. Y. Yakunin, and A. B. Lysenko, "Formation and decomposition of a noncrystalline phase in a Li-25 at% Ag alloy quenched from the liquid state," *Sov. Phys. Solid State*, vol. 17, pp. 1194, 1195, 1975.

- [107] P. M. Nast, K. Samwer, and G. v. Minnigerode, "Electrical resistivity and superconductivity of amorphous La-Ag alloys," *Z. Physik B Condensed Matter*, vol. 38, pp. 89-92, 1980.
- [108] K. Agyeman, R. Muller, and C. C. Tsuei, "Alloying effect on superconductivity in amorphous La-based alloys," *Phys. Rev. B*, vol. 19, pp. 193-195, 1979.
- [109] W. L. Jonson, S. J. Poon, and P. Duwez, "Amorphous superconducting La-Au alloys obtained by liquid quenching," *Phys. Rev. B*, vol. 11, pp. 150-153, 1975.
- [110] W. L. Johnson and S. J. Poon, "Superconductivity in amorphous and microcrystalline transition metal alloys," *J. Appl. Phys.*, vol. 46, pp. 1787-1791, 1975.
- [111] K. Matsuzaki, A. Inoue, H. Toribuchi, K. Aoki, and T. Masumoto, "Formation of La-M-Cu (M=Ca, Sr or Ba) amorphous alloys and their oxidization and superconductivity," *Trans. JIM*, vol. 29, pp. 585-588, 1988.
- [112] W. H. Shull, D. G. Naugle, S. J. Poon, and W. L. Johnson, "Calorimetric and resistive measurements of amorphous "splat cooled" $\text{La}_{1-x}\text{Ga}_x$ foils," *Phys. Rev. B*, vol. 18, pp. 3263-3270, 1978.
- [113] U. Mizutani, K. Tanaka, T. Matsuda, N. Suzuki, T. Fukunaga, Y. Ozaki, Y. Yamada, and K. Nakayama, "Electronic structure and electron transport properties amorphous Mg-Ni-La and Mg-Cu-Y alloys," *J. Non-Cryst. Sol.*, vol. 156-158, pp. 297-301, 1993.
- [114] R. Richter, D. Baxter, and J. Strom-Olsen, "Quantum corrections to the conductivity in $\text{Mg}_{70}\text{Cu}_{30-0}\text{Au}_0$, $\text{Mg}_{70}\text{Cu}_{30-1}\text{Au}_1$, $\text{Mg}_{70}\text{Cu}_{30-3}\text{Au}_3$, $\text{Mg}_{70}\text{Cu}_{30-9}\text{Au}_9$ and $\text{Mg}_{70}\text{Zn}_{30-0}\text{Au}_0$ and $\text{Mg}_{70}\text{Zn}_{30-3}\text{Au}_3$," *Mat. Sci. Eng.*, vol. 99, pp. 183-186, 1988.
- [115] N. AUTHOR, "NEED TITLE for Mg-Y, Nd-Ni glasses."
- [116] S. Kim, A. Inoue, and T. Masumoto, "High mechanical strengths of Mg-Ni-Y and Mg-Cu-Y amorphous alloys with significant supercooled liquid region," *Mater. Trans. JIM*, vol. 31, pp. 929-934, 1990.
- [117] B. Predel and K. Hulse, "Thermodynamische eigenschaften metastabiler phasen des systems magnesium-gallium," *J. Less Common Metals*, vol. 63, pp. 245-256, 1979.
- [118] A. Inoue, M. Kohinata, A.-P. Tsai, and T. Masumoto, "Mg-Ni-La amorphous alloys with a wide supercooled liquid region," *Mat. Trans. JIM*, vol. 30, pp. 5-12, 1989.
- [119] H. Horikiri, A. Kato, A. Inoue, and T. Masumoto, "New Mg-based amorphous alloys in Mg---Y-misch metal systems," *Mat. Sci. Eng.*, vol. A179/A180, pp. 702-706, 1994.
- [120] A. Niikura, P. Tsai, N. Nishiyama, A. Inoue, and T. Masumoto, "Amorphous and quasi-crystalline phases in rapidly solidified Mg-Al-Zn alloys," *Mat. Sci. Eng.*, vol. A181/A182, pp. 1387-1391, 1994.
- [121] N. Shiotani, H. Narumi, H. Arai, K. Wakatsuki, Y. Sasa, and T. Mizoguchi, "Crystallization progress of amorphous Mg-Zn alloys," presented at Proc. 4th International Conference on Rapidly Quenched Metals, Sendai, Japan, 1981.
- [122] Z. P. Lu, Y. Li, S. C. Ng, and Y. P. Feng, "Study of glass transition of metallic glasses by temperature-modulated differential scanning calorimetry (MDSC)," *Thermochimica Acta*, vol. 357-358, pp. 65-69, 2000.
- [123] M. Nose, "PhD. Thesis," in *Department of Materials Science*. Sendai, Japan: Tohoku University, 1988.

- [124] K. Togano, H. Kumakura, and K. Tachikawa, "Liquid quenching on hot substrate," presented at Proc. 4th International Conference on Rapidly Quenched Metals, Sendai, Japan, 1981.
- [125] S. Davis, M. Fischer, B. C. Giessen, and D. E. Polk, "Formation and properties of refractory metallic glasses: T5-T9 glasses (T5=Nb,Ta T9=Rh,Ir)," presented at Rapidly Quenched Metals III, Proc. 3rd International Conference on Rapidly Quenched Metals, Brighton, England, 1978.
- [126] R. Ruhl, B. Giessen, M. Cohen, and N. Grant, "New microcrystalline phases in the Nb-Ni and Ta-Ni systems," *Acta metall.*, vol. 15, pp. 1699-1701, 1967.
- [127] D. Polk, "GET CITATION."
- [128] N. AUTHORS, "NEED TITLE for Nb-Si glasses."
- [129] T. Masumoto, A. Inoue, S. Sakai, H. Kimura, and A. Hoshi, "Superconductivity of ductile Nb-based amorphous alloys," *Trans. JIM*, vol. 21, pp. 115-122, 1980.
- [130] K. Tanaka, M. Yamada, T. Okamoto, Y. Narita, and H. Takaki, "Photoemission study of electronic structures of Nd-Fe and Nd-Fe-B alloy glasses," *Mat. Sci. Eng.*, vol. A181/A182, pp. 932-936, 1991.
- [131] B. Fogarassy, A. Cziraki, I. Bakonyi, K. Wetzig, G. Ziess, and I. Szabo, presented at Proc. 5th International Conference on Rapidly Quenched Metals, Wurzburg, Germany, 1985.
- [132] A. Inoue, T. Nakamura, and T. Masumoto, "Boron-rich Ni-B-C amorphous alloys prepared by rapid quenching," *J. Mat. Sci. Lett.*, vol. 5, pp. 1178-1180, 1986.
- [133] B. Punge-Witteler and U. Koster, "Crystallization of Ni-B glasses with high boron contents," *Mat. Sci. Eng.*, vol. 97, pp. 343-346, 1997.
- [134] L. Xia, W. H. Li, S. S. Fang, B. C. Wei, and Y. D. Dong, "Binary Ni-Nb bulk metallic glasses," *J. Appl. Phys.*, vol. 99, pp. 026103, 2006.
- [135] Z. P. Lu, Y. Liu, and C. T. Liu, "Evaluation of Glass-Forming Ability," in *Bulk Metallic Glasses*, M. Miller and P. Liaw, Eds. New York, NY: Springer, 2008, pp. 87-115.
- [136] K. Asami, A. Kawashima, and K. Hashimoto, "Chemical properties and applications of some amorphous alloys," *Mat. Sci. Eng.*, vol. 99, pp. 475-481, 1988.
- [137] M. H. Lee, W. T. Kim, D. H. Kim, and Y. B. Kim, "The effect of Al addition on the thermal properties and crystallization behavior of Ni₆₀Nb₄₀ metallic glass," *Mat. Sci. Eng.*, vol. A375-377, pp. 336-340, 2004.
- [138] A. Kawashima, K. Asami, and K. Hashimoto, "Change in corrosion behavior of amorphous Ni-P alloys by alloying with chromium, molybdenum or tungsten," *J. Non-Cryst. Sol.*, vol. 70, pp. 69-83, 1985.
- [139] B. P. Zhang, E. Akiyama, H. Habazaki, A. Kawashima, K. Asami, and H. Hashimoto, "Highly corrosion-resistant amorphous Cr-Ni-P alloys," *Mat. Sci. Eng.*, vol. A181/A182, pp. 1111-1118, 1994.
- [140] K. Aoki, M. Kamachi, and T. Masumoto, "Morphology of Zr or Ti based amorphous alloys after hydrogen absorption and desorption cycles," *Sci. Rep. Res. Inst. Tohoku University (Sendai)*, vol. 31A, pp. 191-199, 1983.

- [141] D. Louzguine-Luzgin, L. Louzguina-Luzgina, G. Xie, S. Li, W. Zhang, and A. Inoue, "Glass-forming ability and crystallization behavior of some binary and ternary Ni-based glassy alloys," *J. Alloys Compds.*, vol. 460, pp. 409-413, 2007.
- [142] A. Inoue, T. Zhang, and T. Masumoto, "Zr-Al-Ni amorphous alloys with high glass transition temperature and significant supercooled liquid region," *Mat. Trans. JIM*, vol. 31, pp. 177-183, 1990.
- [143] M. Ellner, M. El-Boragy, and B. Predel, presented at Proc. 5th International Conference on Rapidly Quenched Metals, Wurzburg, Germany, 1985.
- [144] N. Hayachi, T. Fukunaga, M. Ueno, and K. Suzuki, "Nearest neighbor short range structure of Pd-Ge alloys glasses by pulsed neutron total scattering," presented at Proc. 4th International Conference on Rapidly Quenched Metals, Sendai, Japan, 1981.
- [145] K. Suzuki, K. Shibata, and H. Mizuseki, "The medium- and short-range collective atomic motion in Pd-Si(Ge) amorphous alloys," *J. Non-Cryst. Sol.*, vol. 156-158, pp. 58-62, 1993.
- [146] N. Chen, P. Feng, and J. Sun, presented at Proc. 5th International Conference on Rapidly Quenched Metals, Wurzburg, Germany, 1985.
- [147] M. Hara, K. Hashimoto, and T. Masumoto, "The anodic polarization behavior of amorphous Pd-T-P alloys in NaCl solutions," *Electrochim. Acta*, vol. 25, pp. 1215-1220, 1980.
- [148] P. Duwez, R. Willens, and R. Crewdson, "Amorphous phase in palladium-silicon alloys," *J. Appl. Phys.*, vol. 36, pp. 2267-2269, 1965.
- [149] H. S. Chen and D. Turnbull, "Formation, stability and structure of palladium-silicon based alloy glasses," *Acta metall.*, vol. 17, pp. 1021-1031, 1969.
- [150] C.-P. Chou and D. Turnbull, "Transformation behavior of Pd-Au-Si metallic glasses," *J. Non-Cryst. Sol.*, vol. 17, pp. 169-188, 1975.
- [151] P. Ramachandrarao, B. Cantor, and R. W. Cahn, "Free volume theories of the glass transition and the special case of metallic glasses," *J. Mat. Sci.*, vol. 12, pp. 2488-2502, 1977.
- [152] H. S. Chen, Y. Waseda, and K. T. Aust, "Structure of Pt₇₅P₂₅ glass," *phys. stat. sol. (a)*, vol. 65, pp. 695-699, 1981.
- [153] G. Marchal, P. Mangin, M. Piecuch, B. Rodmacq, and C. Janot, "Electrical resistivity of amorphous Fe_xSn_{1-x} alloys," presented at Rapidly Quenched Metals III, Proc. 3rd International Conference on Rapidly Quenched Metals, London, England, 1978.
- [154] Y. Waseda and H. Chen, "The structure of amorphous metal-metal alloys," presented at Rapidly Quenched Metals III, Proc. 3rd International Conference on Rapidly Quenched Metals, London, England, 1978.
- [155] H. Uhlig, L. Rohr, H.-J. Güntherodt, P. Fischer, and P. Lamparter, "Short range order in amorphous Ni₅₀Ta₅₀ alloys by means of X-ray and neutron diffraction," *J. Non-Cryst. Sol.*, vol. 156-158, pp. 165-168, 1993.
- [156] B. Boucher, M. Sanquer, R. Tourbot, P. Chieux, P. Convert, M. Maret, and J. Bigot, "Magnetic behavior in amorphous Tb_xCu_{1-x} alloys (x= 0.18, 0.22, 0.33, 0.50 and 0.65)," *Mat. Sci. Eng.*, vol. 99, pp. 161-164, 1988.
- [157] R. H. Willens, "Dendritic Crystallization of an Amorphous Alloy," *J. Appl. Phys.*, vol. 33, pp. 3269-3270, 1962.

- [158] M. R. Anseau, "Crystallization of $\text{Te}_{100-x}\text{Ti}_x$ alloys ($15 \leq x \leq 50$) obtained by rapid cooling from the liquid state," *J. Appl. Phys.*, vol. 44, pp. 3357-3359, 1973.
- [159] L. E. Tanner, "Physical properties of Ti-Be-Si glass ribbons," *Scripta Metall.*, vol. 12, pp. 703-708, 1978.
- [160] L. E. Tanner and R. Ray, "Phase separation in Zr-Ti-Be metallic glasses," *Scripta Metall.*, vol. 14, pp. 657-662, 1980.
- [161] D. Polk, A. Calka, and B. Giessen, "The preparation and thermal and mechanical properties of new titanium rich metallic glasses," *Acta metall.*, vol. 26, pp. 1097-1103, 1978.
- [162] T. Fukunaga, K. Kai, M. Naka, N. Watanabe, and K. Suzuki, "High resolution short-range structure of Ni-Ti and Cu-Ti alloy glasses by pulsed neutron total scattering," presented at Proc. 4th International Conference on Rapidly Quenched Metals, Sendai, Japan, 1981.
- [163] C. Seeger and P. L. Ryder, "Kinetics of the crystallization of amorphous Ti-Ni and Ti-Ni-Si alloys," *Mat. Sci. Eng.*, vol. A179/A180, pp. 641-644, 1994.
- [164] T. Masumoto and A. Inoue, *Sci. Rep. Res. Inst. Tohoku University (Sendai)*, vol. 28A, pp. 165, 1980.
- [165] A. Inoue, Y. Takahashi, C. Suryanarayana, A. Hoshi, and T. Masumoto, "Crystallization-induced superconductivity in amorphous Ti-Ta-Si alloys," *J. Mat. Sci.*, vol. 16, pp. 3077-3086, 1981.
- [166] B. C. Giessen and R. D. Elliott, "Properties of metallic glasses containing actinide metals: I Thermal properties of U-M glasses (M=V, Cr, Mn, Fe, Co and Ni)," presented at Rapidly Quenched Metals III, Proc. 3rd International Conference on Rapidly Quenched Metals, London, England, 1978.
- [167] U. Mizutani, H. Sugiura, Y. Yamada, Y. Sugiura, and T. Matsuda, "Electronic structure and electron transport properties of Al-Cu-Y and Mg-Cu-Y amorphous alloys," *Mat. Sci. Eng.*, vol. A179/A180, pp. 132-136, 1994.
- [168] L. Jastrow, U. Köster, and M. Meuris, "Catastrophic oxidation of Zr-TM (noble metals) glasses," *Mat. Sci. Eng.*, vol. A375-377, pp. 440-443, 2004.
- [169] R. Hasegawa and L. E. Tanner, "Superconducting transition temperatures of glassy and partially crystalline Be-Nb-Zr alloys," *J. Appl. Phys.*, vol. 49, pp. 1196-1200, 1978.
- [170] H. Riesemeier, K. Lüders, H. C. Freyhardt, and J. Reichelt, "Superconductivity and thermal relaxation of amorphous Be-Nb-Zr alloys," *J. Non-Cryst. Sol.*, vol. 61-62, pp. 991-996, 1984.
- [171] M. ElAmrani, J. Destry, and R. W. Cochrane, "The influence of hydrostatic pressure on superconducting transition temperature and critical field in the amorphous binary metallic alloy M-Zr(M=Fe,Co or Ni)," *Mat. Sci. Eng.*, vol. 99, pp. 309-311, 1988.
- [172] M. L. Trudeau, R. W. Cochrane, and J. Destry, "The Hall effect in paramagnetic Co-Zr metallic glasses," *Mat. Sci. Eng.*, vol. 99, pp. 187-190, 1988.
- [173] I. Kokanovic, B. Leontic, J. Lukatela, and A. Tonejc, "The effect of thermal-relaxation on the short-range order in Zr₈₀Co₂₀ metallic glass," *Mat. Sci. Eng.*, vol. A375-377, pp. 688-692, 2004.
- [174] T. Mizoguchi, T. Kudo, and T. Irisawa, "The structure of a metal-metal amorphous alloy, $\text{Cu}_{0.57}\text{Zr}_{0.43}$, determined by neutron diffraction," pp. 384-389, FIX.

- [175] W. Biegel, H. U. Krebs, C. Michaelson, H. C. Freyhardt, and E. Heustern, *Mat. Sci. Eng.*, vol. 97, pp. 59-62, 1988.
- [176] Y. Takahashi. Sendai, Japan: Tohoku University, 1982.
- [177] J. C. deLima, D. Raoux, J. M. Tonnerre, D. Udron, K. D. Machado, T. A. Grandi, C. E. M. deCampos, and T. I. Morrison, "Structural study of an amorphous NiZr₂ alloy by anomalous wide-angle x-ray scattering and reverse Monte Carlo simulations," *Phys. Rev. B*, vol. 67, pp. 094210, 2003.
- [178] T. Nakamura, E. Matsubara, M. Sakurai, M. Kasai, A. Inoue, and Y. Waseda, "Structural study in amorphous Zr-noble metal (Pd, Pt and Au) alloys," *J. Non-Cryst. Sol.*, vol. 312-314, pp. 517-521, 2002.
- [179] J. R.C. Bowman, M. J. Rosker, and W. L. Johnson, "A study of the properties and NMR spectra of amorphous and crystalline Zr-Pd hydrides," *J. Non-Cryst. Sol.*, vol. 53, pp. 105-122, 1982.
- [180] K. Togano and K. Tachikawa, "Structure and superconductivity of metastable phases in liquid-quenched Zr-Rh alloys," *J. Appl. Phys.*, vol. 46, pp. 3609-3613, 1975.
- [181] A. Inoue, Y. Takahashi, and T. Masumoto, "Formation range, mechanical properties and thermal stability of superconducting Zr-Si amorphous alloys," *Sci. Rep. Res. Inst. Tohoku University (Sendai)*, vol. 29A, pp. 296-303, 1981.
- [182] A. Inoue, R. Toyota, T. Fukase, T. Masumoto, and Y. Takahashi, "Superconductivity of Zr-Nb-Si amorphous alloys," *J. Mat. Sci.*, vol. 18, pp. 114-126, 1983.

Table 1. Metallic radii of atoms in metallic glass structures.

Element	At #	Radius (pm)	Element	At #	Radius (pm)	Element	At #	Radius (pm)
Li	3	152	As	33	115	Eu	63	196
Be	4	112	Se	34	118	Gd	64	174
B	5	88	Rb	37	132	Tb	65	180
C	6	77	Sr	38	212	Dy	66	175
N	7	72	Y	39	179	Ho	67	177
O	8	64	Zr	40	158	Er	68	175
Na	11	180	Nb	41	143	Tm	69	175
Mg	12	160	Mo	42	139	Yb	70	190
Al	13	141	Tc	43	136	Lu	71	175
Si	14	110	Ru	44	134	Hf	72	158
P	15	102	Rh	45	132	Ta	73	145
S	16	103	Pd	46	142	W	74	135
K	19	230	Ag	47	144	Re	75	137
Ca	20	201	Cd	48	157	Os	76	135
Sc	21	162	In	49	155	Ir	77	136
Ti	22	142	Sn	50	155	Pt	78	139
V	23	134	Sb	51	155	Au	79	144
Cr	24	130	Te	52	140	Hg	80	152
Mn	25	132	Cs	55	264	Tl	81	172
Fe	26	125	Ba	56	223	Pb	82	174
Co	27	125	La	57	187	Bi	83	162
Ni	28	126	Ce	58	182	Po	84	168
Cu	29	126	Pr	59	183	Th	90	178
Zn	30	138	Nd	60	178	Pa	91	165
Ga	31	134	Pm	61	185	U	92	158
Ge	32	114	Sm	62	185			

Table 2. Structural sites and site occupancies $S(i_j)$ per α site.

	Species (i)		Site Sum
	Ω	α	
Site (j)	Ω	$S(\Omega_\Omega)$	\hat{S}_Ω
	α	$S(\Omega_\alpha) = 0$	$\hat{S}_\alpha = 1$
	β	$S(\Omega_\beta) = 0$	$\hat{S}_\beta = 1$
	γ	$S(\Omega_\gamma) = 0$	$\hat{S}_\gamma = 2$
Species Sum	$\bar{S}_\Omega = S(\Omega_\Omega)$	\bar{S}_α	$\sum S = \hat{S}_\Omega + 4$

Table 3. Preferred radius ratios, structure and occurrence.

R^*	$\langle Z \rangle$	Occurrence	BMG
0.414	$\langle 6 \rangle$	Rare	Ca-Al Hf-Cu, Zr-Cu
0.518	$\langle 7 \rangle$	None	
0.617	$\langle 8 \rangle$	Uncommon	
0.710	$\langle 9 \rangle$	Common	
0.799	$\langle 10 \rangle$	Common	
0.884	$\langle 11 \rangle$	Unstable [2]	
0.902	$\langle 12 \rangle$	Common	
0.976	$\langle 13 \rangle$	Rare	Ni-Nb Cu-Hf, Cu-Zr
1.047	$\langle 14 \rangle$	None	
1.116	$\langle 15 \rangle$	Common	
1.183	$\langle 16 \rangle$	Rare	
1.248	$\langle 17 \rangle$	Common	
1.311	$\langle 18 \rangle$	Uncommon	
1.373	$\langle 19 \rangle$	None	
1.433	$\langle 20 \rangle$	Uncommon	

H 1																	He 2						
Li 3	Be 4																	B 5	C 6	N 7	O 8	F 9	Ne 10
Na 11	Mg 12																	Al 13	Si 14	P 15	S 16	Cl 17	Ar 18
K 19	Ca 20	Sc 21	Ti 22	V 23	Cr 24	Mn 25	Fe 26	Co 27	Ni 28	Cu 29	Zn 30	Ga 31	Ge 32	As 33	Se 34	Br 35	Kr 36						
Rb 37	Sr 38	Y 39	Zr 40	Nb 41	Mo 42	Tc 43	Ru 44	Rh 45	Pd 46	Ag 47	Cd 48	In 49	Sn 50	Sb 51	Te 52	I 53	Xe 54						
Cs 55	Ba 56	★ 57-70	Lu 71	Hf 72	Ta 73	W 74	Re 75	Os 76	Ir 77	Pt 78	Au 79	Hg 80	Tl 81	Pb 82	Bi 83	Po 84	At 85	Rn 86					
Fr 87	Ra 88	★★ 89-102	Lr 103	Rf 104	Db 105	Sg 106	Bh 107	Hs 108	Mt 109	Ds 110	Rg 111	Uub 112	Uut 113	Uuq 114	Uup 115	Uuh 116	Uus 117	Uuo 118					

★
Lanthanides

★★
Actinides

La 57	Ce 58	Pr 59	Nd 60	Pm 61	Sm 62	Eu 63	Gd 64	Tb 65	Dy 66	Ho 67	Er 68	Tm 69	Yb 70
Ac 89	Th 90	Pa 91	U 92	Np 93	Pu 94	Am 95	Cm 96	Bk 97	Cf 98	Es 99	Fm 100	Md 101	No 102

Figure 1 Periodic table showing the solute and solvent atoms found in binary metallic glasses.

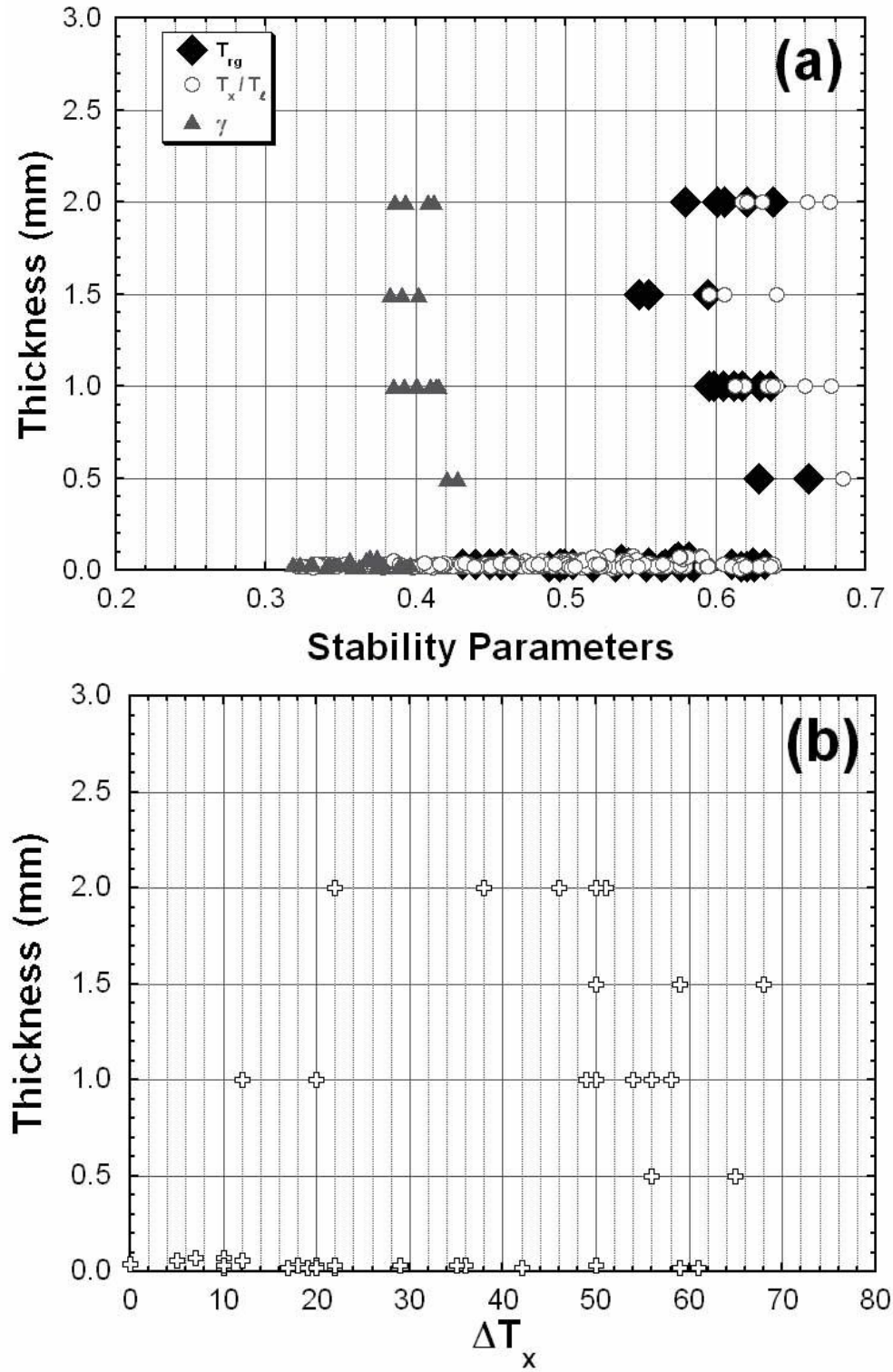
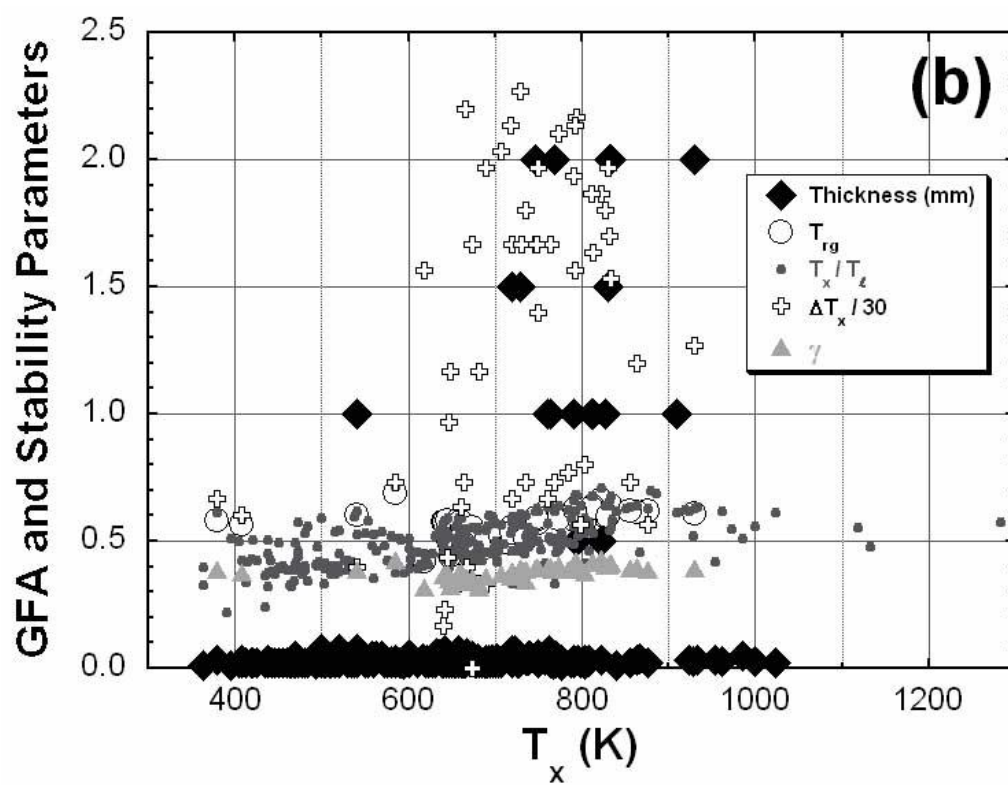
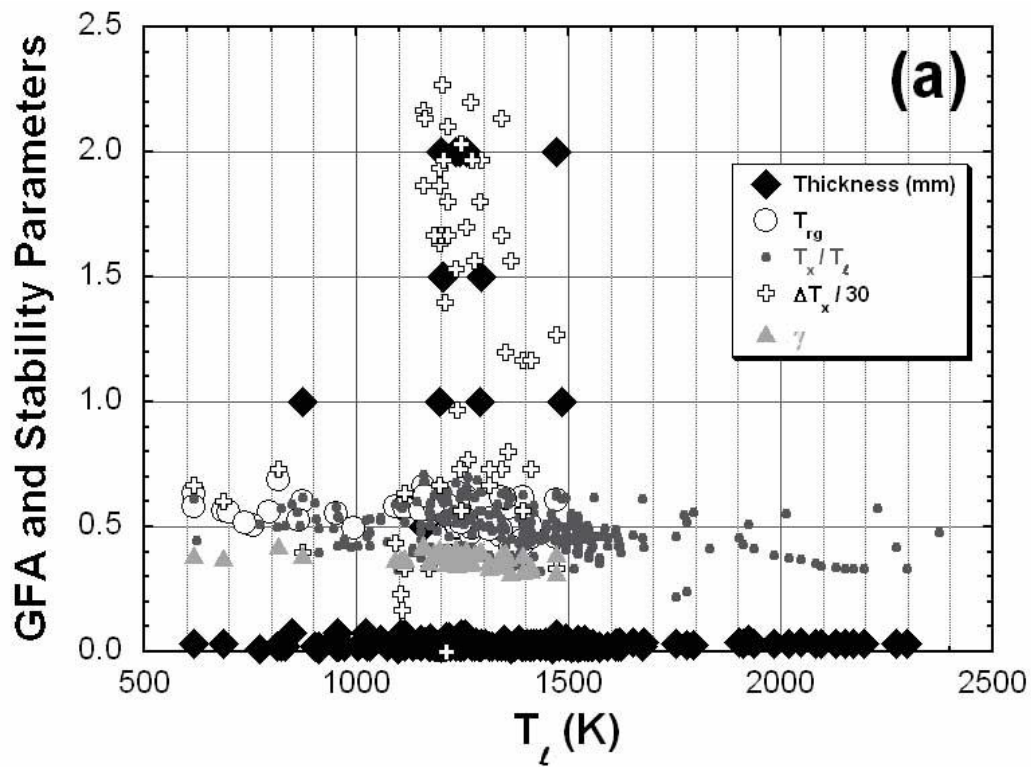


Figure 2 Influence of thermal stability parameters (a) T_{rg} , T_x/T_l and γ , and (b) ΔT_x on reported amorphous thickness. Binary BMGs require minimum values of about 0.55 for T_{rg} ; about 0.59 for T_x/T_l ; 0.38 for γ ; or about 10 K for ΔT_x .



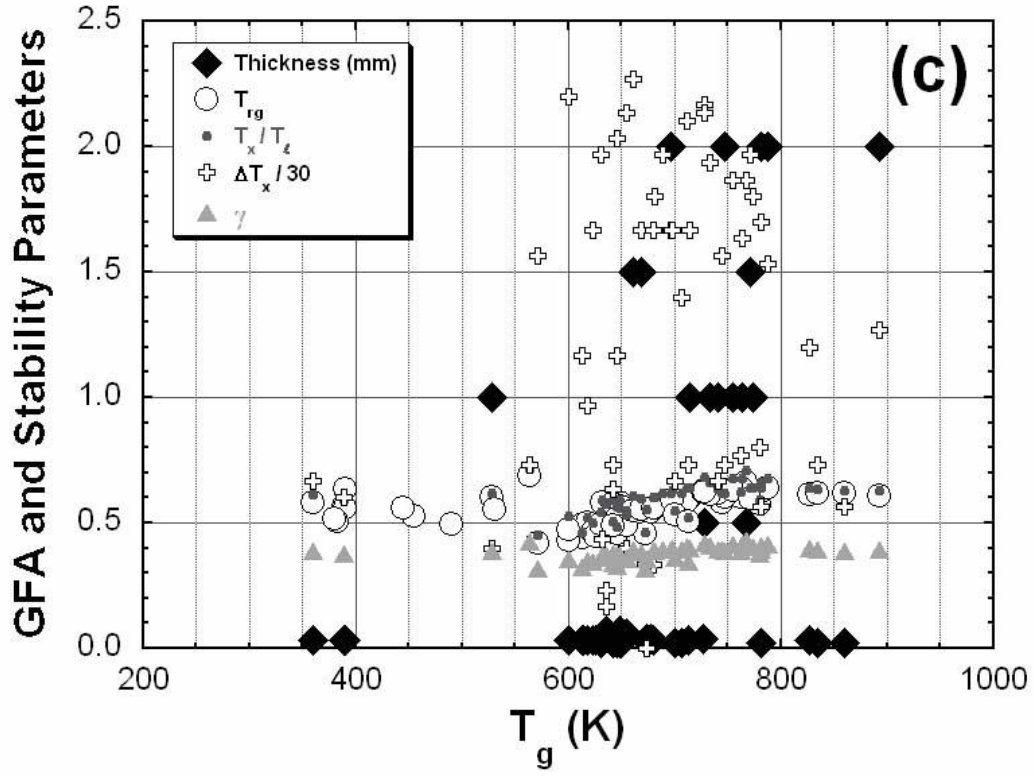


Figure 3 Dependence of the glass forming ability, as measured by the maximum reported amorphous thickness, and derived thermal stability parameters on the primary thermal stability parameters (a) liquidus temperature, T_l ; (b) crystallization temperature T_x ; and (c) glass transition temperature, T_g . For convenience, ΔT_x is reduced by a factor of 30 to fit the same scale.

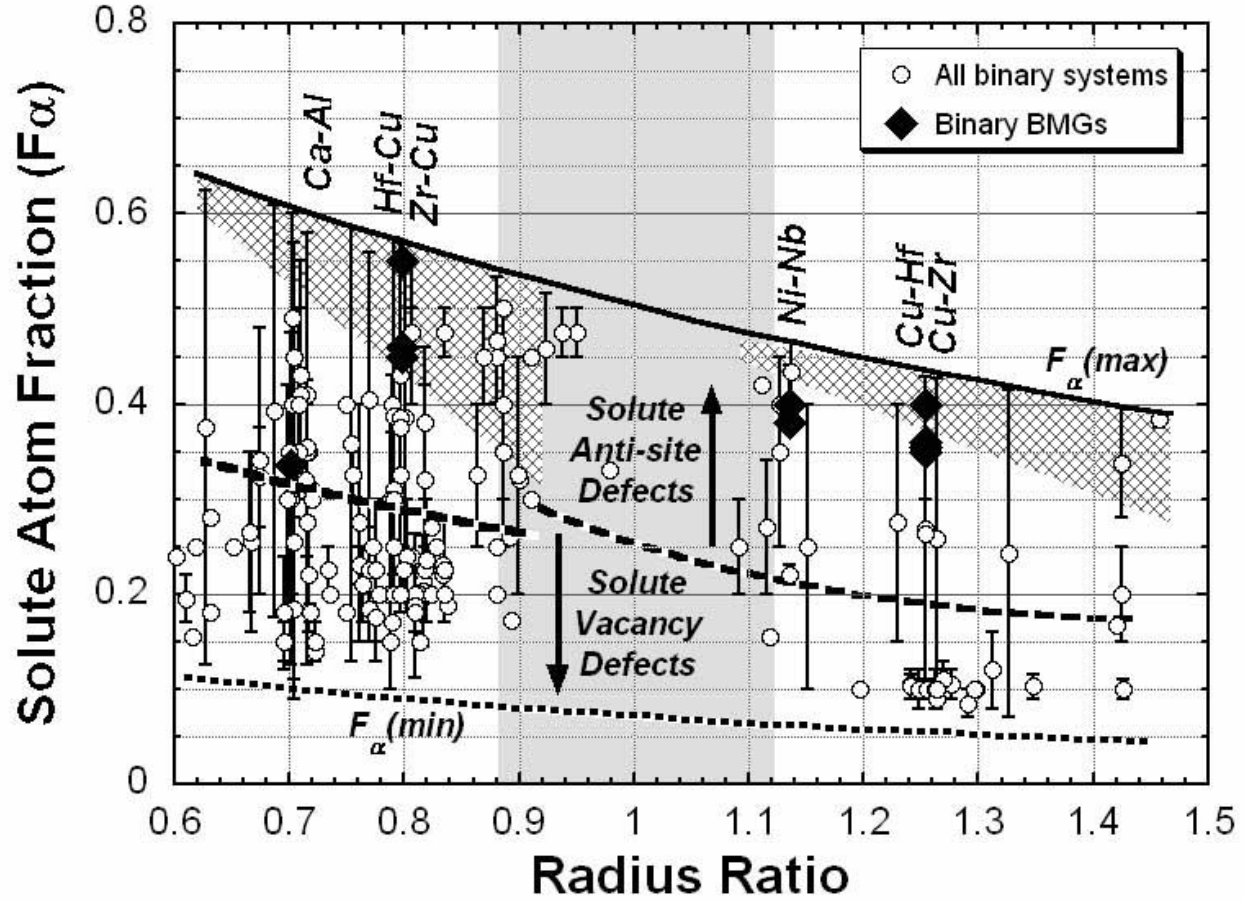


Figure 4 Solute atom fraction vs. nominal radius ratio for all binary metallic glass systems (open symbols) and binary BMGs (filled symbols). The BMG systems are labelled. The solid line is the maximum value of F_{α} at the iso-structure condition from Equation 11. The dashed line represents the boundary at $\bar{S}_{\alpha} = 4$ between solute-lean glasses with solute vacancy defects (below) and solute-rich glasses with solute anti-site defects (above). The dotted line is the minimum solute atom fraction at $\bar{S}_{\alpha} = 1$, where all α sites are filled by α . The gray band is the region of poor GFA from the empirical rule that the preferred difference in solvent and solute radii is greater than $\pm 12\%$. The cross-hatched areas represent regions of maximal global packing efficiency (Section 4.6).

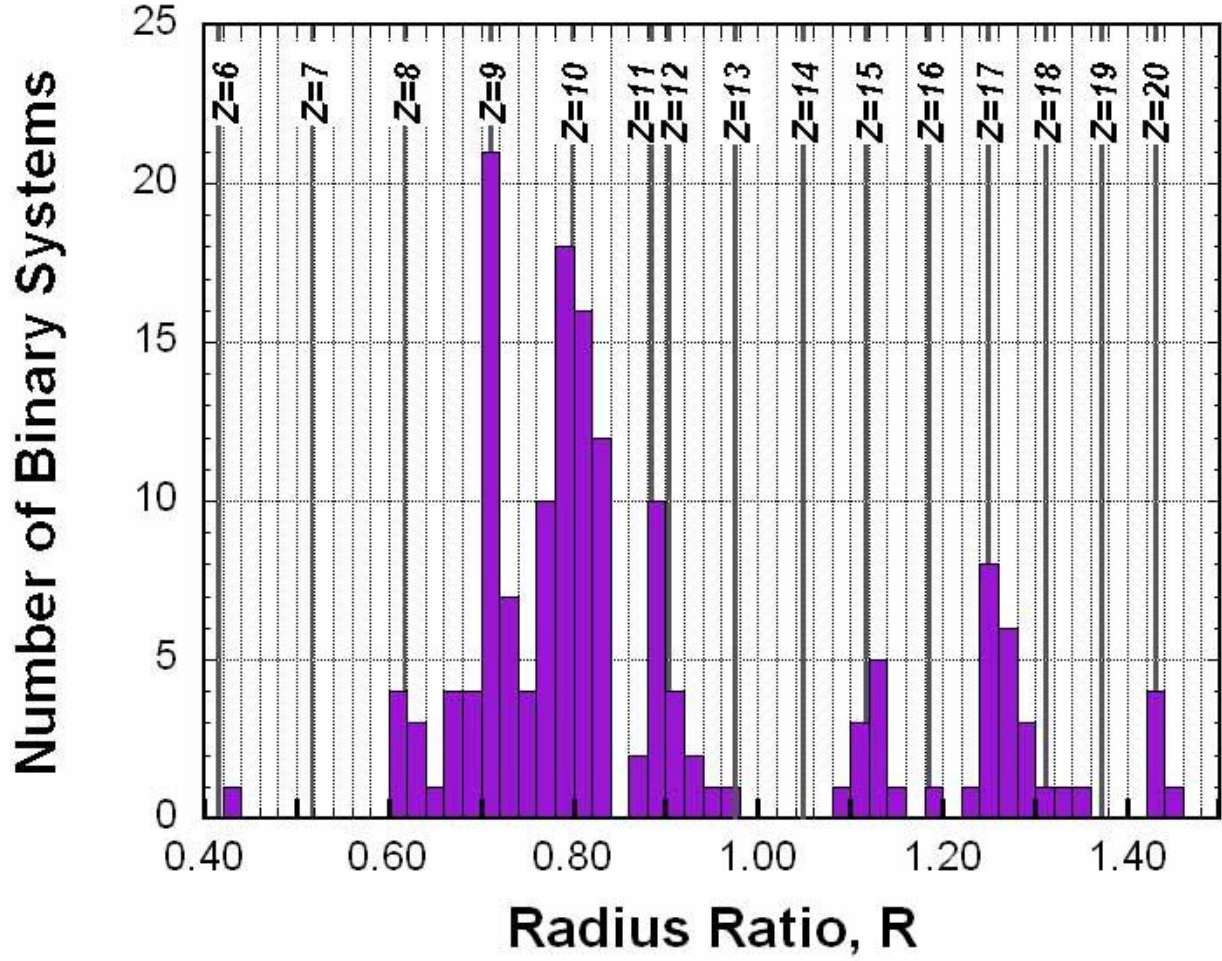


Figure 5 Histogram of the nominal solute-to-solvent radius ratios, $R = r_{\alpha} / r_{\Omega}$, in binary metallic glass systems. The vertical bars represent the number of glass systems with R values in the interval between R and $R+0.02$ as a function of R . The bold vertical lines indicate special radius ratios, R^* , that give efficient local atomic packing of Z solvent atoms around a central α solute.

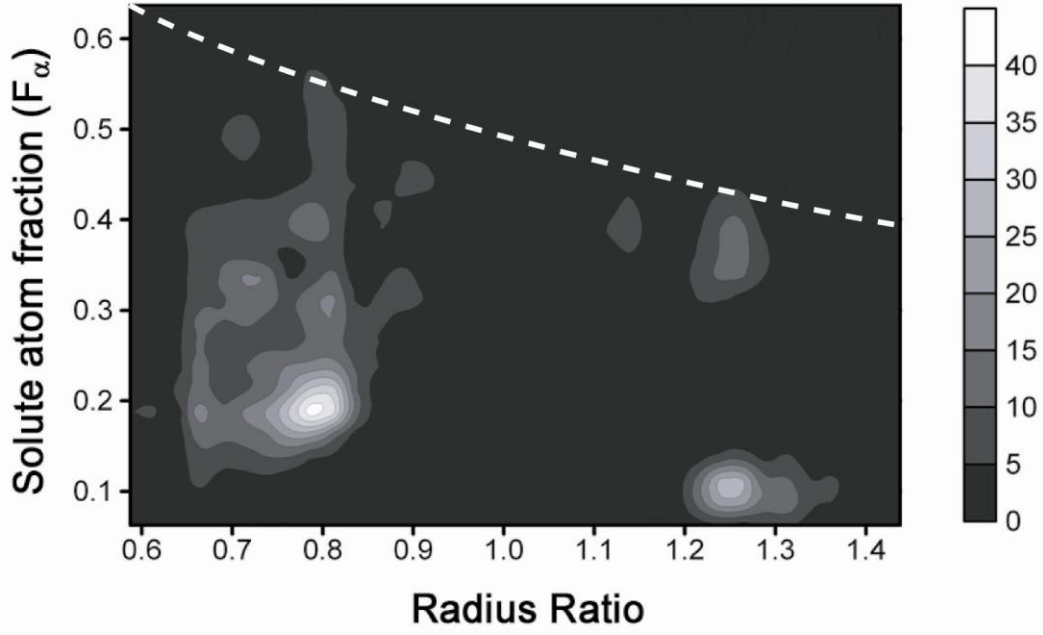


Figure 6 Contour plot of the number of reported alloys within increments $R+0.05R$ and $F_\alpha+0.05F_\alpha$ as a function of R and F_α . The dashed line represents the maximum solute atom fraction at the iso-structural condition from [Equation 11](#).

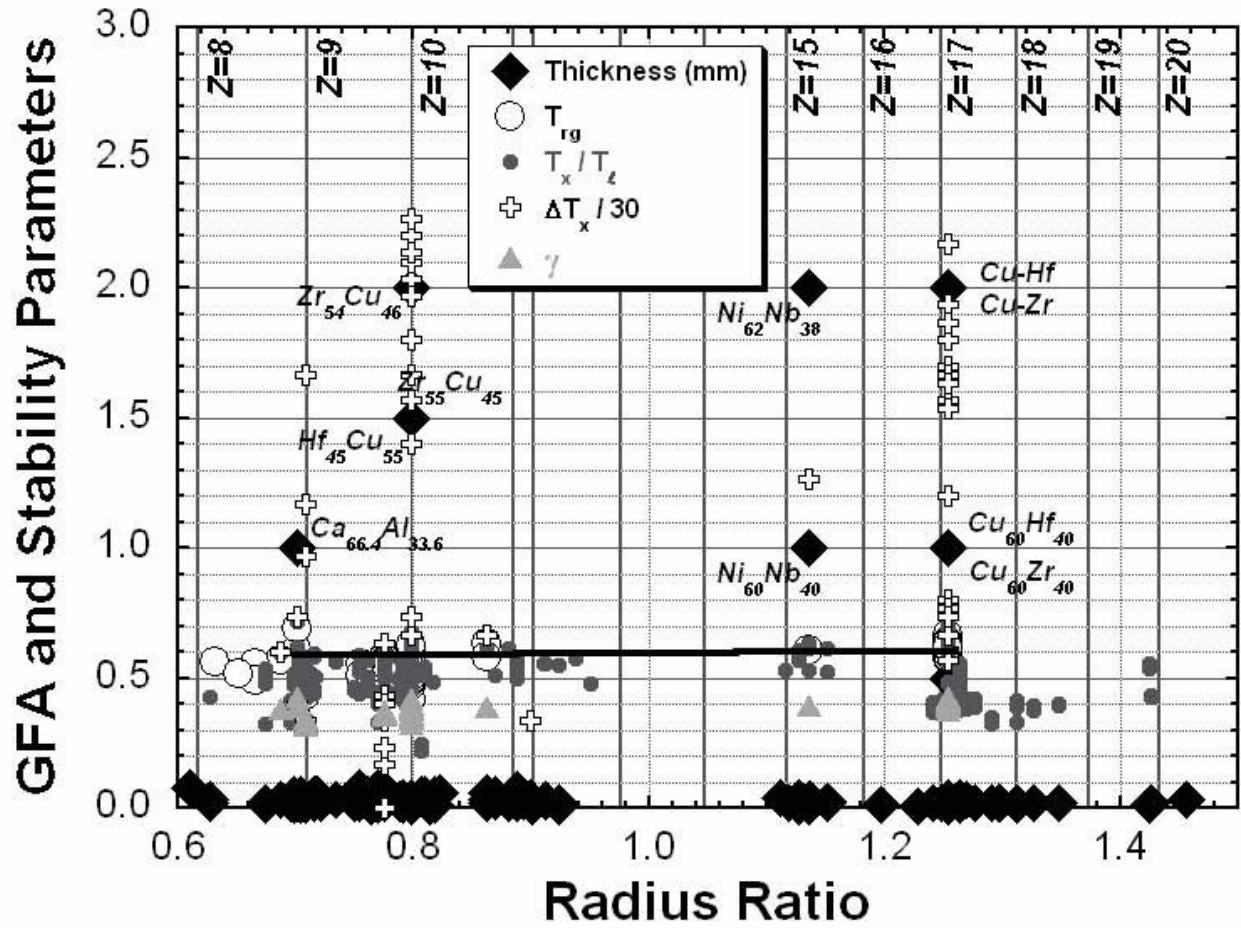


Figure 7 GFA and thermal stability parameters v. R . Values of R^* are shown by the vertical lines. The solid line shows a linear regression from the T_{rg} datapoints for the binary BMGs only. For convenience, ΔT_x is reduced by a factor of 30 to fit the same scale.

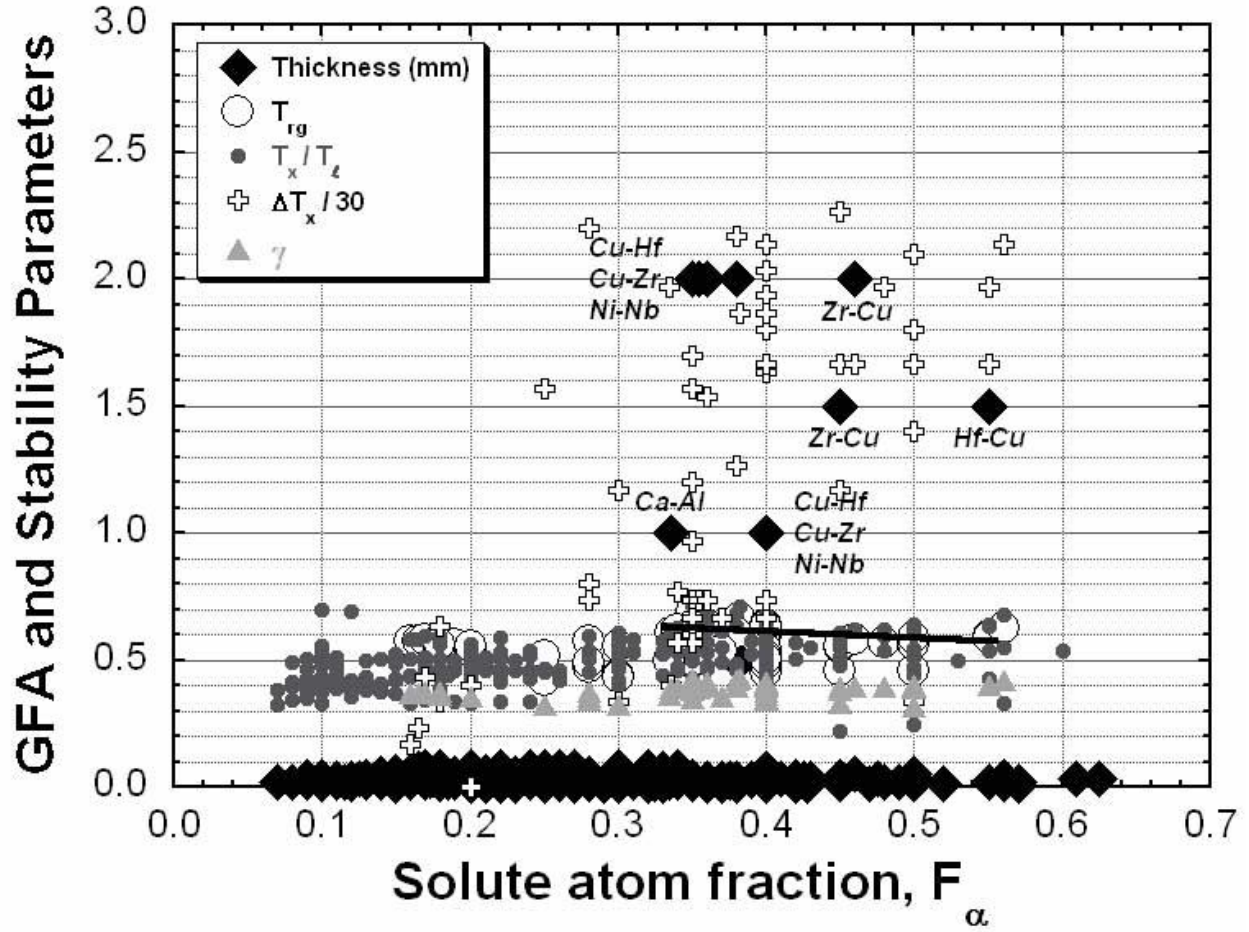


Figure 8 GFA and thermal stability parameters v. F_α . The solid line shows a linear regression from the T_{rg} datapoints for the binary BMGs only. For convenience, ΔT_x is reduced by a factor of 30 to fit the same scale.

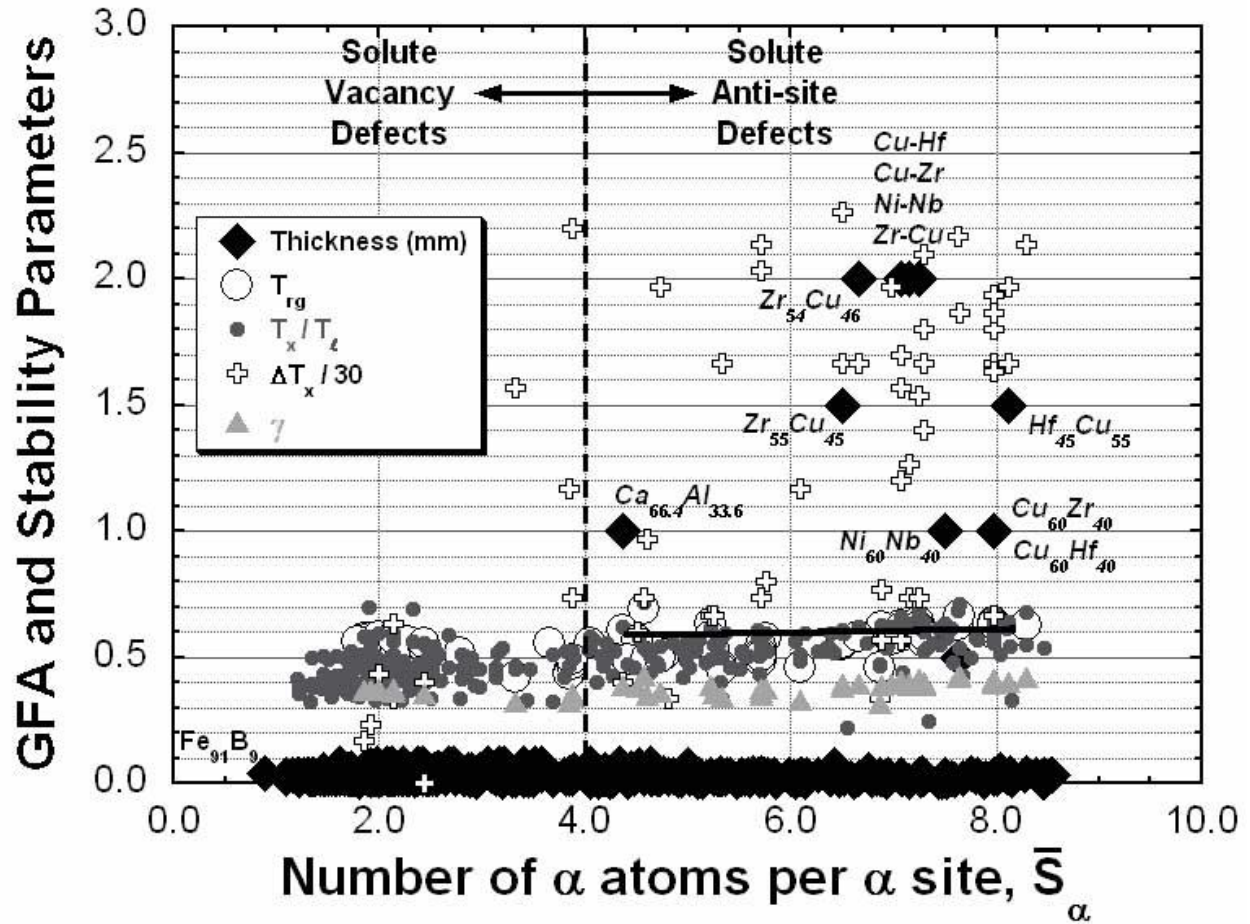


Figure 9 GFA and thermal stability parameters v. the number of α atoms in the structure per α site, \bar{S}_α . All solute sites are filled when $\bar{S}_\alpha = 4$, which defines the boundary between solute-lean and solute-rich structures. The solid line shows a linear regression from the T_{rg} datapoints for the binary BMGs only. For convenience, ΔT_x is reduced by a factor of 30 to fit the same scale.

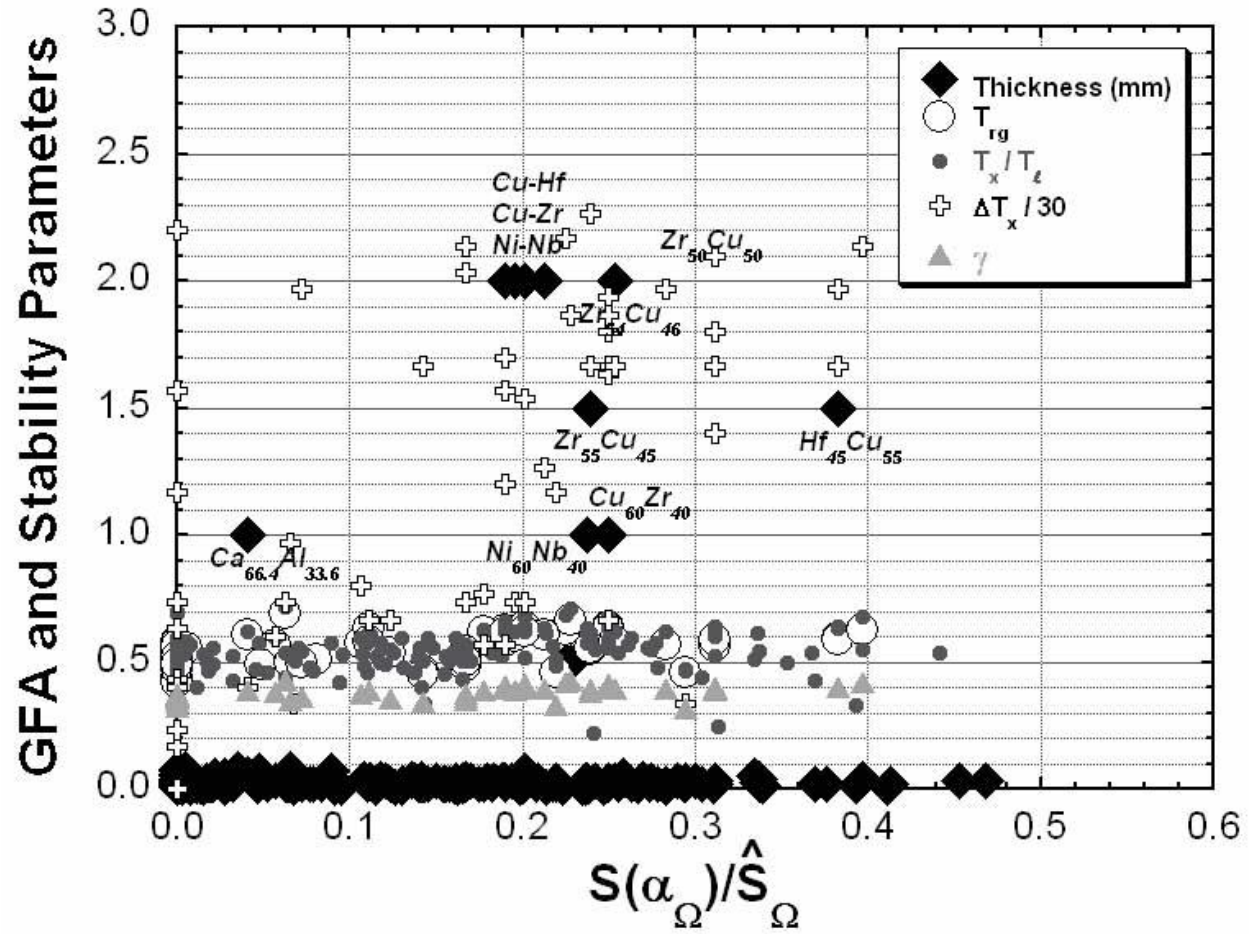


Figure 10 GFA and thermal stability parameters v. the fraction of Ω sites in the structure that are occupied by α atoms. For convenience, ΔT_x is reduced by a factor of 30 to fit the same scale.

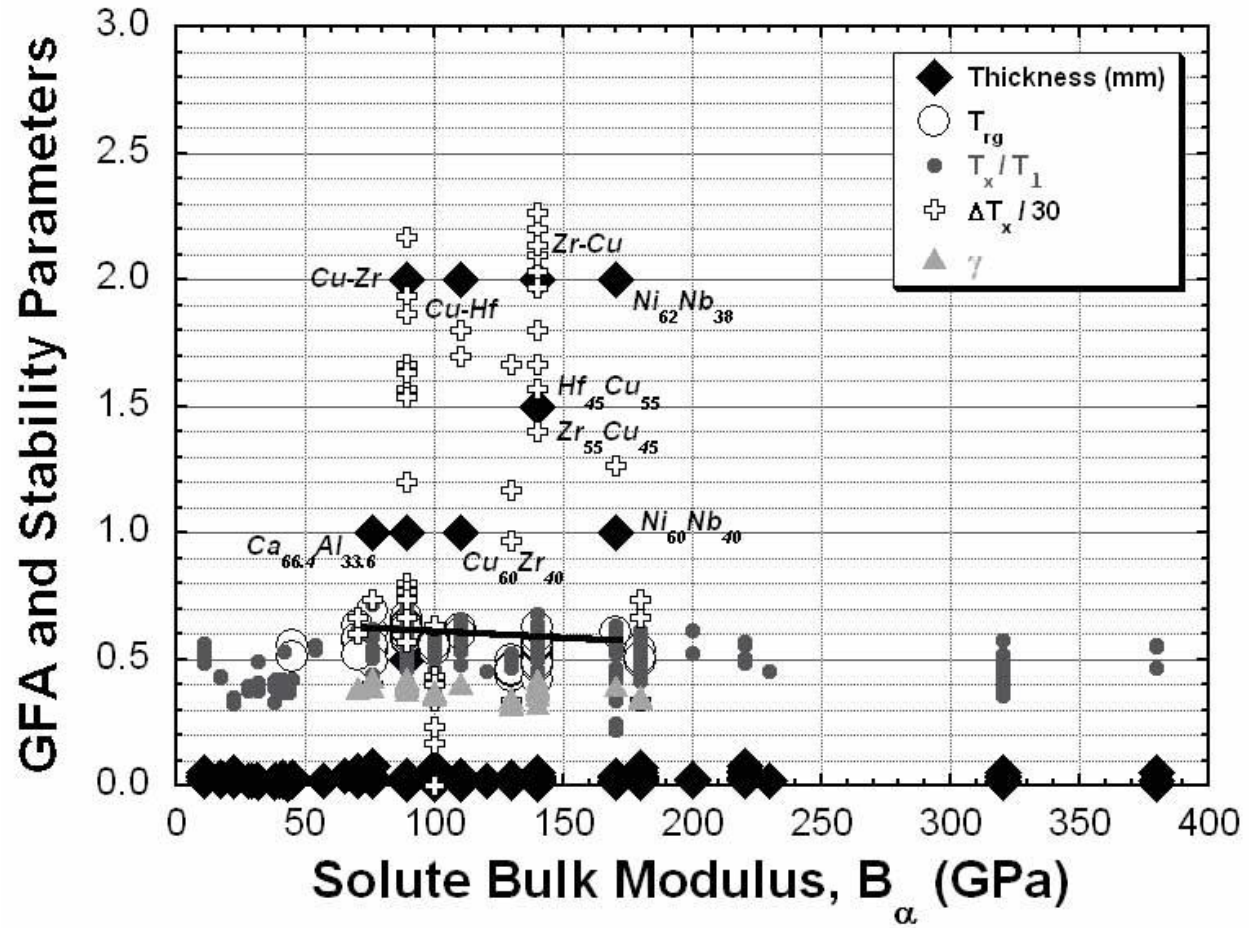


Figure 11 GFA and thermal stability parameters v. the solute bulk modulus, B_{α} . The solid line shows a linear regression from the T_{rg} datapoints for the binary BMGs only. For convenience, ΔT_x is reduced by a factor of 30 to fit the same scale.

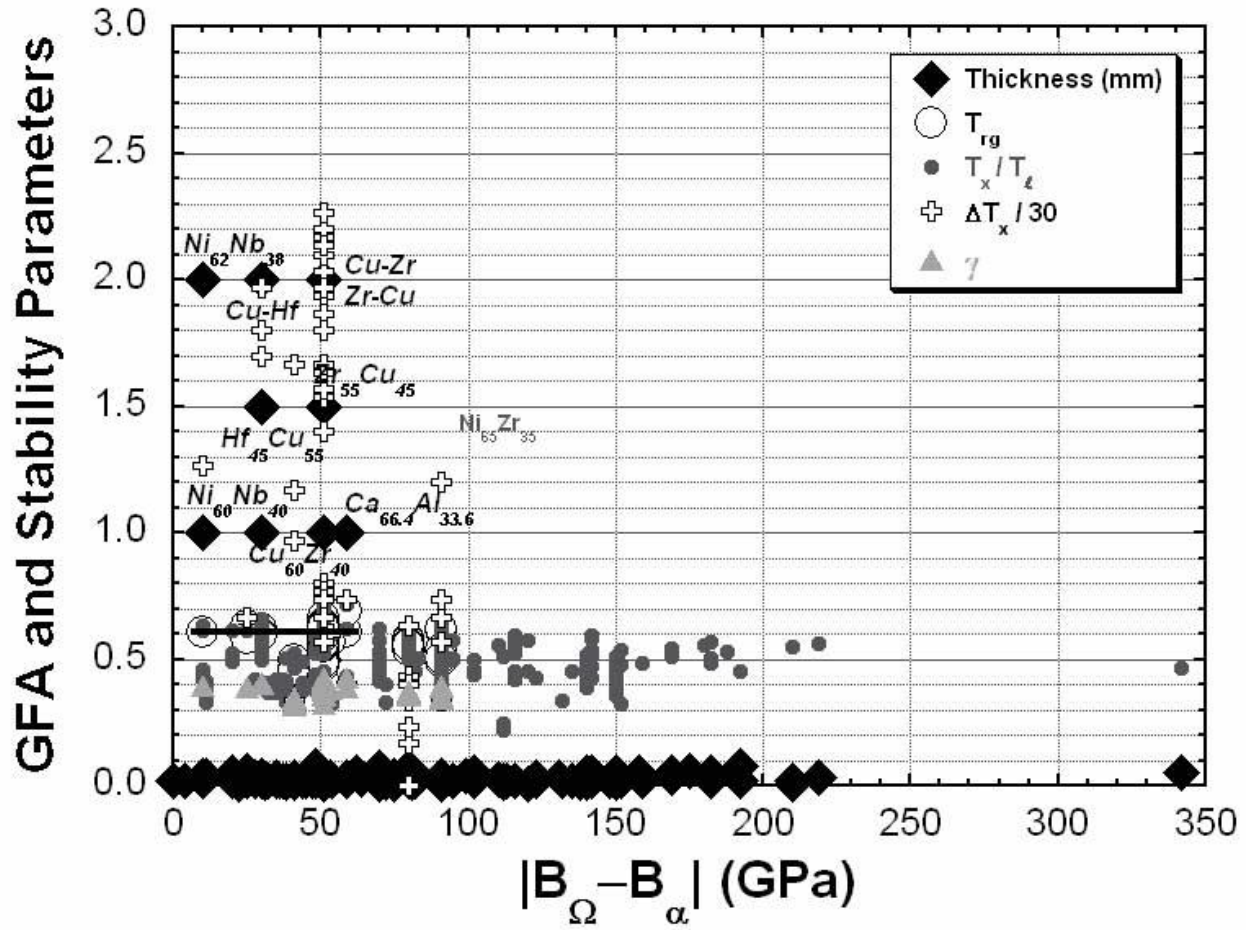


Figure 12 GFA and thermal stability parameters v. the absolute difference in solvent and solute bulk moduli. The solid line shows a linear regression from the T_{rg} datapoints for the binary BMGs only. For convenience, ΔT_x is reduced by a factor of 30 to fit the same scale.

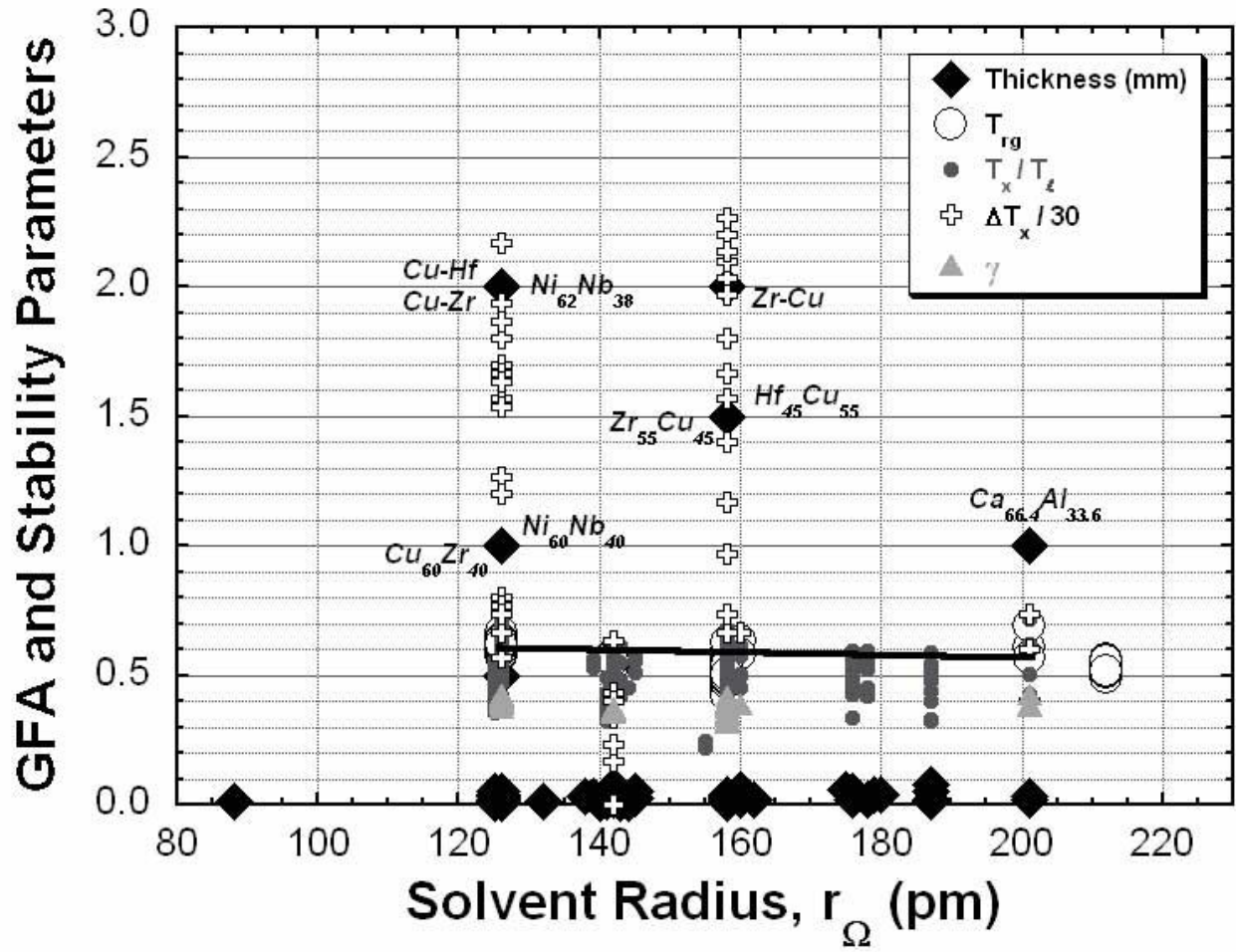


Figure 13 GFA and thermal stability parameters v. the solvent atom radius, r_Ω . The solid curve is a linear regression fit to T_{rg} datapoints for binary BMGs only. For convenience, ΔT_x is reduced by a factor of 30 to fit the same scale.

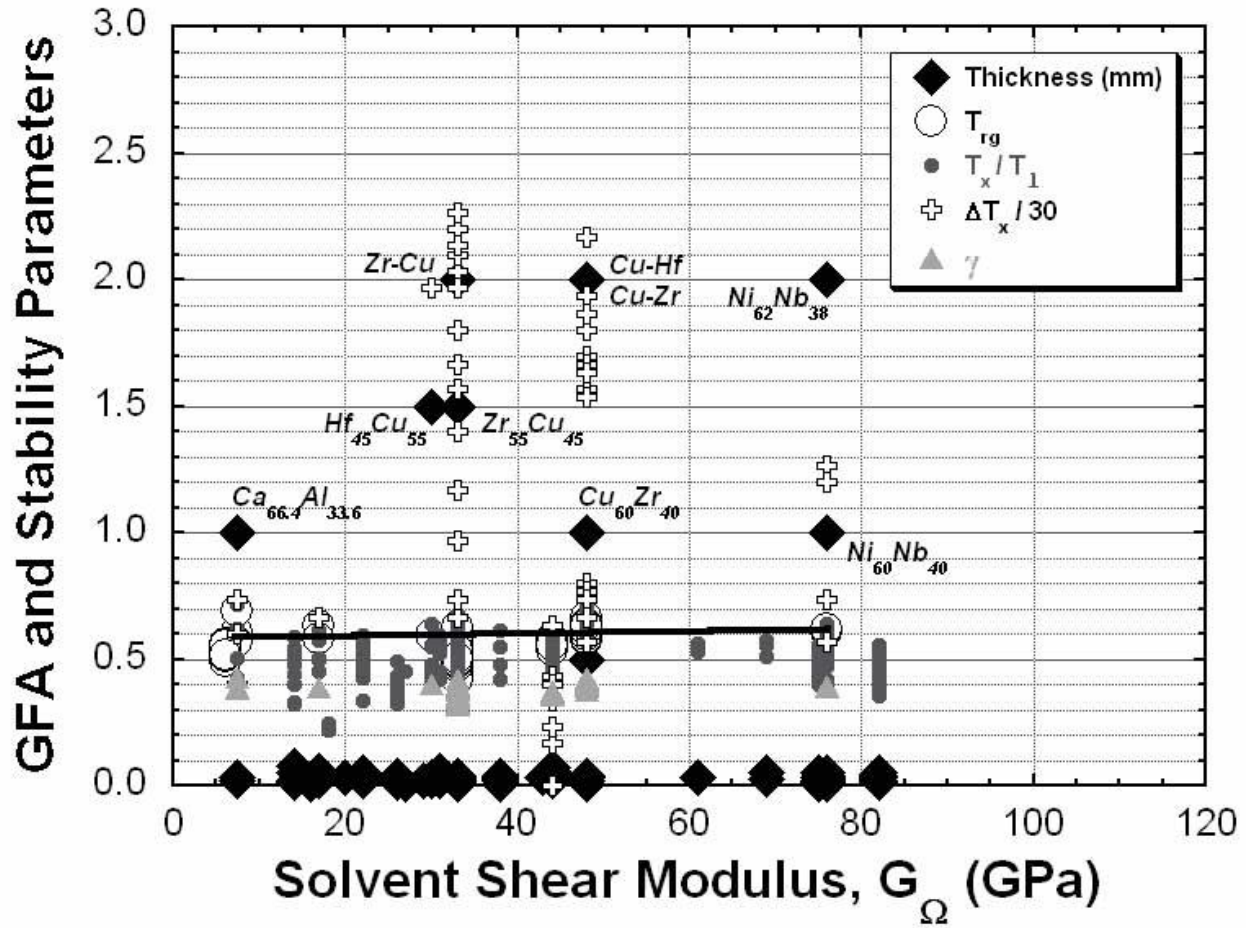


Figure 14 GFA and thermal stability parameters v. the solvent shear modulus, G_{Ω} . The solid curve is a linear regression fit to T_{rg} datapoints for binary BMGs only. For convenience, ΔT_x is reduced by a factor of 30 to fit the same scale.

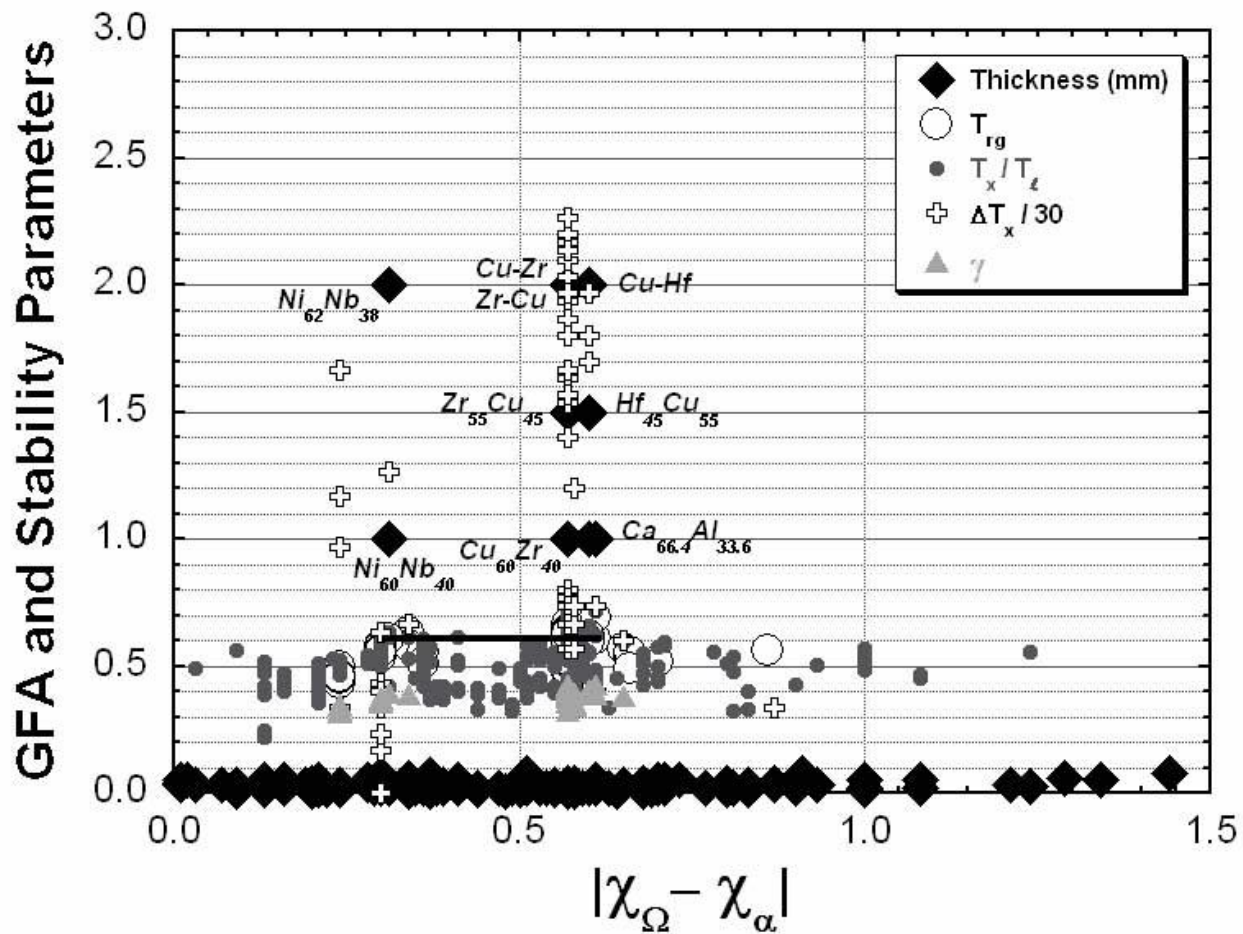


Figure 15 GFA and thermal stability parameters v. the absolute difference in solute and solvent Pauling electronegativities. The solid curve is a linear regression fit to T_{rg} datapoints for binary BMGs only. For convenience, ΔT_x is reduced by a factor of 30 to fit the same scale.

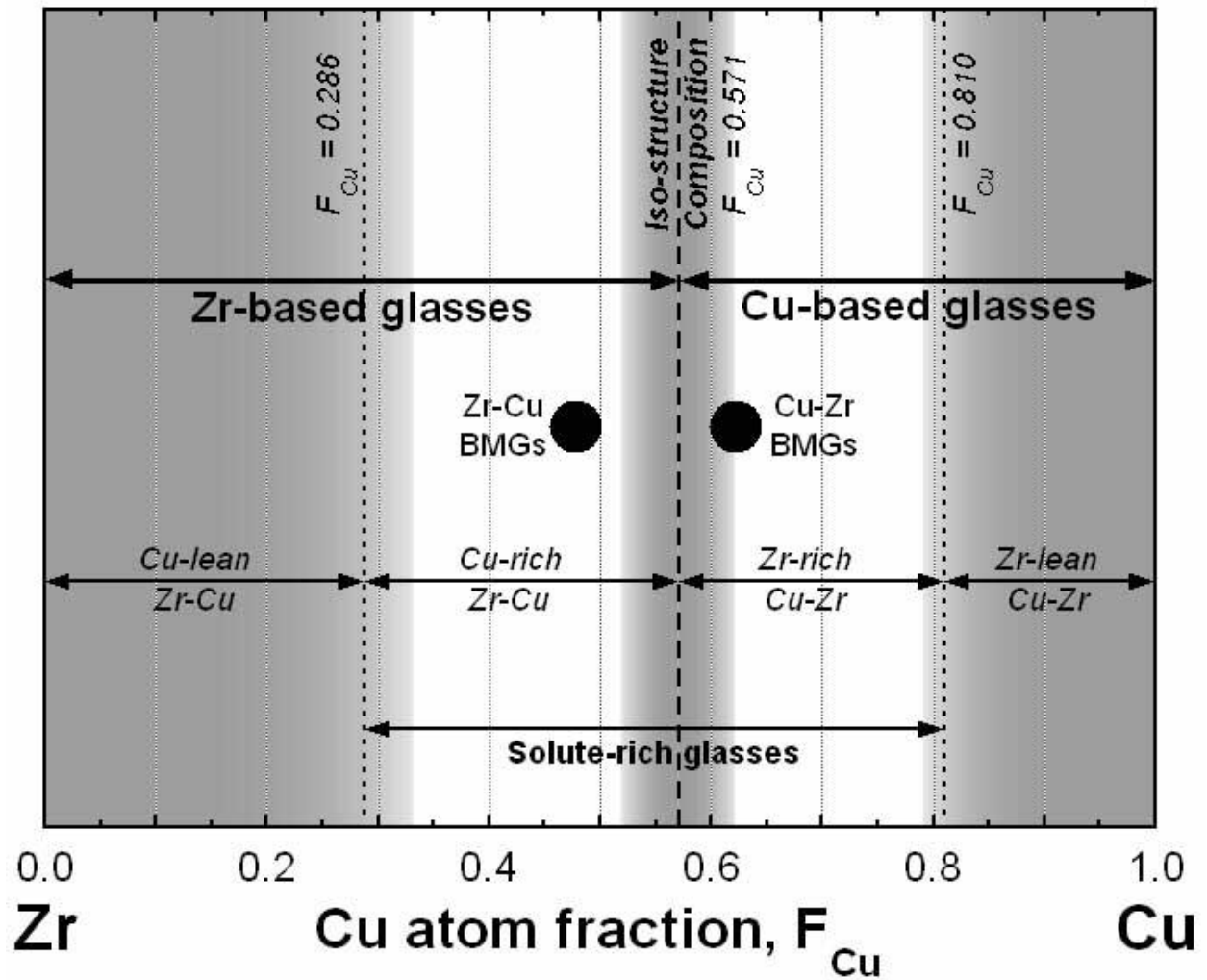


Figure 16 Illustration of composition ranges for Zr-Cu and Cu-Zr binary systems. Solute-rich Zr-Cu BMGs and solute-rich Cu-Zr BMGs both approach the iso-structural composition. The iso-structural composition and the compositions of the boundaries between solute-rich and solute lean structures depend explicitly on the radius ratio of the glass system.

Appendix

Table A1. Binary metallic glass constitutions, densities, characteristic temperatures and structural parameters.

Ω	α	F_α	R	$\rho, \text{g cm}^{-3}$	T_g, K	T_x, K	T_l, K	T_{rg}	ΔT_x	T_x/T_l	γ	S_β	S_α	S_β	$S(\alpha_\alpha)$	$S(\alpha_\beta)$	$S(\alpha_\gamma)$	$S(\alpha_\Omega)$	$Z_{\alpha\alpha}$	$Z_{\alpha\Omega}$	$Z_{\Omega\alpha}$	$Z_{\Omega\Omega}$	Citations
Al	Ca	0.090	1.426			408	955		0.427			19.88	1.97	19.88	1	0.97	0	0					[26]
Al	Ca	0.100	1.426			419	973		0.431			19.88	2.21	19.88	1	1	0.21	0					[26]
Al	Ca	0.110	1.426			425	1003		0.424			19.88	2.46	19.88	1	1	0.46	0					[26]
Al	Ce	0.070	1.291			437	1360		0.321			17.67	1.33	17.67	1	0.33	0	0					[27]
Al	Ce	0.080	1.291			468	1370		0.342			17.67	1.54	17.67	1	0.54	0	0					[27]
Al	Ce	0.090	1.291			483	1390		0.347			17.67	1.75	17.67	1	0.75	0	0					[27]
Al	Ce	0.100	1.291			463	1410		0.328			17.67	1.96	17.67	1	0.96	0	0					[27]
Al	Cu	0.173	0.894									11.12	2.33	11.12	1	1	0.33	0					[28]
Al	Dy	0.090	1.241			478	1278		0.374			16.89	1.67	16.89	1	0.67	0	0					[29]
Al	Dy	0.100	1.241			520	1353		0.384			16.89	1.88	16.89	1	0.88	0	0					[29]
Al	Dy	0.110	1.241			530	1363		0.389			16.89	2.09	16.89	1	1	0.09	0					[29]
Al	Dy	0.120	1.241			515	1393		0.370			16.89	2.30	16.89	1	1	0.3	0					[29]
Al	Er	0.090	1.241			435	1183		0.368			16.89	1.67	16.89	1	0.67	0	0					[29]
Al	Er	0.100	1.241			460	1193		0.386			16.89	1.88	16.89	1	0.88	0	0					[29]
Al	Er	0.115	1.241			505	1233		0.410			16.89	2.19	16.89	1	1	0.19	0					[29]
Al	Gd	0.080	1.248			470	1133		0.415			17.00	1.48	17.00	1	0.48	0	0					[29]
Al	Gd	0.100	1.248			505	1223		0.413			17.00	1.89	17.00	1	0.89	0	0					[29]
Al	Gd	0.120	1.248			510	1273		0.401			17.00	2.32	17.00	1	1	0.32	0					[29]
Al	Ho	0.090	1.255			445	1192		0.373			17.11	1.69	17.11	1	0.69	0	0					[29]
Al	Ho	0.100	1.255			495	1223		0.405			17.11	1.90	17.11	1	0.9	0	0					[29]
Al	Ho	0.110	1.255			530	1253		0.423			17.11	2.12	17.11	1	1	0.12	0					[29]

Corresponding Author:

Dr. Daniel B. Miracle
Air Force Research Laboratory, 2230 Tenth Street
Wright-Patterson AFB, OH 45433-7817 USA
Email: Daniel.miracle@wpafb.af.mil

Al	La	0.070	1.326		442	1153	0.383		18.24	1.37	18.24	1	0.37	0	0					[29, 30]
Al	La	0.080	1.326		472	1188	0.397		18.24	1.59	18.24	1	0.59	0	0					[29]
Al	La	0.090	1.326		480	1233	0.389		18.24	1.80	18.24	1	0.8	0	0					[29]
Al	La	0.100	1.326		477	1273	0.375		18.24	2.03	18.24	1	1	0.03	0					[29, 31]
Al	La	0.140	1.326		540	1418	0.381		18.24	2.97	18.24	1	1	0.97	0					[30]
Al	La	0.414	1.326						16.53	8.50	12.03	1	1	2	4.5					[30]
Al	Nd	0.080	1.262		450	913	0.493		17.22	1.50	17.22	1	0.5	0	0					[29, 32]
Al	Nd	0.100	1.262		500	1223	0.409		17.22	1.91	17.22	1	0.91	0	0					[29, 32]
Al	Nd	0.120	1.262		511	1373	0.372		17.22	2.35	17.22	1	1	0.35	0					[29, 32]
Al	Pr	0.100	1.298						17.79	1.98	17.79	1	0.98	0	0					[29]
Al	Sm	0.080	1.312		455	1133	0.402		18.01	1.57	18.01	1	0.57	0	0					[29, 33]
Al	Sm	0.100	1.312		493	1200	0.411		18.01	2.00	18.01	1	1	0	0					[29]
Al	Sm	0.120	1.312		505	1253	0.403		18.01	2.46	18.01	1	1	0.46	0					[29]
Al	Sm	0.140	1.312		509	1313	0.388		18.01	2.93	18.01	1	1	0.93	0					[29]
Al	Sm	0.160	1.312		502	1513	0.332		18.01	3.43	18.01	1	1	1.43	0					[29]
Al	Tb	0.090	1.277		468	1203	0.389		17.45	1.73	17.45	1	0.73	0	0					[29]
Al	Tb	0.100	1.277		502	1243	0.404		17.45	1.94	17.45	1	0.94	0	0					[29]
Al	Tb	0.110	1.277		535	1273	0.420		17.45	2.16	17.45	1	1	0.16	0					[29]
Al	Tb	0.120	1.277		505	1293	0.391		17.45	2.38	17.45	1	1	0.38	0					[29]
Al	Y	0.090	1.27		437	1153	0.379		17.34	1.71	17.34	1	0.71	0	0					[27]
Al	Y	0.100	1.27		496	1174	0.422		17.34	1.93	17.34	1	0.93	0	0	10.7	1.6	14.1	1.1	[27, 34]
Al	Y	0.110	1.27		502	1213	0.414		17.34	2.14	17.34	1	1	0.14	0					[27]
Al	Y	0.120	1.27		526	1243	0.423		17.34	2.36	17.34	1	1	0.36	0					[27]
Al	Y	0.130	1.27		518	1283	0.404		17.34	2.59	17.34	1	1	0.59	0					[27]
Al	Yb	0.090	1.348		450	1133	0.397		18.59	1.84	18.59	1	0.84	0	0					[29]
Al	Yb	0.100	1.348		455	1153	0.395		18.59	2.07	18.59	1	1	0.07	0					[29]
Al	Yb	0.115	1.348		480	1198	0.401		18.59	2.42	18.59	1	1	0.42	0					[29]
Au	Si	0.170	0.764						9.60	1.97	9.60	1	0.97	0	0					[35]
Au	Si	0.186	0.764		280	623	0.449		9.60	2.19	9.60	1	1	0.19	0					[36]
Au	Si	0.200	0.764						9.60	2.40	9.60	1	1	0.4	0					[35]
Au	Si	0.250	0.764						9.60	3.20	9.60	1	1	1.2	0					[37]
B	N	0.220	0.818						10.22	2.88	10.22	1	1	0.88	0					[38]

B	N	0.420	0.818	1.96	528	540	873	0.605	0.619	12	0.385	10.59	6.13	8.46	1	1	2	2.13				[38]
Ba	Al	0.280	0.632									8.17	3.18	8.17	1	1	1.18	0				[39]
Ba	Ga	0.240	0.601									7.84	2.48	7.84	1	1	0.48	0				[39]
Ba	Mg	0.350	0.717									9.24	4.63	8.61	1	1	2	0.63				[39]
Ba	Zn	0.250	0.619									8.02	2.67	8.02	1	1	0.67	0				[39]
Ca	Ag	0.125	0.716									9.07	1.30	9.07	1	0.3	0	0				[40]
Ca	Ag	0.350	0.716									9.23	4.63	8.60	1	1	2	0.63				[40, 41]
Ca	Ag	0.425	0.716									9.51	5.74	7.77	1	1	2	1.74				[40]
Ca	Al	0.125	0.701									8.91	1.27	8.91	1	0.27	0	0				[40]
Ca	Al	0.336	0.701									9.00	4.37	8.63	1	1	2	0.37				[42]
Ca	Al	0.350	0.701	563	585	818	0.688	0.715	22	0.424	9.05	4.57	8.49	1	1	2	0.57	[39, 40]				
Ca	Al	0.400	0.701	9.25	5.30	7.95	1	1	2	1.3	[43]											
Ca	Al	0.475	0.701	9.55	6.44	7.11	1	1	2	2.44	[40]											
Ca	Au	0.350	0.716	9.23	4.63	8.60	1	1	2	0.63	[41]											
Ca	Cu	0.125	0.627	1.81	8.11	1.16	8.11	1	0.16	0	0	[40]										
Ca	Cu	0.300	0.627	8.11	3.48	8.11	1	1	1.48	0	[44]											
Ca	Cu	0.350	0.627	441	1033	8.19	4.27	7.92	1	1	2	0.27	[40, 41]									
Ca	Cu	0.500	0.627	8.87	6.44	6.44	1	1	2	2.44	[40]											
Ca	Cu	0.625	0.627	9.55	8.47	5.08	1	1	2	4.47	[40]											
Ca	Ga	0.160	0.667	8.53	1.62	8.53	1	0.62	0	0	[39]											
Ca	Ga	0.350	0.667	8.65	4.43	8.22	1	1	2	0.43	[41]											
Ca	Mg	0.225	0.796	9.97	2.89	9.97	1	1	0.89	0	[40]											
Ca	Mg	0.270	0.796	9.97	3.69	9.97	1	1	1.69	0	[39]											
Ca	Mg	0.300	0.796	1.45	10.00	4.20	9.80	1	1	2	0.2	[44]										
Ca	Mg	0.350	0.796	414	987	10.15	4.95	9.19	1	1	2	0.95	[40, 41]									
Ca	Mg	0.400	0.796	1.47	10.29	5.72	8.57	1	1	2	1.72	[43]										
Ca	Mg	0.425	0.796	10.37	6.11	8.26	1	1	2	2.11	[40]											
Ca	Pd	0.350	0.706	9.11	4.59	8.52	1	1	2	0.59	[41]											
Ca	Zn	0.175	0.687	8.75	1.86	8.75	1	0.86	0	0	[40]											
Ca	Zn	0.270	0.687	8.75	3.23	8.75	1	1	1.23	0	[39]											
Ca	Zn	0.350	0.687	389	407	687	0.566	0.592	18	0.378	8.88	4.51	8.37	1	1	2	0.51	[40]				
Ca	Zn	0.500	0.687	9.50	6.75	6.75	1	1	2	2.75	[40]											

Ca	Zn	0.609	0.687						10.01	8.53	5.48	1	1	2	4.53				[40]
Ce	Au	0.200	0.791						9.91	2.48	9.91	1	1	0.48	0				[45]
Co	B	0.110	0.704						8.94	1.10	8.94	1	0.1	0	0				[46]
Co	B	0.120	0.704						8.94	1.22	8.94	1	0.22	0	0				[46]
Co	B	0.160	0.704	8.225					8.94	1.70	8.94	1	0.7	0	0				[46, 47]
Co	B	0.170	0.704	8.34					8.94	1.83	8.94	1	0.83	0	0				[48]
Co	B	0.180	0.704		656	1403	0.468		8.94	1.96	8.94	1	0.96	0	0				[49]
Co	B	0.180	0.704	8.205	603	1403	0.430		8.94	1.96	8.94	1	0.96	0	0				[47, 50]
Co	B	0.185	0.704	8.29	603	1383	0.436		8.94	2.03	8.94	1	1	0.03	0				[51]
Co	B	0.200	0.704		659	1393	0.473		8.94	2.23	8.94	1	1	0.23	0				[49]
Co	B	0.200	0.704	8.11					8.94	2.23	8.94	1	1	0.23	0				[51]
Co	B	0.200	0.704	8.185					8.94	2.23	8.94	1	1	0.23	0				[46, 47]
Co	B	0.220	0.704		660	1433	0.461		8.94	2.52	8.94	1	1	0.52	0				[49]
Co	B	0.220	0.704	8.12	638	1433	0.445		8.94	2.52	8.94	1	1	0.52	0				[47, 50]
Co	B	0.230	0.704	8.16					8.94	2.67	8.94	1	1	0.67	0				[48]
Co	B	0.240	0.704		660	1468	0.450		8.94	2.82	8.94	1	1	0.82	0				[49]
Co	B	0.240	0.704	8.055					8.94	2.82	8.94	1	1	0.82	0				[46, 47]
Co	B	0.250	0.704	8.02					8.94	2.98	8.94	1	1	0.98	0				[51]
Co	B	0.260	0.704		671	1503	0.446		8.94	3.14	8.94	1	1	1.14	0				[49]
Co	B	0.260	0.704		690	1503	0.459		8.94	3.14	8.94	1	1	1.14	0				[50]
Co	B	0.280	0.704		696	1538	0.453		8.94	3.47	8.94	1	1	1.47	0				[49]
Co	B	0.280	0.704	7.93					8.94	3.47	8.94	1	1	1.47	0				[46, 47]
Co	B	0.300	0.704	7.73					8.94	3.83	8.94	1	1	1.83	0				[51]
Co	B	0.300	0.704	7.86					8.94	3.83	8.94	1	1	1.83	0				[47, 50]
Co	B	0.310	0.704	7.815					8.94	4.01	8.93	1	1	2	0.01				[47]
Co	B	0.320	0.704						8.97	4.15	8.82	1	1	2	0.15				[46]
Co	B	0.330	0.704						9.01	4.29	8.72	1	1	2	0.29				[46]
Co	B	0.340	0.704						9.05	4.44	8.61	1	1	2	0.44				[52]
Co	B	0.350	0.704	7.59					9.08	4.58	8.50	1	1	2	0.58				[51]
Co	B	0.360	0.704		704	1523	0.462		9.12	4.72	8.40	1	1	2	0.72				[50, 53]
Co	B	0.380	0.704		725	1573	0.461		9.20	5.01	8.18	1	1	2	1.01				[50, 53]
Co	B	0.400	0.704	7.44	647	1623	0.399		9.27	5.31	7.96	1	1	2	1.31				[50, 51, 53]

Co	P	0.190	0.816	7.97								10.20	2.39	10.20	1	1	0.39	0									[54, 55]
Co	P	0.200	0.816									10.20	2.55	10.20	1	1	0.55	0	0	8.9	2.23	10.1					[56]
Co	P	0.203	0.816	7.94								10.20	2.60	10.20	1	1	0.6	0									[54]
Co	P	0.220	0.816	7.89								10.20	2.88	10.20	1	1	0.88	0									[54]
Co	P	0.236	0.816	7.9								10.20	3.15	10.20	1	1	1.15	0									[54]
Co	Ti	0.210	1.136									15.28	4.05	15.23	1	1	2	0.05									[57]
Co	Ti	0.220	1.136		777	1463		0.531				15.26	4.24	15.02	1	1	2	0.24									[57]
Co	Ti	0.230	1.136									15.23	4.42	14.81	1	1	2	0.42									[57]
Co	Zr	0.090	1.264		779	1543		0.505				17.25	1.71	17.25	1	0.71	0	0									[58]
Co	Zr	0.100	1.264		776	1505		0.516				17.25	1.92	17.25	1	0.92	0	0									[58]
Co	Zr	0.100	1.264		833	1505		0.553				17.25	1.92	17.25	1	0.92	0	0									[59, 60]
Co	Zr	0.100	1.264		804	1505		0.534				17.25	1.92	17.25	1	0.92	0	0									[61]
Co	Zr	0.100	1.264		764	1505		0.508				17.25	1.92	17.25	1	0.92	0	0									[62]
Co	Zr	0.110	1.264		768	1506		0.510				17.25	2.13	17.25	1	1	0.13	0									[58]
Co	Zr	0.120	1.264									17.25	2.35	17.25	1	1	0.35	0									[60]
Co	Zr	0.400	1.264									16.04	8.01	12.02	1	1	2	4.01									[63]
Co	Zr	0.426	1.264									15.90	8.48	11.42	1	1	2	4.48									[63]
Cu	Hf	0.300	1.254									16.47	6.14	14.33	1	1	2	2.14									[64]
Cu	Hf	0.350	1.254	781	832	1259	0.621	0.661	51	0.408		16.20	7.07	13.13	1	1	2	3.07									[65]
Cu	Hf	0.400	1.254	773	827	1290	0.599	0.641	54	0.401		15.94	7.98	11.96	1	1	2	3.98									[64, 66]
Cu	Hf	0.428	1.254									15.80	8.47	11.32	1	1	2	4.47									[64]
Cu	Te	0.420	1.111									14.47	7.76	10.71	1	1	2	3.76									[67]
Cu	Ti	0.250	1.127									15.05	4.76	14.29	1	1	2	0.76									[68]
Cu	Ti	0.270	1.127									15.00	5.13	13.87	1	1	2	1.13									[68, 69]
Cu	Ti	0.300	1.127		692	1143		0.605				14.92	5.68	13.25	1	1	2	1.68									[68-71]
Cu	Ti	0.340	1.127		697	1173		0.594				14.82	6.40	12.42	1	1	2	2.4									[71]
Cu	Ti	0.350	1.127									14.80	6.58	12.22	1	1	2	2.58									[70]
Cu	Ti	0.400	1.127	6.69								14.67	7.47	11.20	1	1	2	3.47									[68, 69, 72]
Cu	Ti	0.420	1.127		701	1228		0.571				14.63	7.82	10.80	1	1	2	3.82									[71]
Cu	Ti	0.430	1.127									14.60	8.00	10.60	1	1	2	4									[73]
Cu	Ti	0.450	1.127									14.55	8.35	10.20	1	1	2	4.35									[68]
Cu	Y	0.167	1.421									19.80	3.97	19.80	1	1	1.97	0	10.4	2.8	14	0					[56, 74]

Cu	Zr	0.100	1.254	7.54		880	1263		0.697			17.09	1.90	17.09	1	0.9	0	0					[75]
Cu	Zr	0.120	1.254				885	1285		0.688			17.09	2.33	17.09	1	1	0.33	0				[75]
Cu	Zr	0.250	1.254										16.75	5.19	15.56	1	1	2	1.19				[70]
Cu	Zr	0.280	1.254			780	804	1358	0.574	0.592	24	0.376	16.58	5.76	14.82	1	1	2	1.76				[76]
Cu	Zr	0.300	1.254				788	1333		0.591			16.47	6.14	14.33	1	1	2	2.14				[64, 75]
Cu	Zr	0.340	1.254			762	785	1263	0.603	0.622	23	0.388	16.25	6.89	13.37	1	1	2	2.89				[77, 78]
Cu	Zr	0.350	1.254			781	798	1248	0.626	0.639	17	0.393	16.20	7.07	13.13	1	1	2	3.07				[75, 79]
Cu	Zr	0.350	1.254			745	792	1279	0.582	0.619	47	0.391	16.20	7.07	13.13	1	1	2	3.07				[76]
Cu	Zr	0.355	1.254			747	769	1243	0.601	0.618	22	0.386	16.17	7.16	13.01	1	1	2	3.16				[80]
Cu	Zr	0.360	1.254			787	833	1233	0.638	0.676	46	0.412	16.15	7.25	12.89	1	1	2	3.25				[72, 78]
Cu	Zr	0.380	1.254			728	793	1158	0.629	0.685	65	0.421	16.04	7.62	12.43	1	1	2	3.62				[75]
Cu	Zr	0.382	1.254			767	823	1158	0.662	0.711	56	0.428	16.03	7.65	12.38	1	1	2	3.65				[78]
Cu	Zr	0.400	1.254			740	760	1198	0.618	0.634	20	0.392	15.94	7.98	11.96	1	1	2	3.98				[36, 64, 81]
Cu	Zr	0.400	1.254			714	764	1198	0.596	0.638	50	0.400	15.94	7.98	11.96	1	1	2	3.98				[76]
Cu	Zr	0.400	1.254			763	812	1198	0.637	0.677	49	0.414	15.94	7.98	11.96	1	1	2	3.98				[79]
Cu	Zr	0.400	1.254			733	791	1198	0.612	0.660	58	0.410	15.94	7.98	11.96	1	1	2	3.98				[66]
Cu	Zr	0.400	1.254		755	811	1198	0.630	0.677	56	0.415	15.94	7.98	11.96	1	1	2	3.98				[78]	
Cu	Zr	0.428	1.254									15.80	8.47	11.32	1	1	2	4.47				[64, 70]	
Dy	Al	0.400	0.806									10.40	5.76	8.64	1	1	2	1.76				[82]	
Dy	Al	0.450	0.806									10.54	6.54	8.00	1	1	2	2.54				[82]	
Dy	Al	0.500	0.806									10.69	7.34	7.34	1	1	2	3.34				[82]	
Dy	Al	0.550	0.806									10.84	8.16	6.68	1	1	2	4.16				[82]	
Dy	Au	0.200	0.823									10.28	2.57	10.28	1	1	0.57	0				[45]	
Dy	Cu	0.300	0.72			540						9.11	3.90	9.11	1	1	1.9	0				[75]	
Dy	Ni	0.310	0.72									9.13	4.07	9.06	1	1	2	0.07	3	10.8	4.85	12.4	[56]
Er	Au	0.200	0.823									10.28	2.57	10.28	1	1	0.57	0				[45]	
Er	Cu	0.300	0.72			566						9.11	3.90	9.11	1	1	1.9	0				[75]	
Er	Fe	0.320	0.714									9.10	4.19	8.90	1	1	2	0.19				[74]	
Eu	Au	0.200	0.735									9.27	2.32	9.27	1	1	0.32	0				[45]	
Fe	B	0.090	0.704									8.94	0.88	8.94	0.88	0	0	0				[83]	
Fe	B	0.110	0.704									8.94	1.10	8.94	1	0.1	0	0				[83]	
Fe	B	0.120	0.704	7.44		595	1573		0.378			8.94	1.22	8.94	1	0.22	0	0				[83]	

Fe	B	0.120	0.704			560	1573	0.356			8.94	1.22	8.94	1	0.22	0	0																																																																																																																																																																																																																																																																																																																																																																																																																																																																																																																																																																																																																																																																																																																																																																																																																																																																																																																																																																																																																																																																																																																																																																																																																																																																																																																																																																																																														
----	---	-------	-------	--	--	-----	------	-------	--	--	------	------	------	---	------	---	---	--	--	--	--	--	--	--	--	--	--	--	--	--	--	--	--	--	--	--	--	--	--	--	--	--	--	--	--	--	--	--	--	--	--	--	--	--	--	--	--	--	--	--	--	--	--	--	--	--	--	--	--	--	--	--	--	--	--	--	--	--	--	--	--	--	--	--	--	--	--	--	--	--	--	--	--	--	--	--	--	--	--	--	--	--	--	--	--	--	--	--	--	--	--	--	--	--	--	--	--	--	--	--	--	--	--	--	--	--	--	--	--	--	--	--	--	--	--	--	--	--	--	--	--	--	--	--	--	--	--	--	--	--	--	--	--	--	--	--	--	--	--	--	--	--	--	--	--	--	--	--	--	--	--	--	--	--	--	--	--	--	--	--	--	--	--	--	--	--	--	--	--	--	--	--	--	--	--	--	--	--	--	--	--	--	--	--	--	--	--	--	--	--	--	--	--	--	--	--	--	--	--	--	--	--	--	--	--	--	--	--	--	--	--	--	--	--	--	--	--	--	--	--	--	--	--	--	--	--	--	--	--	--	--	--	--	--	--	--	--	--	--	--	--	--	--	--	--	--	--	--	--	--	--	--	--	--	--	--	--	--	--	--	--	--	--	--	--	--	--	--	--	--	--	--	--	--	--	--	--	--	--	--	--	--	--	--	--	--	--	--	--	--	--	--	--	--	--	--	--	--	--	--	--	--	--	--	--	--	--	--	--	--	--	--	--	--	--	--	--	--	--	--	--	--	--	--	--	--	--	--	--	--	--	--	--	--	--	--	--	--	--	--	--	--	--	--	--	--	--	--	--	--	--	--	--	--	--	--	--	--	--	--	--	--	--	--	--	--	--	--	--	--	--	--	--	--	--	--	--	--	--	--	--	--	--	--	--	--	--	--	--	--	--	--	--	--	--	--	--	--	--	--	--	--	--	--	--	--	--	--	--	--	--	--	--	--	--	--	--	--	--	--	--	--	--	--	--	--	--	--	--	--	--	--	--	--	--	--	--	--	--	--	--	--	--	--	--	--	--	--	--	--	--	--	--	--	--	--	--	--	--	--	--	--	--	--	--	--	--	--	--	--	--	--	--	--	--	--	--	--	--	--	--	--	--	--	--	--	--	--	--	--	--	--	--	--	--	--	--	--	--	--	--	--	--	--	--	--	--	--	--	--	--	--	--	--	--	--	--	--	--	--	--	--	--	--	--	--	--	--	--	--	--	--	--	--	--	--	--	--	--	--	--	--	--	--	--	--	--	--	--	--	--	--	--	--	--	--	--	--	--	--	--	--	--	--	--	--	--	--	--	--	--	--	--	--	--	--	--	--	--	--	--	--	--	--	--	--	--	--	--	--	--	--	--	--	--	--	--	--	--	--	--	--	--	--	--	--	--	--	--	--	--	--	--	--	--	--	--	--	--	--	--	--	--	--	--	--	--	--	--	--	--	--	--	--	--	--	--	--	--	--	--	--	--	--	--	--	--	--	--	--	--	--	--	--	--	--	--	--	--	--	--	--	--	--	--	--	--	--	--	--	--	--	--	--	--	--	--	--	--	--	--	--	--	--	--	--	--	--	--	--	--	--	--	--	--	--	--	--	--	--	--	--	--	--	--	--	--	--	--	--	--	--	--	--	--	--	--	--	--	--	--	--	--	--	--	--	--	--	--	--	--	--	--	--	--	--	--	--	--	--	--	--	--	--	--	--	--	--	--	--	--	--	--	--	--	--	--	--	--	--	--	--	--	--	--	--	--	--	--	--	--	--	--	--	--	--	--	--	--	--	--	--	--	--	--	--	--	--	--	--	--	--	--	--	--	--	--	--	--	--	--	--	--	--	--	--	--	--	--	--	--	--	--	--	--	--	--	--	--	--	--	--	--	--	--	--	--	--	--	--	--	--	--	--	--	--	--	--	--	--	--	--	--	--	--	--	--	--	--	--	--	--	--	--	--	--	--	--	--	--	--	--	--	--	--	--	--	--	--	--	--	--	--	--	--	--	--	--	--	--	--	--	--	--	--	--	--	--	--	--	--	--	--	--	--	--	--	--	--	--	--	--	--	--	--	--	--	--	--	--	--	--	--	--	--	--	--	--	--	--	--	--	--	--	--	--	--	--	--	--	--	--	--	--	--	--	--	--	--	--	--	--	--	--	--	--	--	--	--	--	--	--	--	--	--	--	--	--	--	--	--	--	--	--	--	--	--	--	--	--	--	--	--	--	--	--	--	--	--	--	--	--	--	--	--	--	--	--	--	--	--	--	--	--	--	--	--	--	--	--	--	--	--	--	--	--	--	--	--	--	--	--	--	--	--	--	--	--	--	--	--	--	--	--	--	--	--	--	--	--	--	--	--	--	--	--	--	--	--	--	--	--	--	--	--	--	--	--	--	--	--	--	--	--	--	--	--	--	--	--	--	--	--	--	--	--	--	--	--	--	--	--	--	--	--	--	--	--	--	--	--	--	--	--	--	--	--	--	--	--	--	--	--	--	--	--	--	--	--	--	--	--	--	--	--	--	--	--	--	--	--	--	--	--	--	--	--	--	--	--	--	--	--	--	--	--	--	--	--	--	--	--	--	--	--	--	--	--	--	--	--	--	--	--	--	--	--	--	--	--	--	--	--	--	--	--	--	--	--	--	--	--	--	--	--	--	--	--	--	--	--	--	--	--	--	--	--	--	--	--	--	--	--	--	--	--	--	--	--	--	--	--	--	--	--	--	--	--	--	--	--	--	--	--	--	--	--	--	--	--	--	--	--	--	--	--	--	--	--	--	--	--	--	--	--	--	--	--	--	--	--	--	--	--	--	--	--	--	--	--	--	--	--	--	--	--	--	--	--	--	--	--	--	--	--	--	--	--	--	--	--	--	--	--	--	--	--	--	--	--	--	--	--	--	--	--	--	--	--	--	--	--	--	--	--	--	--	--	--	--	--	--	--	--	--	--	--	--	--	--	--	--	--	--	--	--	--	--	--	--	--	--	--	--	--	--	--	--	--	--	--	--	--	--	--	--	--	--	--	--	--	--	--	--	--	--	--	--	--	--	--	--	--	--	--	--	--	--	--	--	--	--	--	--	--

Fe	B	0.240	0.704		677	1593	0.425		8.94	2.82	8.94	1	1	0.82	0					[84]
Fe	B	0.250	0.704	7.27					8.94	2.98	8.94	1	1	0.98	0					[54, 87]
Fe	B	0.250	0.704	7.22					8.94	2.98	8.94	1	1	0.98	0					[48]
Fe	B	0.260	0.704	7.215	734	1618	0.454		8.94	3.14	8.94	1	1	1.14	0					[54]
Fe	B	0.260	0.704		685	1618	0.423		8.94	3.14	8.94	1	1	1.14	0					[84]
Fe	B	0.270	0.704	7.18					8.94	3.30	8.94	1	1	1.3	0					[54]
Fe	B	0.280	0.704	7.09					8.94	3.47	8.94	1	1	1.47	0					[84]
Fe	C	0.155	0.616						7.99	1.47	7.99	1	0.47	0	0					[12]
Fe	Hf	0.090	1.264						17.25	1.71	17.25	1	0.71	0	0					[12]
Fe	Nd	0.150	1.424						19.85	3.50	19.85	1	1	1.5	0					[79]
Fe	Nd	0.180	1.424						19.72	4.27	19.45	1	1	2	0.27					[79]
Fe	Nd	0.210	1.424						19.39	4.91	18.48	1	1	2	0.91					[79]
Fe	Nd	0.250	1.424						18.97	5.74	17.22	1	1	2	1.74					[79]
Fe	P	0.145	0.816	7.285					10.20	1.73	10.20	1	0.73	0	0					[47]
Fe	P	0.145	0.816	7.25					10.20	1.73	10.20	1	0.73	0	0					[54]
Fe	P	0.150	0.816						10.20	1.80	10.20	1	0.8	0	0					[88]
Fe	P	0.160	0.816	7.27					10.20	1.94	10.20	1	0.94	0	0					[47]
Fe	P	0.160	0.816	7.2					10.20	1.94	10.20	1	0.94	0	0					[54]
Fe	P	0.170	0.816	7.26	640	1321	0.484		10.20	2.09	10.20	1	1	0.09	0					[47, 86, 88]
Fe	P	0.180	0.816	7.225					10.20	2.24	10.20	1	1	0.24	0					[47, 88]
Fe	P	0.182	0.816	7.14					10.20	2.27	10.20	1	1	0.27	0					[54]
Fe	P	0.190	0.816	7.175					10.20	2.39	10.20	1	1	0.39	0					[47]
Fe	P	0.200	0.816	7.118					10.20	2.55	10.20	1	1	0.55	0					[47, 88]
Fe	P	0.200	0.816	7.1					10.20	2.55	10.20	1	1	0.55	0					[54]
Fe	P	0.216	0.816	7.03					10.20	2.81	10.20	1	1	0.81	0					[54]
Fe	P	0.240	0.816						10.20	3.22	10.20	1	1	1.22	0					[88]
Fe	P	0.250	0.816						10.20	3.40	10.20	1	1	1.4	0	3.5	8.1	2.6	10.4	[88]
Fe	P	0.260	0.816						10.20	3.58	10.20	1	1	1.58	0					[88]
Fe	Sc	0.100	1.296						17.76	1.97	17.76	1	0.97	0	0					[89]
Fe	Si	0.250	0.88						10.95	3.65	10.95	1	1	1.65	0					[87]
Fe	Th	0.280	1.424		813	1523	0.534		18.66	6.34	16.31	1	1	2	2.34					[90]
Fe	Th	0.300	1.424		808	1458	0.554		18.46	6.74	15.72	1	1	2	2.74					[90]

Fe	Th	0.310	1.424		745	1383	0.539		18.36	6.93	15.43	1	1	2	2.93				[90]
Fe	Th	0.330	1.424		745	1383	0.539		18.17	7.32	14.85	1	1	2	3.32				[90, 91]
Fe	Th	0.395	1.424						17.56	8.52	13.05	1	1	2	4.52				[90, 91]
Fe	Zr	0.080	1.264						17.25	1.50	17.25	1	0.5	0	0				[92]
Fe	Zr	0.090	1.264		774	1653	0.468		17.25	1.71	17.25	1	0.71	0	0				[58, 93, 94]
Fe	Zr	0.100	1.264		775	1610	0.481		17.25	1.92	17.25	1	0.92	0	0				[58, 92, 93]
Fe	Zr	0.100	1.264		791	1610	0.491		17.25	1.92	17.25	1	0.92	0	0				[61, 62, 95]
Fe	Zr	0.110	1.264		770	1673	0.460		17.25	2.13	17.25	1	1	0.13	0				[58, 93]
Fe	Zr	0.120	1.264						17.25	2.35	17.25	1	1	0.35	0				[92, 93]
Gd	Ag	0.300	0.818						10.27	4.28	9.99	1	1	2	0.28				[96, 97]
Gd	Ag	0.460	0.818						10.70	6.76	7.94	1	1	2	2.76				[96]
Gd	Al	0.220	0.801		591	1173	0.504		10.03	2.83	10.03	1	1	0.83	0				[96-98]
Gd	Al	0.400	0.801						10.35	5.74	8.61	1	1	2	1.74				[82]
Gd	Al	0.450	0.801						10.49	6.52	7.97	1	1	2	2.52				[82]
Gd	Al	0.500	0.801						10.64	7.32	7.32	1	1	2	3.32				[82]
Gd	Al	0.550	0.801						10.80	8.14	6.66	1	1	2	4.14				[82]
Gd	Au	0.200	0.818						10.22	2.56	10.22	1	1	0.56	0				[45, 96, 97]
Gd	Au	0.250	0.818						10.22	3.41	10.22	1	1	1.41	0				[99]
Gd	C	0.200	0.438						6.22	1.55	6.22	1	0.55	0	0				[97]
Gd	Co	0.310	0.71		550	1033	0.532		9.01	4.03	8.98	1	1	2	0.03				[98]
Gd	Co	0.400	0.71						9.34	5.34	8.01	1	1	2	1.34				[100]
Gd	Co	0.450	0.71		590	1153	0.512		9.54	6.09	7.45	1	1	2	2.09				[98, 100]
Gd	Co	0.500	0.71		600	1273	0.471		9.74	6.87	6.87	1	1	2	2.87				[100]
Gd	Co	0.550	0.71		575	1353	0.425		9.96	7.68	6.28	1	1	2	3.68				[98]
Gd	Cu	0.240	0.716		473	1073	0.441		9.07	2.86	9.07	1	1	0.86	0				[98]
Gd	Cu	0.300	0.716		470	948	0.496		9.07	3.89	9.07	1	1	1.89	0				[96-98]
Gd	Cu	0.340	0.716		473	1025	0.461		9.19	4.48	8.70	1	1	2	0.48				[98]
Gd	Cu	0.580	0.716						10.14	8.20	5.94	1	1	2	4.2				[75]
Gd	Fe	0.320	0.71						9.05	4.18	8.87	1	1	2	0.18				[98]
Gd	Fe	0.400	0.71		413	1223	0.338		9.34	5.34	8.01	1	1	2	1.34				[98]
Gd	Fe	0.500	0.71						9.74	6.87	6.87	1	1	2	2.87				[98]
Gd	Ga	0.210	0.761		558	1153	0.484		9.57	2.54	9.57	1	1	0.54	0				[96-98]

Gd	Ga	0.250	0.761								9.57	3.19	9.57	1	1	1.19	0																																																																																																																																																																																																																																																																																																																																																																																																																																																																																																																																																																																																																																																																																																																																																																																																																																																																																																																																																																																																																																																																																																																																																																																																																																																																																																																																																																																																																																																																																					</
----	----	-------	-------	--	--	--	--	--	--	--	------	------	------	---	---	------	---	--	--	--	--	--	--	--	--	--	--	--	--	--	--	--	--	--	--	--	--	--	--	--	--	--	--	--	--	--	--	--	--	--	--	--	--	--	--	--	--	--	--	--	--	--	--	--	--	--	--	--	--	--	--	--	--	--	--	--	--	--	--	--	--	--	--	--	--	--	--	--	--	--	--	--	--	--	--	--	--	--	--	--	--	--	--	--	--	--	--	--	--	--	--	--	--	--	--	--	--	--	--	--	--	--	--	--	--	--	--	--	--	--	--	--	--	--	--	--	--	--	--	--	--	--	--	--	--	--	--	--	--	--	--	--	--	--	--	--	--	--	--	--	--	--	--	--	--	--	--	--	--	--	--	--	--	--	--	--	--	--	--	--	--	--	--	--	--	--	--	--	--	--	--	--	--	--	--	--	--	--	--	--	--	--	--	--	--	--	--	--	--	--	--	--	--	--	--	--	--	--	--	--	--	--	--	--	--	--	--	--	--	--	--	--	--	--	--	--	--	--	--	--	--	--	--	--	--	--	--	--	--	--	--	--	--	--	--	--	--	--	--	--	--	--	--	--	--	--	--	--	--	--	--	--	--	--	--	--	--	--	--	--	--	--	--	--	--	--	--	--	--	--	--	--	--	--	--	--	--	--	--	--	--	--	--	--	--	--	--	--	--	--	--	--	--	--	--	--	--	--	--	--	--	--	--	--	--	--	--	--	--	--	--	--	--	--	--	--	--	--	--	--	--	--	--	--	--	--	--	--	--	--	--	--	--	--	--	--	--	--	--	--	--	--	--	--	--	--	--	--	--	--	--	--	--	--	--	--	--	--	--	--	--	--	--	--	--	--	--	--	--	--	--	--	--	--	--	--	--	--	--	--	--	--	--	--	--	--	--	--	--	--	--	--	--	--	--	--	--	--	--	--	--	--	--	--	--	--	--	--	--	--	--	--	--	--	--	--	--	--	--	--	--	--	--	--	--	--	--	--	--	--	--	--	--	--	--	--	--	--	--	--	--	--	--	--	--	--	--	--	--	--	--	--	--	--	--	--	--	--	--	--	--	--	--	--	--	--	--	--	--	--	--	--	--	--	--	--	--	--	--	--	--	--	--	--	--	--	--	--	--	--	--	--	--	--	--	--	--	--	--	--	--	--	--	--	--	--	--	--	--	--	--	--	--	--	--	--	--	--	--	--	--	--	--	--	--	--	--	--	--	--	--	--	--	--	--	--	--	--	--	--	--	--	--	--	--	--	--	--	--	--	--	--	--	--	--	--	--	--	--	--	--	--	--	--	--	--	--	--	--	--	--	--	--	--	--	--	--	--	--	--	--	--	--	--	--	--	--	--	--	--	--	--	--	--	--	--	--	--	--	--	--	--	--	--	--	--	--	--	--	--	--	--	--	--	--	--	--	--	--	--	--	--	--	--	--	--	--	--	--	--	--	--	--	--	--	--	--	--	--	--	--	--	--	--	--	--	--	--	--	--	--	--	--	--	--	--	--	--	--	--	--	--	--	--	--	--	--	--	--	--	--	--	--	--	--	--	--	--	--	--	--	--	--	--	--	--	--	--	--	--	--	--	--	--	--	--	--	--	--	--	--	--	--	--	--	--	--	--	--	--	--	--	--	--	--	--	--	--	--	--	--	--	--	--	--	--	--	--	--	--	--	--	--	--	--	--	--	--	--	--	--	--	--	--	--	--	--	--	--	--	--	--	--	--	--	--	--	--	--	--	--	--	--	--	--	--	--	--	--	--	--	--	--	--	--	--	--	--	--	--	--	--	--	--	--	--	--	--	--	--	--	--	--	--	--	--	--	--	--	--	--	--	--	--	--	--	--	--	--	--	--	--	--	--	--	--	--	--	--	--	--	--	--	--	--	--	--	--	--	--	--	--	--	--	--	--	--	--	--	--	--	--	--	--	--	--	--	--	--	--	--	--	--	--	--	--	--	--	--	--	--	--	--	--	--	--	--	--	--	--	--	--	--	--	--	--	--	--	--	--	--	--	--	--	--	--	--	--	--	--	--	--	--	--	--	--	--	--	--	--	--	--	--	--	--	--	--	--	--	--	--	--	--	--	--	--	--	--	--	--	--	--	--	--	--	--	--	--	--	--	--	--	--	--	--	--	--	--	--	--	--	--	--	--	--	--	--	--	--	--	--	--	--	--	--	--	--	--	--	--	--	--	--	--	--	--	--	--	--	--	--	--	--	--	--	--	--	--	--	--	--	--	--	--	--	--	--	--	--	--	--	--	--	--	--	--	--	--	--	--	--	--	--	--	--	--	--	--	--	--	--	--	--	--	--	--	--	--	--	--	--	--	--	--	--	--	--	--	--	--	--	--	--	--	--	--	--	--	--	--	--	--	--	--	--	--	--	--	--	--	--	--	--	--	--	--	--	--	--	--	--	--	--	--	--	--	--	--	--	--	--	--	--	--	--	--	--	--	--	--	--	--	--	--	--	--	--	--	--	--	--	--	--	--	--	--	--	--	--	--	--	--	--	--	--	--	--	--	--	--	--	--	--	--	--	--	--	--	--	--	--	--	--	--	--	--	--	--	--	--	--	--	--	--	--	--	--	--	--	--	--	--	--	--	--	--	--	--	--	--	--	--	--	--	--	--	--	--	--	--	--	--	--	--	--	--	--	--	--	--	--	--	--	--	--	--	--	--	--	--	--	--	--	--	--	--	--	--	--	--	--	--	--	--	--	--	--	--	--	--	--	--	--	--	--	--	--	--	--	--	--	--	--	--	--	--	--	--	--	--	--	--	--	--	--	--	--	--	--	--	--	--	--	--	--	--	--	--	--	--	--	--	--	--	--	--	--	--	--	--	--	--	--	--	--	--	--	--	--	--	--	--	--	--	--	--	--	--	--	--	--	--	--	--	--	--	--	--	--	--	--	--	--	--	--	--	--	--	--	--	--	--	--	--	--	--	--	--	--	--	--	--	--	--	--	--	--	--	--	--	--	--	--	--	--	--	--	--	--	--	--	--	--	--	--	--	--	--	--	--	--	--	--	--	--	--	--	--	--	--	--	--	--	--	--	--	--	--	--	--	--	--	--	--	--	--	--	--	--	--	--	--	--	--	--	--	--	--	--	--	--	--	--	--	--	--	--	--	--	--	--	--	--	--	--	--	--	--	--	--	--	--	--	--	--	--	--	--	--	--	--	--	--	--	--	--	--	--	--	--	--	--	--	--	--	--	--	--	--	--	--	--	--	--	--	----

Hf	Ni	0.571	0.797							10.83	8.47	6.36	1	1	2	4.47				[64]
Hf	Si	0.130	0.696							8.85	1.32	8.85	1	0.32	0	0				[104, 105]
Hf	Si	0.150	0.696							8.85	1.56	8.85	1	0.56	0	0				[104, 105]
Hf	Si	0.170	0.696							8.85	1.81	8.85	1	0.81	0	0				[104, 105]
Ho	Au	0.200	0.814							10.17	2.54	10.17	1	1	0.54	0				[45]
La	Ag	0.250	0.77							9.67	3.22	9.67	1	1	1.22	0				[106]
La	Ag	0.260	0.77							9.67	3.40	9.67	1	1	1.4	0				[107]
La	Ag	0.300	0.77	363	913			0.398		9.69	4.11	9.59	1	1	2	0.11				[107]
La	Ag	0.400	0.77							10.01	5.60	8.40	1	1	2	1.6				[107]
La	Ag	0.560	0.77	363	1098			0.331		10.56	8.15	6.40	1	1	2	4.15				[107]
La	Al	0.130	0.754							9.49	1.42	9.49	1	0.42	0	0				[30]
La	Al	0.180	0.754							9.49	2.08	9.49	1	1	0.08	0				[108]
La	Al	0.200	0.754							9.49	2.37	9.49	1	1	0.37	0				[31, 108]
La	Al	0.220	0.754	500	848			0.590		9.49	2.68	9.49	1	1	0.68	0				[30, 108]
La	Al	0.250	0.754							9.49	3.16	9.49	1	1	1.16	0				[108]
La	Al	0.270	0.754							9.49	3.51	9.49	1	1	1.51	0				[108]
La	Al	0.300	0.754	520	955			0.545		9.50	4.05	9.45	1	1	2	0.05				[31, 108]
La	Al	0.320	0.754							9.56	4.34	9.22	1	1	2	0.34				[108]
La	Al	0.340	0.754	540	1023			0.528		9.63	4.63	9.00	1	1	2	0.63				[30, 108]
La	Al	0.360	0.754	560	1058			0.529		9.70	4.93	8.77	1	1	2	0.93				[30]
La	Al	0.400	0.754	580	1113			0.521		9.83	5.53	8.30	1	1	2	1.53				[30, 31]
La	Al	0.500	0.754	620	1413			0.439		10.18	7.09	7.09	1	1	2	3.09				[30, 31]
La	Al	0.550	0.754							10.37	7.90	6.47	1	1	2	3.9				[30]
La	Al	0.585	0.754							10.51	8.49	6.02	1	1	2	4.49				[30]
La	Au	0.180	0.77							9.67	2.12	9.67	1	1	0.12	0				[108, 109]
La	Au	0.200	0.77							9.67	2.42	9.67	1	1	0.42	0				[108, 109]
La	Au	0.220	0.77							9.67	2.73	9.67	1	1	0.73	0				[109]
La	Au	0.240	0.77							9.67	3.05	9.67	1	1	1.05	0				[108-110]
La	Au	0.250	0.77							9.67	3.22	9.67	1	1	1.22	0				[108]
La	Au	0.260	0.77							9.67	3.40	9.67	1	1	1.4	0				[109]
La	Au	0.270	0.77							9.67	3.58	9.67	1	1	1.58	0				[108]
La	Cu	0.270	0.674							8.61	3.18	8.61	1	1	1.18	0				[111]

La	Cu	0.300	0.674	6.07	395	773	0.511			8.61	3.69	8.61	1	1	1.69	0				[31, 75]
La	Cu	0.370	0.674							8.81	4.74	8.07	1	1	2	0.74				[111]
La	Cu	0.375	0.674							8.83	4.81	8.02	1	1	2	0.81				[111]
La	Ga	0.160	0.717							9.07	1.73	9.07	1	0.73	0	0				[112]
La	Ga	0.180	0.717							9.07	1.99	9.07	1	0.99	0	0				[112]
La	Ga	0.200	0.717							9.07	2.27	9.07	1	1	0.27	0				[112]
La	Ga	0.220	0.717							9.07	2.56	9.07	1	1	0.56	0				[112]
La	Ga	0.240	0.717							9.07	2.87	9.07	1	1	0.87	0				[112]
La	Ga	0.260	0.717							9.07	3.19	9.07	1	1	1.19	0				[112]
La	Ga	0.280	0.717							9.07	3.53	9.07	1	1	1.53	0				[112]
La	Ge	0.170	0.61							7.93	1.62	7.93	1	0.62	0	0				[108]
La	Ge	0.200	0.61							7.93	1.98	7.93	1	0.98	0	0				[108]
La	Ge	0.220	0.61	7.93	2.24	7.93	1	1	0.24	0	[108]									
La	Ni	0.200	0.674	465	1433	0.324			8.61	2.15	8.61	1	1	0.15	0				[30]	
La	Ni	0.300	0.674						8.61	3.69	8.61	1	1	1.69	0				[30]	
La	Ni	0.400	0.674						8.93	5.17	7.76	1	1	2	1.17				[30, 113]	
La	Ni	0.480	0.674						9.28	6.37	6.90	1	1	2	2.37				[30]	
Mg	Cu	0.200	0.788						9.87	2.47	9.87	1	1	0.47	0				[114-116]	
Mg	Cu	0.300	0.788						9.90	4.17	9.73	1	1	2	0.17				[114-116]	
Mg	Cu	0.400	0.788						10.20	5.68	8.52	1	1	2	1.68				[114-116]	
Mg	Ga	0.187	0.838						10.45	2.41	10.45	1	1	0.41	0				[117]	
Mg	Ni	0.100	0.788						9.87	1.10	9.87	1	0.1	0	0				[114, 118]	
Mg	Ni	0.150	0.788						9.87	1.74	9.87	1	0.74	0	0				[114, 118]	
Mg	Ni	0.200	0.788						9.87	2.47	9.87	1	1	0.47	0				[115, 116, 118]	
Mg	Y	0.150	1.119						15.04	2.65	15.04	1	1	0.65	0				[114, 119]	
Mg	Y	0.160	1.119	15.04	2.86	15.04	1	1	0.86	0	[115]									
Mg	Zn	0.250	0.863	10.74	3.58	10.74	1	1	1.58	0	[40, 120]									
Mg	Zn	0.281	0.863	10.76	4.15	10.61	1	1	2	0.15	[121]									
Mg	Zn	0.292	0.863	10.78	4.32	10.47	1	1	2	0.32	[121]									
Mg	Zn	0.300	0.863	10.80	4.44	10.36	1	1	2	0.44	[120]									
Mg	Zn	0.321	0.863	10.84	4.76	10.08	1	1	2	0.76	[121]									
Mg	Zn	0.350	0.863	390	616	0.633			10.90	5.22	9.69	1	1	2	1.22				[40]	

Mg	Zn	0.350	0.863		359	379	616	0.583	0.615	20	0.389	10.90	5.22	9.69	1	1	2	1.22					[120, 122]												
Mg	Zn	0.400	0.863																					11.01	6.00	9.00	1	1	2	2				[120]	
Mn	Si	0.230	0.833																					10.40	3.11	10.40	1	1	1.11	0				[12]	
Mn	Zr	0.100	1.197																					16.21	1.80	16.21	1	0.8	0	0				[123]	
Mo	Zr	0.400	1.137																					14.77	7.51	11.26	1	1	2	3.51				[124]	
Mo	Zr	0.450	1.137																					14.64	8.39	10.25	1	1	2	4.39				[124]	
Mo	Zr	0.466	1.137																					14.60	8.67	9.93	1	1	2	4.67				[124]	
Nb	Ir	0.450	0.951									8.86		1133	2373		0.477							12.84	7.58	9.26	1	1	2	3.58					[125]
Nb	Ir	0.500	0.951																					12.88	8.44	8.44	1	1	2	4.44					[125]
Nb	Ni	0.400	0.881									8.91		961	1560		0.616							12.01	6.40	9.60	1	1	2	2.4	3.8	8.2	5.5	9	[56, 74, 110]
Nb	Ni	0.500	0.881		961	1560		0.616				12.21	8.10						8.10	1	1	2		4.1	5	7.4	7.4	7.5	[56, 74, 126, 127]						
Nb	Rh	0.400	0.923									12.48	6.59						9.89	1	1	2		2.59				[125]							
Nb	Rh	0.420	0.923									12.51	6.93						9.58	1	1	2		2.93				[110]							
Nb	Rh	0.450	0.923			973	1773		0.549			12.55	7.45						9.10	1	1	2		3.45				[125]							
Nb	Rh	0.515	0.923									12.64	8.57						8.07	1	1	2		4.57				[125]							
Nb	Si	0.150	0.769									9.66	1.70						9.66	1	0.7	0		0				[128]							
Nb	Si	0.160	0.769									9.66	1.84						9.66	1	0.84	0		0				[128]							
Nb	Si	0.170	0.769									9.66	1.98						9.66	1	0.98	0		0				[129]							
Nb	Si	0.180	0.769									9.66	2.12						9.66	1	1	0.12		0				[128, 129]							
Nb	Si	0.190	0.769									9.66	2.27	9.66	1	1	0.27	0				[128, 129]													
Nb	Si	0.200	0.769			953	2273		0.419			9.66	2.42	9.66	1	1	0.42	0				[128, 129]													
Nb	Si	0.210	0.769									9.66	2.57	9.66	1	1	0.57	0				[129]													
Nb	Si	0.220	0.769									9.66	2.72	9.66	1	1	0.72	0				[124]													
Nd	Au	0.200	0.809	8.36		533	1383	0.385				10.12	2.53	10.12	1	1	0.53	0	0	9.3	2.18	10.8	[45]												
Nd	Fe	0.490	0.702																					9.62	6.67	6.95	1	1	2	2.67			[130]		
Nd	Ni	0.300	0.708																					8.98	3.85	8.98	1	1	1.85	0			[115]		
Nd	Ni	0.400	0.708																					9.32	5.33	7.99	1	1	2	1.33			[115]		
Ni	B	0.180	0.698																					8.87	1.95	8.87	1	0.95	0	0				[48, 50]	
Ni	B	0.185	0.698																					8.87	2.01	8.87	1	1	0.01	0				[131]	
Ni	B	0.190	0.698																					8.87	2.08	8.87	1	1	0.08	0	0	9.3	2.18	10.8	[56]
Ni	B	0.200	0.698																					8.87	2.22	8.87	1	1	0.22	0	0	5.8	1.45	10.8	[56, 74]
Ni	B	0.280	0.698																					8.87	3.45	8.87	1	1	1.45	0					[132]

Ni	B	0.300	0.698			585	1393		0.420			8.87	3.80	8.87	1	1	1.8	0								150, 394
Ni	B	0.330	0.698									8.94	4.27	8.67	1	1	2	0.27	0.9	9	4.43	9.4				[56, 74]
Ni	B	0.340	0.698			658	1398		0.471			8.98	4.41	8.57	1	1	2	0.41								[50, 52, 53, 132, 133]
Ni	B	0.360	0.698			662	1393		0.475			9.06	4.70	8.36	1	1	2	0.7	1.1	8.7	4.9	9.2				[53, 56, 133]
Ni	B	0.380	0.698			659	1353		0.487			9.13	4.99	8.14	1	1	2	0.99								[50, 53, 132]
Ni	B	0.400	0.698			663	1291		0.514			9.21	5.28	7.93	1	1	2	1.28								[50, 53]
Ni	B	0.420	0.698			655	1304		0.502			9.29	5.58	7.71	1	1	2	1.58								[50, 53, 132]
Ni	Hf	0.110	1.254			728	1523		0.478			17.09	2.11	17.09	1	1	0.11	0								[102]
Ni	Hf	0.300	1.254									16.47	6.14	14.33	1	1	2	2.14								[64]
Ni	Hf	0.360	1.254			923	1493		0.618			16.15	7.25	12.89	1	1	2	3.25								[102]
Ni	Hf	0.400	1.254									15.94	7.98	11.96	1	1	2	3.98								[64]
Ni	Hf	0.428	1.254									15.80	8.47	11.32	1	1	2	4.47								[64]
Ni	Nb	0.370	1.135	8.95								14.83	6.97	11.87	1	1	2	2.97	6.6	5.9	10	5.6				[56, 74]
Ni	Nb	0.380	1.135		892	930	1473	0.606	0.631	38	0.393	14.81	7.15	11.66	1	1	2	3.15	6.1	5.7	9.3	5.5				[56, 134]
Ni	Nb	0.400	1.135			910	1484		0.613			14.76	7.50	11.25	1	1	2	3.5								[36, 135]
Ni	Nb	0.400	1.135			933	1473		0.633			14.76	7.50	11.25	1	1	2	3.5								[136, 137]
Ni	Nb	0.400	1.135			918	1473		0.623			14.76	7.50	11.25	1	1	2	3.5								[127]
Ni	Nb	0.440	1.135	8.92								14.65	8.21	10.45	1	1	2	4.21	5.5	6.6	8.4	6.5				[56, 74]
Ni	P	0.112	0.81	8.31								10.12	1.28	10.12	1	0.28	0	0								[54]
Ni	P	0.152	0.81	8.16								10.12	1.81	10.12	1	0.81	0	0								[54]
Ni	P	0.180	0.81									10.12	2.22	10.12	1	1	0.22	0								[138, 139]
Ni	P	0.185	0.81	8								10.12	2.30	10.12	1	1	0.3	0								[54]
Ni	P	0.190	0.81									10.12	2.37	10.12	1	1	0.37	0								[139]
Ni	P	0.200	0.81	7.9		635	1173		0.541			10.12	2.53	10.12	1	1	0.53	0	0	9.3	2.33	9.4				340, 114, 306, 393, 3
Ni	P	0.200	0.81			600	1173		0.512			10.12	2.53	10.12	1	1	0.53	0	0	9.3	2.33	9.4				[36]
Ni	P	0.210	0.81	7.94								10.12	2.69	10.12	1	1	0.69	0								[54]
Ni	P	0.222	0.81	7.8								10.12	2.89	10.12	1	1	0.89	0								[54]
Ni	P	0.240	0.81	7.8								10.12	3.20	10.12	1	1	1.2	0								[54]
Ni	P	0.263	0.81	7.73								10.12	3.61	10.12	1	1	1.61	0								[54]
Ni	Ta	0.100	1.151									15.51	1.72	15.51	1	0.72	0	0								[136]
Ni	Ta	0.200	1.151									15.51	3.88	15.51	1	1	1.88	0								[136]

Pd	Ge	0.248	0.803	11.1		523						10.04	3.31	10.04	1	1	1.31	0								[144]
Pd	Ge	0.300	0.803									10.09	4.23	9.86	1	1	2	0.23								[70]
Pd	Ni	0.500	0.887									12.27	8.14	8.14	1	1	2	4.14								[146]
Pd	P	0.170	0.718									9.09	1.86	9.09	1	0.86	0	0								[143]
Pd	P	0.180	0.718									9.09	2.00	9.09	1	1	0	0								[143]
Pd	P	0.190	0.718									9.09	2.13	9.09	1	1	0.13	0								[147]
Pd	Sb	0.200	1.092									14.64	3.66	14.64	1	1	1.66	0								[70]
Pd	Sb	0.300	1.092									14.48	5.55	12.94	1	1	2	1.55								[70]
Pd	Si	0.150	0.775			633	1213		0.522			9.72	1.72	9.72	1	0.72	0	0								[148, 149]
Pd	Si	0.160	0.775		635	640	1108	0.573	0.578	5	0.367	9.72	1.85	9.72	1	0.85	0	0								[55, 149]
Pd	Si	0.165	0.775		635	642	1105	0.575	0.581	7	0.369	9.72	1.92	9.72	1	0.92	0	0								[150]
Pd	Si	0.170	0.775		632	645	1092	0.579	0.591	13	0.374	9.72	1.99	9.72	1	0.99	0	0								[36, 148]
Pd	Si	0.180	0.775	10.25	648	658	1113	0.582	0.591	10	0.374	9.72	2.13	9.72	1	1	0.13	0								[149, 151]
Pd	Si	0.180	0.775		648	658	1170	0.554	0.562	10	0.362	9.72	2.13	9.72	1	1	0.13	0								[77, 150]
Pd	Si	0.180	0.775		642	661	1113	0.577	0.594	19	0.377	9.72	2.13	9.72	1	1	0.13	0								[62]
Pd	Si	0.190	0.775		650		1153	0.564				9.72	2.28	9.72	1	1	0.28	0								[85]
Pd	Si	0.200	0.775	10.3	655	667	1220	0.537	0.547	12	0.356	9.72	2.43	9.72	1	1	0.43	0	0	6.6	1.65	10.6				[56, 70, 72, 77, 148, 149]
Pd	Si	0.200	0.775		673	673	1213	0.555	0.555	0	0.357	9.72	2.43	9.72	1	1	0.43	0								[81, 85]
Pd	Si	0.210	0.775			640	1253		0.511			9.72	2.58	9.72	1	1	0.58	0								[145, 149]
Pd	Si	0.230	0.775			673	1349		0.499			9.72	2.90	9.72	1	1	0.9	0								[148]
Pd	Si	0.250	0.775									9.72	3.24	9.72	1	1	1.24	0								[135]
Pd	Si	0.300	0.775									9.75	4.12	9.62	1	1	2	0.12								[70]
Pr	Au	0.200	0.787									9.86	2.47	9.86	1	1	0.47	0								[45]
Pt	Ge	0.170	0.82									10.25	2.10	10.25	1	1	0.1	0								[12]
Pt	Ge	0.200	0.82									10.25	2.56	10.25	1	1	0.56	0	0	5.6	1.4	10.3				[56, 70]
Pt	Ge	0.300	0.82									10.29	4.29	10.01	1	1	2	0.29								[70]
Pt	P	0.200	0.734			483	861		0.561			9.26	2.32	9.26	1	1	0.32	0								[36]
Pt	P	0.250	0.734	15.8								9.26	3.09	9.26	1	1	1.09	0								[152]
Pt	Sb	0.200	1.115									14.98	3.75	14.98	1	1	1.75	0								[70]
Pt	Sb	0.300	1.115									14.78	5.63	13.14	1	1	2	1.63								[70]
Pt	Sb	0.340	1.115			480	905		0.530			14.69	6.35	12.33	1	1	2	2.35								[36]
Pt	Si	0.200	0.791									9.91	2.48	9.91	1	1	0.48	0								[70]

[illegible]

Te	Tl	0.380	1.229						15.79	7.52	12.27	1	1	2	3.52				[158]
Te	Tl	0.400	1.229						15.69	7.88	11.82	1	1	2	3.88				[158]
Th	Fe	0.200	0.702		647	1553	0.417		8.92	2.23	8.92	1	1	0.23	0				[90, 91]
Th	Fe	0.250	0.702		645	1418	0.455		8.92	2.97	8.92	1	1	0.97	0				[91]
Th	Fe	0.300	0.702		638	1213	0.526		8.92	3.82	8.92	1	1	1.82	0				[90, 91]
Th	Fe	0.330	0.702		631	1205	0.524		8.99	4.29	8.70	1	1	2	0.29				[91]
Th	Fe	0.350	0.702		643	1198	0.537		9.06	4.57	8.49	1	1	2	0.57				[91]
Th	Fe	0.400	0.702		654	1173	0.558		9.25	5.30	7.95	1	1	2	1.3				[90, 91]
Th	Fe	0.450	0.702		691	1233	0.560		9.45	6.05	7.40	1	1	2	2.05				[90, 91]
Th	Fe	0.480	0.702		698	1173	0.595		9.58	6.52	7.06	1	1	2	2.52				[90, 91]
Th	Fe	0.500	0.702						9.66	6.83	6.83	1	1	2	2.83				[90]
Th	Fe	0.550	0.702		745	1383	0.539		9.88	7.64	6.25	1	1	2	3.64				[90]
Th	Fe	0.600	0.702		745	1383	0.539		10.11	8.47	5.64	1	1	2	4.47				[90, 91]
Ti	Be	0.370	0.789	3.83	668	1353	0.493		10.12	5.22	8.90	1	1	2	1.22				[63, 135, 159]
Ti	Be	0.380	0.789						10.15	5.38	8.77	1	1	2	1.38				[159]
Ti	Be	0.390	0.789						10.18	5.53	8.65	1	1	2	1.53				[159]
Ti	Be	0.400	0.789	3.77	669				10.21	5.68	8.53	1	1	2	1.68				[63, 159, 160]
Ti	Be	0.410	0.789	3.72	670				10.24	5.84	8.40	1	1	2	1.84				[63, 160]
Ti	Be	0.420	0.789						10.27	5.99	8.28	1	1	2	1.99				[160]
Ti	Be	0.430	0.789						10.30	6.15	8.15	1	1	2	2.15				[160]
Ti	Cu	0.300	0.887						11.10	4.53	10.57	1	1	2	0.53				[69]
Ti	Cu	0.350	0.887		639	1281	0.499		11.18	5.31	9.87	1	1	2	1.31				[68, 71]
Ti	Cu	0.390	0.887		657	1257	0.523		12.06	6.26	9.80	1	1	2	2.26				[71]
Ti	Cu	0.400	0.887						12.08	6.43	9.65	1	1	2	2.43				[68, 69]
Ti	Cu	0.430	0.887		680	1233	0.552		12.13	6.94	9.20	1	1	2	2.94				[71]
Ti	Cu	0.450	0.887						12.17	7.28	8.90	1	1	2	3.28				[68]
Ti	Cu	0.500	0.887	6.25	680	1257	0.541		12.27	8.14	8.14	1	1	2	4.14	4.5	6	6	6.4 [56, 68, 69, 71, 72, 161]
Ti	Ni	0.250	0.887						11.04	3.68	11.04	1	1	1.68	0				[161]
Ti	Ni	0.260	0.887						11.04	3.88	11.04	1	1	1.88	0				[162]
Ti	Ni	0.300	0.887		720	1247	0.577		11.10	4.53	10.57	1	1	2	0.53				[63, 68, 161, 163]
Ti	Ni	0.330	0.887		723	1256	0.576		11.15	5.00	10.15	1	1	2	1				[68, 140, 162, 163]

Ti	Ni	0.350	0.887	6.06		760	1328	0.433	0.572	35	0.323	11.18	5.31	9.87	1	1	2	1.31	2.3	7.9	5.27	8.1	[69, 161]								
Ti	Ni	0.400	0.887			762	1472		0.518			12.08	6.43	9.65	1	1	2	2.43					[56, 68, 161, 163]								
Ti	Ni	0.450	0.887			12.17	7.28		8.90			1	1	2	3.28	[63, 68]															
Ti	Pt	0.330	0.979			13.08	5.63		11.44			1	1	2	1.63	[69]															
Ti	Si	0.130	0.775			702	1620		0.419			9.72	1.45	9.72	1	0.45	0	0					[164, 165]								
Ti	Si	0.150	0.775			702	1677		0.419			9.72	1.72	9.72	1	0.72	0	0					[105, 165]								
Ti	Si	0.160	0.775			9.72	1.85		9.72			1	0.85	0	0	0	9.4	1.79					11.5	[56, 74]							
Ti	Si	0.200	0.775			867	1903		0.456			9.72	2.43	9.72	1	1	0.43	0					[63, 69, 105, 159, 161]								
Ti	Si	0.220	0.775			9.72	2.74		9.72			1	1	0.74	0								[164]								
Tm	Au	0.200	0.823			10.28	2.57		10.28			1	1	0.57	0								[45]								
U	Co	0.200	0.791	9.91	2.48	9.91	1	1	0.48	0				[166]																	
U	Cr	0.270	0.823	10.28	3.80	10.28	1	1	1.8	0				[166]																	
U	Fe	0.200	0.791	9.91	2.48	9.91	1	1	0.48	0				[166]																	
U	Mn	0.200	0.835	10.42	2.61	10.42	1	1	0.61	0				[166]																	
U	Ni	0.200	0.797	9.98	2.50	9.98	1	1	0.5	0				[166]																	
Y	Cu	0.330	0.704	6.06		535		0.440	0.465	35	0.323	9.01	4.29	8.72	1	1	2	0.29	2.9	8.4	4.14	10.7	[56, 75]								
Y	Cu	0.400	0.704			517						9.27	5.31	7.96	1	1	2	1.31					[113, 167]								
Y	Cu	0.570	0.704			522						9.99	7.97	6.01	1	1	2	3.97	2.9	8.4	11.1	10.7	[75]								
Y	Ni	0.330	0.704									9.01	4.29	8.72	1	1	2	0.29	1.9	9.3	4.58	9.5	[56, 74]								
Zn	Ca	0.375	1.457	5.72	613	648	1393	0.496	0.523	29	0.349	18.05	8.27	13.78	1	1	2	4.27	2	7.1	5.35	6.2	[40]								
Zn	Ca	0.390	1.457									17.91	8.54	13.36	1	1	2	4.54					[40]								
Zr	Al	0.260	0.892									11.10	3.90	11.10	1	1	1.9	0					[12]								
Zr	Au	0.300	0.911									12.20	4.86	11.34	1	1	2	0.86					[168]								
Zr	Be	0.300	0.709									5.72	600	1393	0.431	8.99	3.85	8.99					1	1	1.85	0	[63, 160]				
Zr	Be	0.300	0.709									5.72	600	1393	0.431	8.99	3.85	8.99					1	1	1.85	0	[169]				
Zr	Be	0.325	0.709									9.05	4.24	8.81	1	1	2	0.24					[170]								
Zr	Be	0.350	0.709									5.65	614	1238	0.496	9.14	4.60	8.54					1	1	2	0.6	[169]				
Zr	Be	0.350	0.709									5.48	618	647	1238	0.499	0.523	29					0.349	9.14	4.60	8.54	1	1	2	0.6	[63, 135, 160]
Zr	Be	0.400	0.709									5.46	623	673	1343	0.464	0.501	50					0.342	9.33	5.33	8.00	1	1	2	1.33	[63, 160]
Zr	Be	0.400	0.709	5.48	625		1393	0.449				9.33	5.33	8.00	1	1	2	1.33	[169]												
Zr	Be	0.430	0.709									9.45	5.78	7.66	1	1	2	1.78	2	7.1	5.35	6.2	[38]								

Zr	Be	0.450	0.709	5.18	646	681	1413	0.457	0.482	35	0.331	9.52	6.09	7.44	1	1	2	2.09				[63, 160]
Zr	Be	0.500	0.709	5.08	672	682	1473	0.456	0.463	10	0.318	9.73	6.87	6.87	1	1	2	2.87				[63, 160]
Zr	Co	0.200	0.791	6.8		580	1388		0.418			9.91	2.48	9.91	1	1	0.48	0				[171-173]
Zr	Co	0.220	0.791			643	1254		0.513			9.91	2.80	9.91	1	1	0.8	0				[59, 79]
Zr	Co	0.270	0.791									9.91	3.67	9.91	1	1	1.67	0				[63]
Zr	Co	0.300	0.791	7								9.95	4.18	9.76	1	1	2	0.18				[172]
Zr	Co	0.300	0.791	6.68		700	1394		0.502			9.95	4.18	9.76	1	1	2	0.18				[59, 154, 172]
Zr	Co	0.330	0.791	7.12								10.03	4.63	9.40	1	1	2	0.63				[171, 172]
Zr	Co	0.350	0.791	7.2								10.09	4.93	9.16	1	1	2	0.93				[172]
Zr	Co	0.360	0.791			740	1394		0.531			10.12	5.08	9.04	1	1	2	1.08				[59]
Zr	Co	0.400	0.791	7.35		767	1523		0.504			10.24	5.70	8.54	1	1	2	1.7				[79, 171, 172]
Zr	Co	0.450	0.791	7.4								10.39	6.48	7.91	1	1	2	2.48				[172]
Zr	Co	0.470	0.791	7.63								10.45	6.79	7.66	1	1	2	2.79				[172]
Zr	Co	0.500	0.791									10.55	7.27	7.27	1	1	2	3.27				[140]
Zr	Co	0.520	0.791	7.7								10.61	7.60	7.01	1	1	2	3.6				[172]
Zr	Co	0.530	0.791			785	1585		0.495			10.64	7.76	6.88	1	1	2	3.76				[59]
Zr	Co	0.573	0.791									10.79	8.47	6.31	1	1	2	4.47				[63]
Zr	Cu	0.200	0.797									9.98	2.50	9.98	1	1	0.5	0				[76]
Zr	Cu	0.250	0.797		571	618	1363	0.419	0.454	47	0.320	9.98	3.33	9.98	1	1	1.33	0				[75]
Zr	Cu	0.280	0.797		600	666	1268	0.473	0.525	66	0.356	9.98	3.88	9.98	1	1	1.88	0				[75]
Zr	Cu	0.300	0.797									10.02	4.21	9.82	1	1	2	0.21				[64]
Zr	Cu	0.335	0.797		631	690	1273	0.496	0.542	59	0.362	10.12	4.73	9.39	1	1	2	0.73				[76]
Zr	Cu	0.400	0.797		677		1248	0.542				10.31	5.72	8.58	1	1	2	1.72				[64, 70, 81]
Zr	Cu	0.400	0.797		646	707	1248	0.518	0.567	61	0.373	10.31	5.72	8.58	1	1	2	1.72				[76]
Zr	Cu	0.400	0.797		654	718	1343	0.487	0.534	64	0.359	10.31	5.72	8.58	1	1	2	1.72				[75]
Zr	Cu	0.450	0.797		661	729	1203	0.549	0.606	68	0.391	10.46	6.51	7.95	1	1	2	2.51				[75]
Zr	Cu	0.450	0.797		669	719	1206	0.555	0.596	50	0.383	10.46	6.51	7.95	1	1	2	2.51				[66]
Zr	Cu	0.460	0.797		696	746	1201	0.580	0.621	50	0.393	10.49	6.66	7.82	1	1	2	2.66				[135]
Zr	Cu	0.480	0.797		689	749	1207	0.571	0.620	59	0.395	10.55	6.98	7.56	1	1	2	2.98				[75]
Zr	Cu	0.500	0.797		707	749	1208	0.585	0.620	42	0.391	10.61	7.30	7.30	1	1	2	3.3				[64, 79]
Zr	Cu	0.500	0.797	7.33	681	735	1214	0.561	0.605	54	0.388	10.61	7.30	7.30	1	1	2	3.3				[72, 77, 127]
Zr	Cu	0.500	0.797		680	730	1214	0.560	0.602	50	0.386	10.61	7.30	7.30	1	1	2	3.3				[76]

Zr	Cu	0.500	0.797	6.45	711	774	1214	0.586	0.638	63	0.402	10.61	7.30	7.30	1	1	2	3.3	5.4	5	6.7	5.9	[75]	
Zr	Cu	0.550	0.797		698	748	1183	0.590	0.632	50	0.398	10.77	8.12	6.65	1	1	2	4.12					[76]	
Zr	Cu	0.560	0.797		727		1163	0.625				10.80	8.29	6.51	1	1	2	4.29					[81]	
Zr	Cu	0.560	0.797		728	792	1163	0.626	0.681	64	0.419	10.80	8.29	6.51	1	1	2	4.29					[75]	
Zr	Cu	0.570	0.797									10.83	8.45	6.38	1	1	2	4.45					[70, 73, 174]	
Zr	Fe	0.200	0.791									9.91	2.48	9.91	1	1	0.48	0					[171]	
Zr	Fe	0.240	0.791									9.91	3.13	9.91	1	1	1.13	0					[94, 95, 175]	
Zr	Fe	0.250	0.791									9.91	3.30	9.91	1	1	1.3	0					[63, 89, 171]	
Zr	Fe	0.280	0.791									9.91	3.85	9.91	1	1	1.85	0					[94]	
Zr	Fe	0.300	0.791			663	1433		0.463			9.95	4.18	9.76	1	1	2	0.18					[154, 175]	
Zr	Fe	0.330	0.791			682	1553		0.439			10.03	4.63	9.40	1	1	2	0.63					[79]	
Zr	Fe	0.350	0.791									10.09	4.93	9.16	1	1	2	0.93					[63, 95]	
Zr	Fe	0.400	0.791									10.24	5.70	8.54	1	1	2	1.7					[95]	
Zr	Ge	0.130	0.722									9.13	1.36	9.13	1	0.36	0	0					[105, 176]	
Zr	Ge	0.150	0.722									9.13	1.61	9.13	1	0.61	0	0					[105, 176]	
Zr	Ge	0.170	0.722								9.13	1.87	9.13	1	0.87	0	0	[105, 176]						
Zr	Mn	0.450	0.835								10.84	6.68	8.16	1	1	2	2.68	[63]						
Zr	Mn	0.500	0.835								10.97	7.49	7.49	1	1	2	3.49	[63]						
Zr	Mo	0.400	0.88								11.19	6.08	9.11	1	1	2	2.08	[63]						
Zr	Mo	0.533	0.88								12.26	8.67	7.60	1	1	2	4.67	[63]						
Zr	Ni	0.180	0.797								9.98	2.19	9.98	1	1	0.19	0	[30]						
Zr	Ni	0.200	0.797		660	1423		0.464			9.98	2.50	9.98	1	1	0.5	0	[70, 142, 171]						
Zr	Ni	0.220	0.797		611	1343		0.455			9.98	2.82	9.98	1	1	0.82	0	[59]						
Zr	Ni	0.240	0.797		638	1233		0.517			9.98	3.15	9.98	1	1	1.15	0	[59, 63]						
Zr	Ni	0.250	0.797								9.98	3.33	9.98	1	1	1.33	0	[171]						
Zr	Ni	0.280	0.797	6.71	642	664	1313	0.489	0.506	22	0.340	9.98	3.88	9.98	1	1	1.88	0	[79]					
Zr	Ni	0.300	0.797			660	1338		0.493			10.02	4.21	9.82	1	1	2	0.21	[64, 142, 154]					
Zr	Ni	0.330	0.797									10.11	4.65	9.45	1	1	2	0.65	[140, 171]					
Zr	Ni	0.333	0.797									10.11	4.70	9.41	1	1	2	0.7	1.3	8.4	4.2	11.6	[74, 177]	
Zr	Ni	0.350	0.797									10.16	4.96	9.21	1	1	2	0.96	3.3	8.6	4.8	11	[177]	
Zr	Ni	0.360	0.797			730	1293		0.565			10.19	5.11	9.08	1	1	2	1.11	2.3	7.9	3.9	9.1	[59, 177]	
Zr	Ni	0.370	0.797		700	720	1313	0.533	0.548	20	0.358	10.22	5.26	8.96	1	1	2	1.26						[79]

Zr	Ni	0.400	0.797		713	735	1413	0.505	0.520	22	0.346	10.31	5.72	8.58	1	1	2	1.72						[64, 70, 79, 142]
Zr	Ni	0.500	0.797			795	1523		0.522			10.61	7.30	7.30	1	1	2	3.3	3.3	6.7	6.7	7.8		[56, 64, 140, 142]
Zr	Ni	0.571	0.797									10.83	8.47	6.36	1	1	2	4.47						[30, 63]
Zr	Pd	0.200	0.899									11.18	2.79	11.18	1	1	0.79	0						[70]
Zr	Pd	0.250	0.899									11.18	3.73	11.18	1	1	1.73	0						[63]
Zr	Pd	0.300	0.899	7.53								12.04	4.81	11.23	1	1	2	0.81						[110, 154, 168]
Zr	Pd	0.300	0.899	7.71	680	690				10		12.04	4.81	11.23	1	1	2	0.81	3.6	5.37	2.3	11.5		[36, 178]
Zr	Pd	0.330	0.899	7.9								12.09	5.31	10.78	1	1	2	1.31						[140, 179]
Zr	Pd	0.350	0.899	8.02								12.12	5.64	10.48	1	1	2	1.64						[70, 179]
Zr	Pd	0.450	0.899									12.29	7.33	8.96	1	1	2	3.33						[63]
Zr	Pt	0.200	0.88									10.95	2.74	10.95	1	1	0.74	0						[168, 178]
Zr	Rh	0.170	0.835									10.42	2.14	10.42	1	1	0.14	0						[63]
Zr	Rh	0.180	0.835									10.42	2.29	10.42	1	1	0.29	0						[180]
Zr	Rh	0.270	0.835									10.42	3.86	10.42	1	1	1.86	0						[180]
Zr	Rh	0.280	0.835									10.43	4.04	10.39	1	1	2	0.04						[63]
Zr	Si	0.120	0.696			804	1936		0.416			8.85	1.21	8.85	1	0.21	0	0						[181]
Zr	Si	0.130	0.696			772	1984		0.389			8.85	1.32	8.85	1	0.32	0	0						[105, 181]
Zr	Si	0.140	0.696			757	2019		0.375			8.85	1.44	8.85	1	0.44	0	0						[181]
Zr	Si	0.150	0.696			759	2047		0.371			8.85	1.56	8.85	1	0.56	0	0						[105, 181]
Zr	Si	0.160	0.696			735	2081		0.353			8.85	1.69	8.85	1	0.69	0	0						[181]
Zr	Si	0.170	0.696			720	2095		0.344			8.85	1.81	8.85	1	0.81	0	0						[181, 182]
Zr	Si	0.180	0.696			725	2130		0.340			8.85	1.94	8.85	1	0.94	0	0						[105, 181]
Zr	Si	0.190	0.696			724	2151		0.336			8.85	2.08	8.85	1	1	0.08	0						[105, 181, 182]
Zr	Si	0.200	0.696			720	2172		0.332			8.85	2.21	8.85	1	1	0.21	0						[105, 181, 182]
Zr	Si	0.220	0.696			737	2198		0.335			8.85	2.50	8.85	1	1	0.5	0						[105, 181, 182]
Zr	Si	0.230	0.696									8.85	2.64	8.85	1	1	0.64	0						[182]
Zr	Si	0.240	0.696			768	2297		0.334			8.85	2.79	8.85	1	1	0.79	0						[181]

Table A2. Binary bulk metallic glass constitutions, thicknesses, characteristic temperatures and structural parameters.

Ω	α	F_α	R	Thickness, mm	T_g , K	T_x , K	T_l , K	T_{rg}	ΔT_x	T_x/T_l	γ	\hat{S}_α	\bar{S}_α	\bar{S}_α	$S(\alpha_\alpha)$	$S(\alpha_\beta)$	$S(\alpha_\gamma)$	$S(\alpha_\Omega)$	Citations
Ca	Al	0.336	0.701	1	528	540	873	0.605	0.619	12	0.385	9.00	4.37	8.63	1	1	2	0.37	[42]
Cu	Hf	0.350	1.254	2	781	832	1259	0.621	0.661	51	0.408	16.20	7.07	13.13	1	1	2	3.07	[65]
Cu	Hf	0.400	1.254	1	773	827	1290	0.599	0.641	54	0.401	15.94	7.98	11.96	1	1	2	3.98	[64, 66]
Cu	Zr	0.355	1.254	2	747	769	1243	0.601	0.618	22	0.386	16.17	7.16	13.01	1	1	2	3.16	[80]
Cu	Zr	0.360	1.254	2	787	833	1233	0.638	0.676	46	0.412	16.15	7.25	12.89	1	1	2	3.25	[72, 78]
Cu	Zr	0.400	1.254	1	740	760	1198	0.618	0.634	20	0.392	15.94	7.98	11.96	1	1	2	3.98	[36, 64, 81]
Cu	Zr	0.400	1.254	1	714	764	1198	0.596	0.638	50	0.400	15.94	7.98	11.96	1	1	2	3.98	[76]
Cu	Zr	0.400	1.254	1	763	812	1198	0.637	0.677	49	0.414	15.94	7.98	11.96	1	1	2	3.98	[79]
Cu	Zr	0.400	1.254	1	733	791	1198	0.612	0.660	58	0.410	15.94	7.98	11.96	1	1	2	3.98	[66]
Cu	Zr	0.400	1.254	1	755	811	1198	0.630	0.677	56	0.415	15.94	7.98	11.96	1	1	2	3.98	[78]
Hf	Cu	0.550	0.797	1.5	771	830	1295	0.595	0.641	59	0.402	10.77	8.12	6.65	1	1	2	4.12	[66]
Ni	Nb	0.380	1.135	2	892	930	1473	0.606	0.631	38	0.393	14.81	7.15	11.66	1	1	2	3.15	[56, 134]
Ni	Nb	0.400	1.135	1		910	1484		0.613			14.76	7.50	11.25	1	1	2	3.5	[36, 135]
Zr	Cu	0.450	0.797	1.5	661	729	1203	0.549	0.606	68	0.391	10.46	6.51	7.95	1	1	2	2.51	[75]
Zr	Cu	0.450	0.797	1.5	669	719	1206	0.555	0.596	50	0.383	10.46	6.51	7.95	1	1	2	2.51	[66]
Zr	Cu	0.460	0.797	2	696	746	1201	0.580	0.621	50	0.393	10.49	6.66	7.82	1	1	2	2.66	[135]